

Rowan University

Rowan Digital Works

Theses and Dissertations

12-22-2016

Landfill elevated internal temperature detection and landfill fire index assessment for fire monitoring

Aurora Musilli
Rowan University

Follow this and additional works at: <https://rdw.rowan.edu/etd>



Part of the [Civil and Environmental Engineering Commons](#)

Let us know how access to this document benefits you -
share your thoughts on our feedback form.

Recommended Citation

Musilli, Aurora, "Landfill elevated internal temperature detection and landfill fire index assessment for fire monitoring" (2016). *Theses and Dissertations*. 2340.

<https://rdw.rowan.edu/etd/2340>

This Thesis is brought to you for free and open access by Rowan Digital Works. It has been accepted for inclusion in Theses and Dissertations by an authorized administrator of Rowan Digital Works. For more information, please contact LibraryTheses@rowan.edu.

**LANDFILL ELEVATED INTERNAL TEMPERATURE DETECTION AND
LANDFILL FIRE INDEX ASSESSMENT FOR FIRE MONITORING**

by

Aurora Musilli

A Thesis

Submitted to the
Department of Civil & Environmental Engineering
College of Engineering
In partial fulfillment of the requirement
For the degree of
Master of Science in Civil & Environmental Engineering
at
Rowan University
September 23, 2016

Thesis Chair: Rouzbeh Nazari

© 2016 Aurora Musilli

Dedications

This thesis becomes a reality with the kind support and help of many individuals. I would like to extend my sincere thanks to all of them.

Foremost, I want to offer this endeavor to my family, my dad in particular, and supportive friends for the encouragement which helped me in completion of this paper. My beloved and supportive dad, Egidio Musilli who is always by my side when times I need him most and helped me a lot in conduction this research and overcoming the obstacles encountered in my leadership experience.

Acknowledgements

I would like to express my appreciation to Dr. Rouzbeh Nazari for his support throughout my master program and Dr. Jess W. Everett for his guidance and help throughout the writing of this thesis. The skills and knowledge that I have gained are things that I will take with me into my next professional endeavor.

Abstract

Aurora Musilli

LANDFILL ELEVATED INTERNAL TEMPERATURE DETECTION AND
RISK ASSESSMENT FOR FIRE MONITORING

2016-2017

Rouzbeh Nazari

Master of Science in Civil & Environmental Engineering

Landfill fires are becoming a real threat to both people and environment due to lack of predictions and control methods. Processing of the infrared band from level-1 satellite images was employed and decades worth of archived data from USGS Earth Explorer databases were analyzed to obtain surface temperature values of Atlantic Waste Landfill, Virginia and Bridgeton Landfill, Missouri. Multitemporal thermal maps and frequency of maxima analysis maps of these two landfills showed the hotspots spreading through the waste site. A Landfill Fire Index (LFI) was created by investigating eight factors that give information about the hazardousness of the landfill conditions relative to the presence of a fire occurrence. The application of Analytical Hierarchy Method (AHP) resulted in the determination of the degree of importance of each Landfill Fire Index factor. Several monitoring well data sets were used to calculate the LFI for Bridgeton Landfill, Missouri, and Burlington County Landfill, New Jersey.

Table of Contents

Abstract.....	v
List of Figures	xi
List of Tables.....	xiv
Chapter 1: Introduction and Objectives.....	1
1.1 Scope	6
Chapter 2: Literature Review	8
2.1 Landfill Fires.....	9
2.1.1 Landfill Fire Data Inventory.....	15
2.2 Applications of Satellite Remote Sensing.....	17
2.2.1 Geostationary Satellites.....	19
2.2.2 Polar Orbiting Satellites	20
2.2.3 Landsat Imagery	21
2.2.4 Visible, Near and Thermal Infrared Sensing	22
2.2.5 Normalized Difference Vegetation Index (NDVI)	24
2.2.6 Land Surface Temperature (LST)	26
Chapter 3: Data Acquisition and Case Studies.....	28

Table of Contents (Continued)

3.1 Data Collection and Processing	28
3.1.1 Landsat Imagery/ Instrument	32
3.2 Study Area	34
3.2.1 Bridgeton Landfill (BL)	36
3.2.2 Atlantic Waste Landfill (AWL)	37
3.2.3 Burlington County Landfill (BCL).....	38
Chapter 4: Landfill Elevated Internal Temperature Detection.....	40
4.1 Methodology.....	40
4.1.1 Landsat calibration	41
4.1.2 Spectral radiance scaling method	41
4.1.3 Atmospheric correction: simple dark object subtraction method.....	43
4.1.4 Sun radiation pattern geometry and albedo effect on earth surface ..	43
4.1.5 Comparison of At-Sensor Radiance to Effective At-Satellite Temperatures	47
4.1.6 Calculation of Land Surface Temperature (LST).....	49
4.2 Results.....	50

Table of Contents (Continued)

4.2.1 Comparison of LST and Air Temperature in Two Study Areas53

4.2.2 “LST Detection” Matlab Program.....58

4.2.3 Detection and Delineation of Consistent Hot Spots Through Time
Series Analysis59

4.2.4 Composition of maps of landfills superimposed by heat map and hot
spots.....68

Chapter 5: Development of Landfill Fire Index (LFI).....72

5.1 Methodology and Data75

5.1.1 Landfill Fire Index Data Analysis.....75

5.1.2 Landfill Classification Data Analysis.....78

5.1.3 First Ignition Source Data Analysis.....80

5.2 Landfill Fire Index Factors.....81

5.2.1 Residual Nitrogen84

5.2.2 Oxygen Exceedance86

5.2.3 Methane87

5.2.4. Carbon Monoxide88

5.2.5 Carbon Dioxide89

Table of Contents (Continued)

5.2.6 Moisture Content90

5.2.7 Monitoring Well Temperature91

5.2.8. Buried Waste Density93

5.3 Landfill Fire Index Data for Bridgeton and Burlington Landfills 95

5.4 Analytical Hierarchy Process (AHP) Calculation for Landfill Fire Index
(LFI) Determination97

5.5 Results Summary of AHP Model 106

5.6 Comparison of Calculated Landfill Fire Index Value for Two Landfills..111

 5.6.1 Bridgeton Landfill (BL)111

 5.6.2 Burlington County Landfill (BCL).....121

5.7 Comparison of AHP for 4 and 7 Factors.....128

Chapter 6: Conclusions and Future Work.....131

References136

Appendix A: Bridgeton Landfill Monitoring Wells Raw Data146

Appendix B: Bridgeton Landfill Map of Monitoring Well Locations152

Appendix C: Map of The Smoldering Event in 2013153

List of Figures

Figure	Page
Figure 1. Visual representation of the method workflow	30
Figure 2. Topography of Bridgeton Landfill [45], Missouri a), Atlantic Waste Landfill [46], Virginia b), and Burlington County Landfill [47], Florence, New Jersey c) from Google.....	35
Figure 3. Sun radiation pattern geometry	44
Figure 4. Albedo effect on earth surface	46
Figure 5. Non-calibrated images of Atlantic Waste Landfill January 23rd 2004 (a); April 28th 2004 (b); August 21st 2005 (c); January 26th 2006 (d); February 13th 2008 (e); May 25th 2008 (f); June 29th 2009 (g); October 9th 2011 (h).....	51
Figure 6. Landsat 8 images of Atlantic Waste Landfill after performing atmospheric correction. January 23rd 2004 (a); April 28th 2004 (b); . August 21st 2005 (c); January 26th 2006 (d); February 13th 2008 (e); May 25th 2008 (f); June 29th 2009 (g); October 9th 2011 (h).....	52
Figure 7. Day-by-day comparison of Avg. LST and Air Temperature for AWL, Virginia	54
Figure 8. Day-by-day comparison of Avg. LST, Max. LST and Air Temperature for Bridgeton Landfill, Missouri.	57
Figure 9. Relative temperature differences between a hotspot (blue) and a regular portion of the landfill (green) in a 12 year span for Atlantic Waste Landfill (AWL), Virginia.....	61

Figure 10. Thermal maps of Atlantic Waste Landfill (AWL) displaying the location of the hotspots relative to the perimeter of the landfill throughout the years. (a) January 23rd 2004; (b) April 28th 2004; (c) August 21st 2005; (d) January 26th 2006; (e) February 13th 2008; (f) May 25 th 2008; (g) June 29 th 2009; (h) October 9 th 2011.	63
Figure 11. Relative temperature differences in a 12 year span for BL, Missouri ...	66
Figure 12. Thermal maps of Bridgeton Landfill displaying the location of the hotspots relative to the perimeter of the landfill throughout the years. January 20th 2000 (a); February 17th 2002 (b); July 4th 2002 (c); May 16th 2005 (d); December 22th 2006 (e); August 10th 2007 (f); August 25th 2009 (g); October 21st 2010 (h).	67
Figure 13. Location of frequency of maxima around the landfill site of Atlantic Waste Landfill (AWL), Virginia	69
Figure 14. Location of frequency of maxima around the landfill site of Bridgeton Landfill, Missouri.....	71
Figure 15. Number of Reported Landfill Fires in the United States between 1980 and 2011.....	77
Figure 16. Number of landfill fire occurrences based on landfill classification (1999-2011).....	79
Figure 17. Top ten ignition sources for landfill fires.....	81
Figure 18. Risk factors area of influence around a general landfill	83
Figure 19. Landfill Box Model.....	95

Figure 20. Landfill Fire Index factors: the eight parameters of the LFI.....101

List of Tables

Table	Page
Table 1. Resolution and spectral range of the different spectral bands of Landsat TM.....	33
Table 2. Constant Values for Equation 7.....	49
Table 3. Eight-Step Risk Assessment Process.	74
Table 4. Residual Nitrogen Ranges for Landfills.....	85
Table 5. Explanation of symbols used in Equation 9	100
Table 6. Pair comparison rating parameters for AHP	103
Table 7. Random Index table.....	105
Table 8. Pair-wise Comparison Matrix for V_i (Weights of the LFI factors).....	106
Table 9. Landfill Fire Index (LFI)	110
Table 10. PCM for Bridgeton Landfill weight factors	112
Table 11. Summary of data from monitoring wells in Bridgeton Landfill	114
Table 12. Final Landfill Fire Index for GIW-05 (BL)	115
Table 13. Final Landfill Fire Index for GEW-038 (BL)	116
Table 14. Final Landfill Fire Index for GEW-028R (BL).....	117
Table 15. Final Landfill Fire Index for GEW-10 (BL)	119
Table 16. PCM for Burlington County Landfill weight factors	122
Table 17. LFI Factors Assessment for Burlington County Landfill (BCL)	123

Table 18. LFI for BCL - Landfill 1.....	125
Table 19. LFI for BCL - Landfill 2 (East)	126
Table 20. LFI for BCL - Landfill 2 (West)	127
Table 21. PCM for 7 criteria	129
Table 22. PCM for 4 criteria	130

Chapter 1

Introduction and Objectives

There are serious environmental and public health consequences of landfill fires caused by large amounts of toxic and harmful chemicals being released into the air. Also, damage to the leachate collection system or to the geomembrane liner of the landfill due to a fire may result in the release of biogas and other toxic elements into the surrounding soil, ground water, and atmosphere. Landfill fires and associated environmental pollution is a particularly important issue, especially in rural areas. Soil pollution affects local agriculture and hence endangers jobs in this sector of the economy. The quality of ground water is of critical importance for rural communities because of their wide reliance on personal ground wells as a source of drinking water and water used for irrigation. Leakage of biogas from landfills is another major threat. Unfortunately, biogas movement can happen even in authorized sanitary landfills, especially in the proximity of the edges, where permeability to both gaseous and liquid fluids is increased at the vertical boundaries as compacted landfills stratify horizontally. Due to the unique design characteristics of a landfill, underground or subsurface fires are an ongoing and complex problem. The different dynamics, characteristics and regulations of landfills and the fires that are likely to occur in them suggest that incident response tactics need to be determined on a case by case basis.

Landfill regulations began in 1976 when Congress passed the Resource Conservation and Recovery Act (RCRA). After the Hazardous Solid Waste Amendments of 1984, the EPA began expanding upon the amendments to create federal standards of landfill construction and maintenance. Safety has been the primary motivator for developing the new criteria for landfills. Therefore, landfill fires are an up-and-coming topic as new safety hazards are identified. However, landfills are also a controversial topic, due to perceived notions regarding noxious fume emissions, health and environmental effects and decreased property values in surrounding communities. Subsurface landfill fires can be extremely costly to contain and may result into financial losses from a million dollars upwards to repair the landfill and handle cleanup. These economical aspects should not be overlooked since they can affect federal funds available for clean-up and severely impact the landfill owners managing the active sites, people living nearby the waste site, and the entire community.

Until now, the task of determining either fire and biogas development were given to fire alarm systems installed at landfill sites that rely primarily on aspirating smoke detectors. At large, newer landfills equipped with methane collecting systems, an anomalously high temperature of methane is often used as an indicator of a possible underground fire. Both techniques require substantial

efforts to maintain and are prone to errors causing both delayed fire identification and false fire alarms. A more viable approach to identify and locate landfill fire involves direct thermal imaging of landfill sites and smoldering/fire outbreak prediction.

The technique involves identification of isolated “hotspots” in the thermal image that most likely represent active fire. Internal activities in the landfill cause a change in internal temperature which is not typically a visible sign. However, they can lead to change in surface temperature caused by heat transfer from the interior to the surface that can be detected by thermal infrared sensors. Once these activities begin, the land surface temperature increases in the landfill area but it usually remains unnoticed for long periods of time until the fire ignites, which is too late for interventions. Therefore, if these events could be kept under control, risk of ignition will be lowered and measures to remove the gas build up and stop combustion reactions will be applied hence preventing fires. Thus, thermal imaging can be used to detect underground fires by monitoring changes of the land surface temperature (LST) and identifying strong positive deviations from the “normal” spatial distribution of LST.

A quick and reliable way to monitor large areas of territories such as landfills is the use of space borne remote sensing of thermal imaging employing

satellites. This non-destructive method allows observation of multiple locations over time, making it possible to build an archive of satellite photographs that shows the change in thermal characteristic of a landfill. For this purpose, big data of satellite images can be retrieved from Landsat imagery database which is public domain and can be accessed directly from the United States Geological Survey (USGS) Earth Explorer website [1]. Potentials of infrared-based technique from satellite-based observations have already been actively used in the last two decades for grass and forest fire monitoring. However, no previous studies have shown its direct application to predict and prevent both subsurface and surface fires in landfills. The changes in the land surface temperature captured by series of satellite images spread throughout years can be a powerful tool. Fires exhibit a distinctive and strong thermal signal, which can be easily picked up by infrared sensors observing the landfill site. This makes thermal imaging of landfill sites a viable and efficient way of early fire identification and fire prevention.

Timely landfill fire identification and warnings leading to the prevention or extinction of the fire at an early stage is critical for public welfare and for minimizing environmental and structural damages. The objectives of this study are to:

1. Identify and review landfill fires causes,

2. Identify and review existing method for landfill fires prevention and monitoring,
3. Identify different physical/chemical factors affecting the likability of a landfill to catch fire,
4. Introduce Satellite remote sensing techniques,
5. Analysis of big data of satellite images from USGS Explorer archive using the capabilities of image processing software as ENVI,
6. Develop a user-friendly computer program that uses the capabilities of Matlab to average LSTs on different areas of landfills and combine it with the capabilities of GIS for georeferencing and map creation,
7. Develop a Landfill Fire Index (LFI) for landfill fires prevention from Analytical Hierarchy Process (AHP) model calculations,
8. Apply the “LST detection” Matlab program program to two different case study waste sites in Waverly, Virginia and Bridgeton, Missouri,
9. Apply the Landfill Fire Index to two case studies waste sites in Bridgeton, Missouri and Burlington, New Jersey,
10. Present conclusions on the usefulness of the practicality of the methods presented here and make adequate recommendations and comments on future work.

1.1 Scope

In this paper is illustrated how thermal imaging studies and their correlation to land surface temperature (LST) aid to locate current landfill subsurface events and to predict and locate possible landfill fire outbreaks. Another point that will be made is the usefulness of a Landfill Fire Index for landfill fire prevention based on chemical and physical characteristics of a landfill. This study was finalized to be applied only to Municipal and Construction/Demolition (C&D) Solid Waste Landfills in the United States with a multidisciplinary method that combines the use of ENVI, Matlab, and GIS to retrieve and display temperature data.

In order to fulfill the above-mentioned objectives past and current methods of remote sensing techniques and statistical analysis are applied to a total of three landfills in North America. A literature review of these topics is found in Chapter 2 which goes into the details of the background knowledge that served as backbone for the results and analysis illustrated into the subsequent chapters. Chapter 3 offers an introduction to the data collection of the input images that will be fed to the in-house written computer program. Data processing techniques and instrumentation will be also described in this chapter together with the characterization of the study area. Chapter 4 describes the methodology used for the image processing algorithm and lists the main equations that are behind the

image processing techniques with some key concept that better clarify them. The systematic approach being considered involves observing LST trends over periods of 10 years or more using Landsat images from USGS Explore database for different landfills scattered around the United States. The applications of this method are intended to have a tremendous impact on reduction of risk for the entire community, workers, and environmental pollution, especially in regard of landfill gases (LFG) emissions. This chapter also presents the results of the method by illustrating two case studies located in Waverly, Virginia, and Bridgeton, Missouri respectively. Chapter 5 illustrates how Analytical Hierarchy Process (AHP) models were used to develop the Landfill Fire Index and what are the specific Landfill Fire Index Factors considered. Each of them is described and analyzed taking into account its interrelationships with each other and the levels at which they become hazardous. In fact, the hazardousness of a chemical or physical factor inside the landfill is enhanced depending on the presence and hazardousness of the other ones. The applicability of the Landfill Fire Index is then proved by implementing it to the landfills of Bridgeton, Missouri and Burlington, New Jersey. The last chapter includes the conclusions of this thesis and the appropriate recommendations to be made for future work on the subject.

Chapter 2

Literature Review

Remote sensing and its applications is the concept that this paper is based upon. In particular, remote sensing can be defined as the science or art of gathering information about an object or a collection of objects without coming in contact with it [2]. Even though there are many quantities that can be measured remotely, such as gravitational force, sonic waves, and seismic waves, the study conducted in this paper focuses on detection and measurement of electromagnetic radiation, reflected or emitted from the Earth's surface [3]. The information derived through remote sensing about the soil temperature is a remarkable tool to monitor the subsurface events that can take place below the surface of landfills. It can be used to keep measure of the temperature fluctuations and thus provide useful information as to predicting when a subsurface of surface fire might occur.

From the public health perspective, the response to landfill fires includes many hazardous scenarios for both the population nearby and landfill personnel which outbalance the cost of preventive measures. In the past, the only preventive measures used for fire prevention were monitoring of landfill gases, along with collecting and recycling of methane emissions [4]. Therefore, most of the engineered solutions employed until now regarded: what compounds to monitor, where to position air monitoring devices, deciding between using mobile or fixed

samplers, whether to use integrating or continuous techniques, interpreting of multi-pollutant mixture results across varied averaging times, action levels for warnings, evacuations, and closures, wording of public notices, recommended actions for reducing exposure, and best practices for using dispersion modeling. [5]. Unfortunately, there is an absence of prioritizing on which factor or compound to measure and where to measure it, besides a lack of focus on compound concentrations with inadequate interpretation of the results and public health impact. Past studies seldom incorporate in depth interpretation of data and limit the ability to generalize from the measurements [5].

2.1 Landfill Fires

Due to the variety of materials collected, municipal solid waste (MSW) landfills are prone to combustion events. Most of these types of landfills undergo surface or subsurface fire during their operational time span [6]. While operating landfills are more likely to experience working face fires, closed landfills are predisposed to subsurface smoldering events that can lead to open fires.

Thalhamer (2010) states that smoldering events in the United States are prevalent during the late spring and winter months due to frequent barometric changes [7]. Waste can catch fire due to arson, internal chemical reactions, hot loads, or equipment at any time. If the fire is small and takes place in an open

landfill, the incidents are considered “operational fires”. These incidents are usually resolved by the operators of the landfill that record the event in the facility log, but only if they are required by regulations [6]. If the facility is a closed landfill, then the local fire department or state regulatory agencies usually administer the situation and take proper action.

Classification of different types of landfill fires is crucial to fire prevention. Subsurface smoldering events develop below the ground level and given the right geological conditions, can extend downward beyond 100 feet [6]. On the other hand, surface fires occur when fuel and oxygen are abundant. This type of fires can start on the surface and burn down to 5 feet below the ground. One should note that fire events can occur even deep under the surface due to methanogenic bacteria that are able to survive in anaerobic conditions, thus providing the fuel for combustion to happen [6]. Combustion reactions are exothermic oxidation processes that generate heat [8]. In general, combustion occurs when a combustible fuel, an oxidizer, and energy for ignition is present [8]. In landfills, combustion can take place as either flaming or smoldering [8], [9]. The first type of combustion is pretty straightforward, however, not all combustions are visible to the human eye. For example, both methanol and hydrogen produce colorless flames and their combustion does not produce smoke. Differently from open flame fires,

smoldering events are more difficult to detect, thus making extremely difficult to verify that a landfill is safe. Except for excavation, there are not many techniques that can be used to observe a smoldering event and even signs of a smoldering fire may be concealed by the environmental conditions of a landfill [9]. For example, a vent temperature of 249 °C was recorded in a landfill in San Francisco with no visible trace of smoke. Smoldering events usually outbreak on slopes, at changes in slope, region with poor interim cover, or areas in the proximity of the gas extraction system [6].

The primary byproducts of landfill processes in municipal solid waste (MSW) are heat, gas, and leachate. Biochemical processes and decomposition of organic components are responsible for the heat generation. The elevated temperatures that develop affect the mechanical and hydraulic properties of the wastes and the engineering properties of liners, covers, and soil. Decomposition of wastes increases with increasing temperatures. Mesophilic and thermophilic bacteria decompose waste grow in an environment with optimal temperature between 35 and 40 °C and 50 to 60 °C respectively [10], [4]. Optimal conditions for gas production are in the temperature range of 34 and 41 °C in laboratory studies [11], [12], whereas 40 to 45 °C was identified as the optimum range of for gas production at a landfill in England [13]. Seasonal air temperatures and landfill

temperatures were similar at shallow depths, while they reached their maximum at middle depths and between seasonal and maximum values near the base of the landfill. Increasing temperatures were recognized within days to few months after placement of waste in landfills. Maximum temperatures were observed for wastes placed from less than 1 year up to 8 to 10 years old [14]. Decreasing temperature trends were observed 10 years after placement. Increases in temperature of wastes are also correlated with placement temperature [14]. Short-term increasing temperature trends in wastes are due to aerobic decomposition which was directly correlated with the placement temperature of wastes [15].

The potential for a smoldering or fire event is dependent on the way the waste is covered, compacted and the way landfill operations are directed. In the past, control of the available oxygen, through compaction, use of adequate cover, waste profiling, and gas control partially lowered the risk of smoldering fires [6]. Details to consider while trying to lower exposure of waste to oxygen are: fissures maintenance, rapid settlement, access roads, poorly compacted or inadequate interim covers, uncapped borings, passive venting systems, and any defective environmental control.

One of the most prevalent causes of smoldering events is overdraw of a gas collection system. Biogas comprises methane (from 45 to 65% in volume) and

carbon dioxide (between 35 and 55%) [16] plus other minor components which are present in the putrescible materials of landfills. Significant thermal fluctuations are associated with average temperature values and patterns notably different from the surrounding regions with analogous characteristics in terms of soil, vegetation typology, and anthropic intervention. Methane and other gases exposed by landfill gas control vents can intensify the fire. The burning of some solid wastes can produce harmful volatile fuels that can pollute the air and cause respiratory problems. Also, the landfill gas control systems that vent the gas from the inside of the landfill can spark and cause debris on the surface to ignite. Other illegal debris that is dumped on top of the land can mix with other chemical substances and spontaneously combust. For instance, an oily rag that is dumped on top of a landfill can be a source of ignition [16].

On the other hand, subsurface events are characterized by fires that occur below the surface, and within the landfill itself at different depths. These types of fires are more dangerous than surface ones because the location and intensity of these fires can be difficult to assess from above the ground. If there is no way to detect them, the subsurface fires can burn for months and even years. Since the ignitions happening below ground can be smoldering for months before noticed, the extent of landfill damage cannot be properly determined. Landfill subsurface

fires can cause large portions of waste to be consumed, causing internal structural damage that may result in sections of the landfill to collapse while personnel are trying to contain the fire [17]. Subsurface landfill fires are often harder to dissipate and may cause damage to the liner and leachate collection system. Most subsurface events have no visible flame or burn slowly, making detection harder than surface landfill fires. There is no one way to directly detect an underground fire, however some fires can be confirmed by measuring the areas of settlement over a short period of time, monitoring the smoke or smoldering odor emanated, detecting a levels of CO in excess of 1,000 ppm, detecting an increase in gas temperature in the extraction system, above 140 °F, or well temperatures exceeding 170 °F. If any of the listed items are found to be present, the landfill personnel try to detect if there is a subsurface fire occurring [18]. These physical tests are inadequate because they can be used only when the fire has already caused damage to the landfill and surrounding environment. Moreover, there is not official procedure to be followed that takes into account the interactions between these different factors and physical quantities to be used as a way to predict and prevent fire outbreaks.

2.1.1 Landfill fire data inventory. Subsurface landfill fires can be extremely costly to contain and may cost from a million dollars upwards to repair the landfill and handle cleanup. Few studies have been conducted on landfill fires and their impact on the environment. Landfill regulations began in 1976 when congress passed the Resource Conservation and Recovery Act (RCRA). After the hazardous solid waste amendments of 1984, the EPA began expanding upon the amendments to create federal standards of landfill construction and maintenance. Safety has been the primary motivator for developing the new criteria for landfills. Therefore, landfill fires are an up-and- coming topic as new safety hazards are identified. Landfills are a controversial topic, due to perceived notions regarding noxious fume emissions, health and environmental effects and decreased property values in surrounding communities. The gas extraction system currently in use in landfills is designed to vacuum out landfill gases to limit environmental hazards as well as controlling odor emissions. The landfill gases typically consumed include: ammonia, sulfides, methane, and carbon dioxide. Two methods to disposing of the landfill gases are flaring and collection. Flaring the gas is a method that converts methane to carbon dioxide, making the gas less harmful to the environment. The more expensive method of gas disposal involves converting the methane into a cleaner gas that can be collected and used for energy [19].

Due to the unique design characteristics of a landfill, underground or subsurface fires are an ongoing and complex problem. Landfill fires threaten the environment through toxic pollutants emitted into the air, water and soil. A large landfill fire requires a prompt response of skilled personnel and a lengthy period before it is contained. The different dynamics, characteristics and regulations of landfills and the fires that occur in them suggest that firefighting tactics need to be determined on a case by case basis. Landfill operators, members of the fire service and community residents need to learn as much as possible from past experiences to prevent and mitigate future landfill fires. Data from the National Fire Incident Reporting System (NFIRS) was extrapolated to determine an average of 8,400 reported dump and landfill fires. Reported fires are responsible for about 10 civilian injuries, 30 firefighter injuries and between \$3 and \$8 million per year in property damage losses. From the NFIRS data, the top 5 types of fires occurring on landfill sites determined for the years 1996-1998 were: refuse (77%); trees, brush, grass (12%); outside structure, where material burning has value (6%); vehicle (4%); structure (1%). Surface fires occur on or close to the surface (1 to 4 feet depth). These fires occur in the aerobic decomposition layer and generally burn at lower temperatures. They emit dense white smoke and products of incomplete combustion including organic acids. Higher temperature surface fires are the result of the burning of rubber and plastic and can cause the breakdown of volatile

compounds and emit dense black smoke. Examples of surface fires include: dumping of undetected smoldering materials in the landfill, fires associated with landfill gas control or venting systems, fires cause by human error on the part of the landfill operators or users, fires cause by construction or maintenance work, spontaneous combustion of materials in the landfill, deliberate fires started by landfill personnel to reduce the volume of waste, deliberate arson fires, set with malicious intent. Underground fires occur deep within a landfill, and involve waste materials that are months or years old. Underground fires can cause portions of the landfill to collapse when void spaces are created from disintegrated waste. Underground fires are harder to extinguish than surface fires, and can smolder for months or years without detection.

2.2 Applications of Satellite Remote Sensing

Remote sensing is the science and engineering practice to gather information at a distance [3]. The collection of consistent data over large areas and long intervals of time makes it possible to understand and monitor the effects of both natural anthropological action onto the environment. Satellite remote sensing finds the majority of its application in geographic information systems (GIS), which comprise specialized software to analyze spatially referenced data. Remote

sensing also finds its application to plant, earth, and hydroscopic sciences and urban planning.

The National Oceanic and Atmospheric Administration's (NOAA's) is the institution responsible for the National Environmental Satellite, Data, and Information Service (NESDIS) and any Landsat operation. NESDIS operates the system of satellites in the United States and is responsible to process and distribute the tremendous amount of data obtained daily by the satellites [20]. Their satellite data is distributed to the both federal agencies and the private sector. Even though the primary use is still for weather forecast, satellite imagery has found an increasing popularity in remote sensing, fire management, urban growth, and agriculture [21]. In specific, remote sensing satellites have been used by many private and government-owned associations to gather information about forests, crops, land use, urbanization patterns, and water bodies. Aerial photography is still used, but does not have as many advantages as observation of large areas in a single image (synoptic view), systematic, repetitive coverage, and fine detail. There exist many satellite observation systems that have been evolving since 1960, when the first Earth observation satellite, the Television and Infrared Observation Satellite (TIROS), was launched. Even though meteorological satellites like TIROS have been used to study land resources, there are satellite systems comprising

polar orbiting and geostationary satellites that are specifically tailored to the investigation of land resources by way of passive sensing of radiation in the visible and infrared part of the light spectrum [3].

2.2.1 Geostationary satellites. Geostationary satellites circumnavigate the earth and their orbit follows the equatorial plane at the same speed of the earth rotation (geosynchronous orbit). They complete their orbit in 24 hours. This allows them to hover perpetually over one position on the surface. For this reason, the satellite seems to be stationary and is able to continuously float over one position on the surface.

The first Geostationary Operational Satellite (GOS) was launched in 1966 [22]. Nowadays, the United States is operating GOES-15 and GOES-13. While GOES-14 is being stored in orbit as a replacement for either GOES-15 or GOES-13, in the event of failure. Advantages for using GOS include being situated permanently in the same location of the sky relative to the earth, viewing the entire earth at all times, recording images at a speed of about 1 image per minute, modeling of clouds motion in the atmosphere, and acquisition of data from remote automatic data collection stations around the world. However, disadvantages for the use of GOS include less quality resolution compared to polar orbiting satellites due to their orbit which is much higher. In fact, the orbit of GOS can reach about

35,790 km (22,236 miles) and it is geosynchronous. Having a geosynchronous orbit means

Compared to the first GOS launched in the 1960s, the current satellites are stabilized so that they always face the earth, whereas older satellites maintained motion stability by rotating on themselves and therefore facing the earth only about 10% of the time [22]. GOS contribute with the kind of continuous monitoring indispensable for intensive data analysis.

2.2.2 Polar orbiting satellites. Polar orbiting satellites (POS) are used complementary to geostationary employing polar orbiting satellites and have many advantages. In particular, their data resolution is higher because their altitudes rarely surpass 850 km, which is much lower compared to geostationary satellites. Their orbital period varies between 98 to 102 minutes, which translates into the satellite completing about 14 orbits daily. The scan swath measures about 3000km in width [23]. Moreover, polar orbiting satellites provide a successive orbit overlay with each other, that it, a global coverage necessary for numerical weather prediction (NWP) models used in climatology. The orbit of POS is geocentric and its altitude and inclination are combined so that a POS passes over any location on the earth surface at the same time. Despite the name, POS almost pass over the poles due to their orbit directed to the northwest. This generates a precession in

the orbit so that it passes over locations further west on subsequent orbits. Due to their features, POS cannot provide continuous viewing of one location. One of the main missions of POS is to supply daily global observations of environmental conditions in the form of quantitative data usable for numerical weather prediction.

2.2.3 Landsat imagery. Almost a decade after the project was first conceived, NASA started the Landsat program in 1972 when the first satellite in the series was launched in orbit. The Landsat program is a joint effort of the U.S. Geological survey (USGS) and the national aeronautics and space administration (NASA). It constitutes the longest-running enterprise for continuous acquisition of space borne remote sensing data of earth surface [24]. Satellite images for this research were acquired from the Landsat 5 thematic mapper (TM). Thematic mapper satellites are among the most used satellites to obtain data for environmental studies [25]. The picture obtained from these satellites is composed of seven bands, six of them in the visible and near infrared while only one is located in the thermal infrared region. Atmospheric correction has to be taken into account to remove the atmospheric influences added to the pure signal of the target [26]. Previous research that used Landsat satellite images for landfill monitoring did not take into account atmospheric correction [27], [28]. The use of

atmospheric correction in this thesis allows the collection of optimal results of the LST. Landfill surface temperatures is significant to a range of issues and themes in fire prevention and landfill maintenance and is important for planning and management practices.

2.2.4 Visible, near and thermal infrared sensing. There are several ways to 'sense' the surroundings, which use different types of electromagnetic radiation. The entire depth of the earth atmosphere is the medium through which all the radiation used for remote sensing passes through. When solar energy goes through the atmosphere and then bounces back after hitting the earth surface it is modified by the physical processes of scattering absorption and refraction [3].

The human eye can detect visible radiation from the sun, which is reflected off the objects in the surroundings. That is, the eye can detect light ranging between 390 – 700 nm. Darker objects absorb more radiation than brighter objects. Visible remote sensing apparatus can detect brighter object more easily compared to the dark ones because of albedo [29]. Albedo is a unitless quantity from 0 to 1 used to assess how much solar energy a surface is able to reflect [29]. Intuitively, darker objects have lower albedo while 'whiter' objects have higher albedo. Ideally, an albedo value of 1 indicates that the surface is a 'perfect reflector', while a value of 0 indicates that the surface is a perfect absorber and none of the

incoming energy is reflected. There are some limitations when applying visible remote sensing: first of all, data collection is limited to only daytime because the sensors measure solar radiation. Therefore, data collection during nighttime is not possible and regions of the earth such as sea ice, which is prevalent in Polar Regions remain unmeasurable. Moreover, there are non-negligible atmospheric effects that impact the quality of the images collected by the visible sensors. In particular, clouds reflect visible radiation, and a cloudy sky blocks visible light from being reflected from the earth surface and being detected by the satellites. In the United States, the satellites and sensors used to process visible radiation are: the operational linescan system (OSL), maintained by the Defense Meteorological Satellite Program (DMSP), the advanced very high resolution radiometer (AVHRR) from the National Oceanic and Atmospheric Administration (NOAA), and the Moderate Resolution Imaging Spectroradiometer (MODIS) from the National Aeronautics and Space Administration (NASA).

Near infrared sensing uses radiations from $0.72\ \mu\text{m}$ to $1.30\ \mu\text{m}$ of the light spectrum which is beyond the visible regions of wavelengths. Radiation with shorter wavelengths, which are near the visible, act in manners similar to radiation in the visible spectrum. For this reason, the apparatus used for visible light can also be used with minimal variation to near infrared radiation. This region of

shorter wavelengths is called 'reflective infrared spectrum' but it is more commonly known as near infrared [3].

Remote sensing of the mid- and far infrared is based upon the section of the infrared spectrum that goes from 1.30 μm to 12 μm . The line between mid- and far infrared is drawn somewhere between 4.5 μm and 8 μm but it cannot be clearly defined since some regions of the spectrum are not contiguous because they are unavailable for detection due to atmospheric effects. The mid- and far infrared regions present different kinds of information from the visible and near IR. Thermal scanners are the type of devices employed for MIR and FIR remote sensing which are able to detect geothermal energy and emitted terrestrial radiation respectively. MIR and FIR also interact with the atmosphere in a different way from shorter wavelengths. FIR is virtually free from scattering, however, absorption phenomena start becoming a problem for specific atmospheric windows.

2.2.5 Normalized Difference Vegetation Index (NDVI). Remote sensing is a powerful tool to determine the identity and characteristics of different types of vegetation. This is because different types of vegetation possess characteristic absorption in the red and blue part of the visible spectrum. Noticeably, vegetation has higher green reflectance, especially in the near infra-red (NIR) [30]. Other

typical features recognizable with remote sensing are leaf shape and size, overall plant shape, water content, soil type, vegetation density, and crops. Crops can be monitored in terms of stage growth, predicted productivity and health. Crops are a good example of the value of multitemporal analysis since crop type estimates of output can be achieved by taking several looks at the same field [30]. Leaves are partially transparent which means that part of the solar radiation passes through and reaches the ground, which reflect its own radiometric signature.

Vegetation radiometric signature depends on the nature of the vegetation itself, its interaction with solar radiation, presence of nutrients, and water in the host medium such as wet soil, and humid air. Many remote sensing devices operate in the red, green and NIR regions. Therefore they can discern radiation absorption and vegetation reflectance signals. The NDVI index of a particular portion of land can be analyzed spatially and temporally through the study of remote sensing imagery. Landsat 5 TM was proved to be an efficient tool for this purpose because of its accessibility to archived data, durability, spatial and temporal resolution, and multispectral sensors.

2.2.6 Land Surface Temperature (LST). There are internal activities in the landfill that cause a change in internal temperature which is not typically a visible sign. However, internal activities can lead to change in surface temperature caused by heat transfer from the interior to the surface that can be detected by thermal infrared sensors. Once these activities begin, the land surface temperature increases but it usually remains unnoticed for long periods of time until the fire ignites, which is too late for interventions.

Land surface temperature (LST) is defined as the radiative skin of the ground and it is a critical constituent of the surface radiation budget because it regulates the upward thermal radiation the same way as surface emissivity. Albedo, vegetation cover and the soil moisture are all factors affecting the value of LST. Intuitively, LST values are mostly given by a combination of vegetation and bare soil temperatures. LSTs exhibit great variation within the same geographical region due to rapid changes of incoming radiation from cloud cover, difference between diurnal and nocturnal sun illumination, and aerosol load modification. LST is responsible for energy partition amid sensible and latent heat fluxes between ground and vegetation and between the surface and the air temperature above the ground [31]- [32]. LST is an essential tool for different applications as: evaluation of forecast models for weather prediction (numerical weather prediction, NWP), and environmental monitoring [33], [34], [35], [36]. If LST

fluctuations could be monitored, risk of ignition will be lowered and measures could be taken to remove any gas build up and stop combustion reactions, thus preventing fires that tend to be very costly to the landfill owners, town, neighbors and the entire community.

Chapter 3

Data Acquisition and Case Studies

This Chapter contains a description of the data collection process for the imagery used to test the fire detection software and landfill fire index, it also contains descriptions of the three landfills used as cases studies. The selection process with which the landfills were chosen was based upon engineering report data availability. Whereas satellite data are readily available for most, if not all the territories belonging to the United States, the same cannot be said for technical reports that may need special permissions to be accessed to. Technical reports are needed to prove the efficacy of the hotspot detection method described in Chapter 4 and to assess the risk of fire with the Landfill Fire Index described in Chapter 5.

3.1 Data Collection and Processing

The summary of the entire image processing method and applications is represented by the flow chart in Figure 1. For the sake of this analysis, a directory of images for two case studies in the United States was collected and used as input to the fire detection software. Satellite images from the online U.S. Geological Survey (USGS) [1] database were collected from all years available between 2000 and 2011 for two out of three case studies: Atlantic Waste Landfill (AWL), and Bridgeton Landfill (BL). Burlington County Landfill (BCL) is a third case study

which was used to test the Landfill Fire Index described in Chapter 5 but was not used to obtain results from the fire detection software. The photographs downloaded from the Earth Explorer portal are Level 1 GeoTIFF format which include all seven bands from the visible and thermal infrared region. Notably, all the following data were acquired by the Landsat 5 and 7 which benefit from Enhanced Thematic Mapper Plus (ETM+) sensor.

Satellite mapping sensors such as the ETM+ obtain the images; each image is composed of pixels which store information as a digital number (DN) which can have values ranging from 0 to 255. "DN" is a commonly used term for pixel values. Pixel values which have not yet been calibrated into meaningful data usually fall in this category. Depending on their application, sometimes it is fine to keep DNs as they are without further processing. Other times it is more desirable to interpret the pixel values in terms of quantitative and physically meaningful data like radiance, as in this study [37].

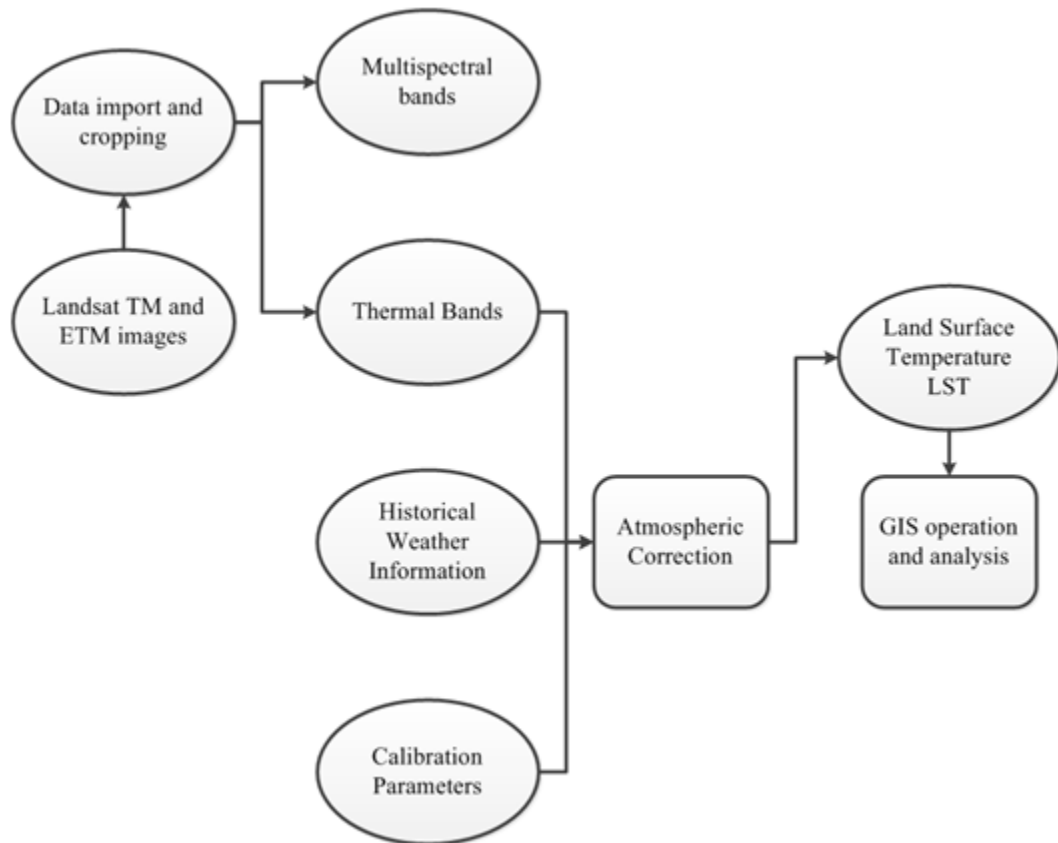


Figure 1. Visual representation of the method workflow

Due to the albedo effect and other physical phenomena, the raw database images cannot be used to directly determine the ground temperature. The scattering of radiation in the atmosphere cause degradation of the images. Another source of bias in satellite images are clouds and cloud-shadows, which cause interference. Detecting and correcting the presence of clouds over a region is important to isolate cloud-free pixels, which are used to retrieve surface properties. Atmospheric effects such as absorption, upward emission, and

downward irradiance reflected from the atmosphere [38], must be corrected before land surface temperatures are obtained. These effects give the images a hazy appearance, thus requiring atmospheric correction to be performed. To deal with this problem, the original database was calibrated to eliminate these effects and obtain more reliable images. The calibration method is described in Chapter 4 and requires the application of Equation 1 (Chapter 4) to all the DNs present in each image. At-surface radiance from cell values was calculated. This last value is then converted to the land surface temperature (LST) in Kelvin. The equations and method used to process the entire database and thus retrieve the LST of each pixel are fully covered in Chapter 4 under the Methodology section.

Surface skin temperature, or LST is defined as the equivalent blackbody temperature of a solid and/or liquid surface that radiates directly to space through the atmosphere [39]. The pre-image processing procedure mentioned in the paragraphs above was conducted by using the software ENVI Classic. Afterwards, the satellite images were cropped to ensure that the landfill was positioned exactly in the center. After atmospheric correction and cropping was performed, the pre-image processing procedure was terminated and the database was ready to be fed into the in-house "LST detection" Matlab program specifically developed for this study. This code processed all the images and turned them into thermal maps.

3.1.1 Landsat imagery/instrument. Landsat Thematic Mapper (TM) is a highly advanced, multispectral, programmable sensor which is present in the satellites series on Landsat 4 and Landsat 5. Thanks to this apparatus the resolution of the images is greatly enhanced. The TM sensor has a swath of 187 km and can cover a portion of land with dimensions of 185 km x 172 km. It also has a spectral range of 0.45 – 12.5 μm . The spectral range of the six bands captured by the tm are listed in Table 1. Spectral range is the part of the electromagnetic spectrum in the form of wavelengths [40] that each band is made of and that is remotely sensed by the TM. Other desirable image properties that are obtained with the tm are sharper spectral separation, improved geometric fidelity and greater radiometric accuracy [41] when compared to images obtained from Landsat 1-3 which uses the Multispectral Scanner System (MSS) technology [42].

Table 1

Resolution and spectral range of the different spectral bands of Landsat TM

Band Number	μm	Resolution
1	0.45-0.52	30 m
2	0.52-0.60	30 m
3	0.63-0.69	30 m
4	0.76-0.90	30 m
5	1.55-1.75	30 m
6	10.41-12.5	120 m
7	2.08-2.35	30 m

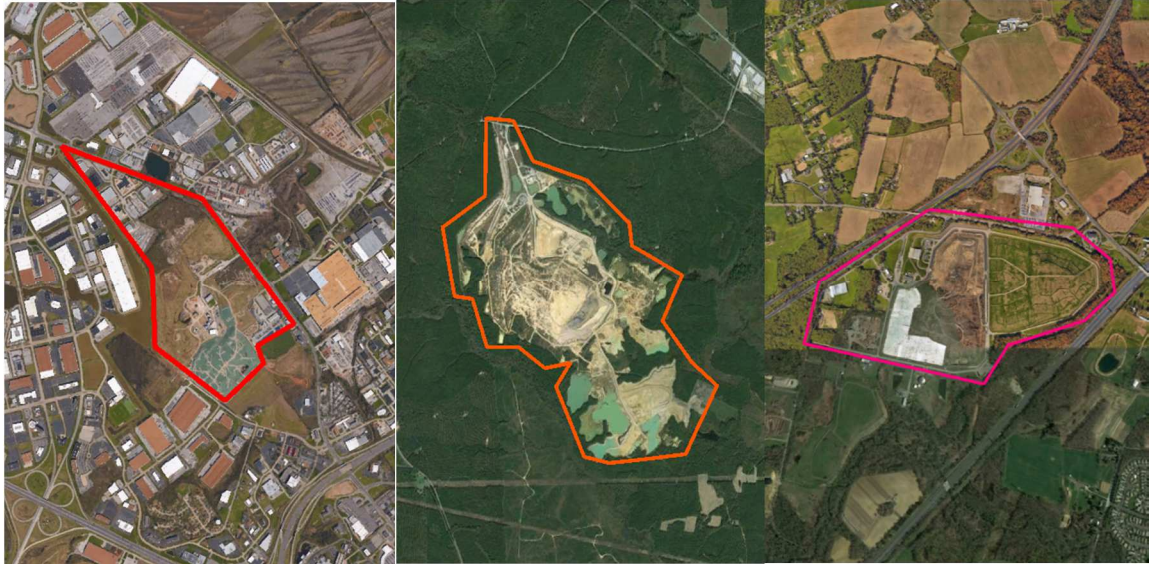
Spectral separation is the process of accurately differentiating the spectral bands comprising each image [43]. A sensor with a sharp spectral separation is able to accurately detect the different bands of the electromagnetic spectrum of all the radiation that hits it. Geometric fidelity refers to the ability to reproduce the geometry of the objects captured in remotely sensed data. Radiometric accuracy simply refers to the ability of the sensor to collect data with the least possible amount of instrumental noise and other type of random errors.

Data captured by the TM are stored simultaneously in seven different spectral bands of which only Band 6 senses thermal infrared radiation. The instantaneous field of view (IFOV) is the measure of the spatial resolution of a remote sensing imaging system [44]. In particular, TM is an opto-mechanical sensor possessing an IFOV of 30m x 30m in bands 1 through 5 and 7, whereas the thermal band 6 has an IFOV of 120 m x 120m on the ground. Even though the spatial resolution of the thermal band is 102 m, the thermal scene is resampled to 30-meter pixels.

3.2 Study area

The territory shown in Figure 2a [45] is the aerial photograph of the Bridgeton Landfill case study at a latitude 38.7687 and longitude -90.4451. The aerial image of the Atlantic Waste Landfill case study at a latitude of 37.0589, and

longitude -77.1757 is shown in Figure 2b [46]. Burlington County Landfill at a latitude of 40.075504 and longitude -74.765362 is in Figure 2c [47]. However, none of the representations contain any information about the temperature of the particular areas captured in the picture and are only meant to illustrate the study area before performing the image processing method.



a)

b)

c)

Figure 2. Topography of Bridgeton Landfill [45], Missouri a), Atlantic Waste Landfill [46], Virginia b), and Burlington County Landfill [47], Florence, New Jersey c) from Google

3.2.1 Bridgeton Landfill (BL). The Bridgeton landfill (BL) complex, in Bridgeton, Missouri, operated in an old limestone quarry complex dating back to 1930. The total area of the complex is 214 acres and includes several subdivisions. There is the North Quarry, the South Quarry, and the so-called OU-1 radiological area. The South Quarry and the North Quarry are separated by a narrow gorge which is referred to as “the neck”. The area covered by both quarries is approximately 52 acres, of which 32 acres are occupied by the south quarry alone. The North Quarry covers the remaining 20 acres [48]. The landfill received municipal solid waste (MSW) from 1979 to 2004. At the end of this period the total waste thickness was reported to be approximately 320 feet, of which 240 feet is below ground level and 80 feet above ground. The landfill received approximately 17 million in-place cubic yards of waste. The MSW landfilled at Bridgeton consists mainly of residential and commercial curbside waste, other materials include demolition waste, automobile tires, and gypsum wallboard [49]. Starting in the early 1950s the quarried areas were used as a site for the disposal of municipal refuse, industrial solid waste, and construction/demolition debris. In 1973, 8,700 tons of radioactive waste from the Manhattan project in the form of barium sulfate was combined with 38,000 tons of soil and disposed in a part of the landfill that was later renamed “west lake landfill” [48]. In 1990, EPA conjointly listed the radiological and the municipal solid waste on the national priority list under the

superfund law of the Comprehensive Environmental, Response, Compensation and Liability act (CERCLA, 1980).

Several fire events have been reported in BL, in which elevated temperatures were registered or subsurface smoldering events (SSE), and subsurface fires (SF) took place. Specifically, fire in the North Quarry was identified in 1992 and permanently extinguished only in 1994. A subsurface elevated temperature event was confirmed in 2010 in the South Quarry and also a subsurface oxidation event was observed on April 3rd 2012 [50]. On February 16th, 2014 a break in a high pressure pneumatic air line that drove a leachate well pump caused a surface fire on the Southeast side of the landfill [50]. Even recently, BL is known to have an ongoing subsurface smoldering event that forced EPA to conduct additional Radiological and Infrared thermal surveys [6]. Given its long history of combustion events, this landfill is an appropriate place to test the proposed fire identification method.

3.2.2 Atlantic Waste Landfill (AWL). The Atlantic Waste Landfill, previously known as Sussex County Landfill, is located in Waverly, Virginia. It is currently operated by a subsidiary of waste management. It is a MSW landfill that has received municipal solid wastes, industrial wastes, refuse, institutional wastes,

commercial wastes, garbage, compost, debris, sledges, demolition wastes, and scrap metal wastes.

AWL is still active and receives waste by rail and road. Since it is an active site, not much information is released to the public. Only recently the landfill started to gain public attention due to complaints by the residents of Waverly about continuous odors from the landfill that became too strong to be attributed simply to uncomplete decomposition of organic material. Finally, state regulators issued notices of violation to the landfill following those complaints. The violations involved leachate flowing outside the disposal area into forested wetlands, and several sinkholes on top of the landfill [51]. Even though a surface fire outbreak has not been officially recorded, it is safe to assume that the unstable conditions of this landfill have provoked thermal fluctuations internally and thus generate a detectable change in land surface temperature. This landfill provides an opportunity to demonstrate how the image processing method described in this thesis can be used to provide early identification of fire location, leading to fire prevention.

3.2.3 Burlington County Landfill (BCL). The Burlington County Resource Recovery Complex, in Florence, New Jersey, is operated by the department of solid waste of Burlington county. This landfill serves all forty

municipalities of the county and collects municipal solid waste, recycling, and household hazardous waste. The total area of the complex is 552 acres. The site was selected in 1981 but landfill operations did not start until 1989, and it is currently active. Landfill operations are predicted to stop in 2027 when the complex is anticipated to complete the disposal needs of the county [52].

The BCL maximum working face width does not exceed 150 feet and the maximum working face slope equals 3:1 (horizontal to vertical). The waste is usually compacted in 2-foot layers whereas the lift height of a daily cell with cover soil does not exceed 12 feet. In total, the exposed waste does not surpass 15,000 square feet [53]. There were no fire events reported for this landfill but nonetheless the Landfill Risk Index developed in Chapter 5 was applied to it in order to assess how a healthy landfill compares to other cases where subsurface and surface events already took place.

Chapter 4

Landfill Elevated Internal Temperature Detection

This chapter focuses on the results obtained from the application of the in-house “LST detection” Matlab program to the satellite images database. It also presents a thorough description of the method used to perform the image processing procedure. Several thermal maps were obtained for the two case studies of Bridgeton Landfill (BL) and Atlantic Waste Landfill (AWL). Successively, weather data related to the location and time of the satellite image acquisition was obtained to be compared to the LST values for both BL and AWL case study. The next step was to detect and delineate consistent hotspots via time series analysis. Multitemporal maps indicating the maximum LST values were further analyzed to obtain a composition of superimposed maps to analyze the frequency of appearance of the hotspots.

4.1 Methodology

The equations described in this chapter refer back to some of the concepts analyzed in the literature review of Chapter 2. For the sake of clarity it was found more useful to write about the following topics in more details in this Chapter whereas only a brief description was offered in Chapter 2.

4.1.1 Landsat Calibration. Imagery calibration is a common pre-processing step for remote sensing analysis where data need to be extracted and reliable scientific results need to be obtained. The purpose of Landsat imagery calibration is to compensate for unpredictable variations in satellite scan angle, radiometric errors due to sensor defects, and system noise. After all these disturbances are taken into account, the resulting image represents true spectral radiance at the sensor. In fact, calculation of at-sensor radiance is the fundamental step in converting image data from multiple sensors into radiometric scales.

4.1.2 Spectral Radiance Scaling Method. After downloading a decade worth of data for both case studies, the two imagery datasets were manually pre-processed via Landsat calibration by using the spectral radiance scaling method [54], [55]. Specifically, the period of time analyzed for Atlantic Waste Landfill covers the years from 2000 to 2010, whereas for Bridgeton Landfill the years covered are from 2001 to 2011. The pre-processing method was conducted with the software ENVI classic (Harris geospatial solutions: www.harrigeospatial.com).

Landsat data are typically delivered as pictures where each pixel is a single byte, possessing a value from 0-255. During the radiometric calibration pixel values from raw, unprocessed data are converted to units of absolute spectral radiance. The two dataset downloaded from USGS Explorer are in GEOTIFF

format. Data were imported into the ENVI software as *Landsat GeoTIFF with Metadata*, in preparation for the calibration step [54]. The temperature data are obtained from the radiation originating from the sun that has bounced back from the earth surface. This information can be recorded by the Thermal Infrared (TIR) sensors present on the satellites and stored as digital numbers (DNs). The equation used to convert DN to radiance values in $W \cdot sr^{-1} \cdot m^{-3}$ [55] is

$$L_{\lambda} = [(L_{\max} - L_{\min}) / (Q_{\text{cal max}} - Q_{\text{cal min}})] * (DN - Q_{\text{cal max}}) + L_{\min}$$

Equation 1

Where DN equals the quantized unitless calibrated pixel value; L_{\min} is the spectral radiance in $W \cdot sr^{-1} \cdot m^{-3}$ that is scaled to $Q_{\text{cal min}}$; L_{\max} is the spectral radiance in $W \cdot sr^{-1} \cdot m^{-3}$ that is scaled to $Q_{\text{cal max}}$; $Q_{\text{cal max}}$ is the maximum quantized unitless calibrated pixel value in DN; and $Q_{\text{cal min}}$ is the minimum quantized unitless calibrated pixel value in DN. The application of this equation results in the removal of errors directly related to the satellite sensor system.

4.1.3 Atmospheric correction: simple dark object subtraction method.

Atmospheric correction is performed following the dark object subtraction (DOS) technique. Several factors are considered when estimating the land surface temperature from satellite observations. This includes the effect of the atmosphere, vegetation, and the land surface emissivity. Atmospheric effects are mostly due to the absorption of infrared radiation by water vapor. This is calculated by the simple dark object subtraction method, which can be seen in equation 2 in the following section [54]. The dos model assumes that within each satellite image are recorded surfaces with negligibly small surface reflectance where the observed top of the atmosphere reflectance (TOA) is explained solely by the atmospheric contribution.

4.1.4 Sun radiation pattern geometry and albedo effect on earth surface.

A graphical representation of the sun radiation geometry pattern can be found in Figure 3. The mathematical representation of the simple dark object subtraction method is in Equation 2.

$$Q = (\pi (L_{\text{sat}} - L_p) d^2) / (E * \cos(x) * T) \quad \text{Equation 1}$$

Where ρ is the TOA reflectance, L_{sat} is the sensor radiance, T is atmospheric transmissivity, θ is the zenithal solar angle, d is the distance from the earth to the sun, and L_p is radiance. This atmospheric correction processes every pixel in the images to obtain TOA reflectance value [55].

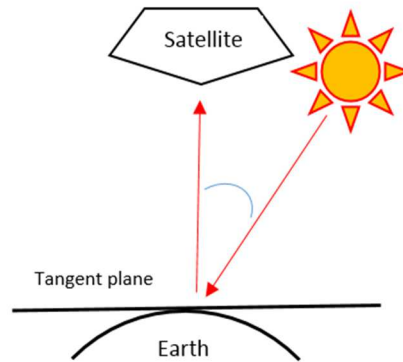


Figure 3. Sun radiation pattern geometry

For accurate land surface temperature estimations it is critical to know the land surface emissivity in the infrared. The implemented approach uses the links between the land surface emissivity and the state of the vegetation cover expressed in the form of the Normalized Difference Vegetation Index (NDVI). Vegetation can falsify land surface temperature calculations. This is because plants perform

photosynthesis: leaves and needles absorb solar radiation while also being very reflective, which is the case for healthy plants. The equation for vegetation corrections can be seen below in Equation 3.

$$\text{NDVI} = (\text{TM}_4 - \text{TM}_3) / (\text{TM}_4 + \text{TM}_3) \quad \text{Equation 2}$$

Where TM_3 is the value of the band 3 (in the visible light spectrum) from the reflected radiation detected by Landsat satellites, and TM_4 is the value of the band 4 (in the infrared region) [56], [56]. The last correction to take into account is for albedo effects. Albedo is the property of the land surface characterizing its potential to reflect shortwave solar radiation (Figure 4). The albedo correction for satellites is calculated by multiplying the reflectance of all points of an image by the energy fraction. When light interacts with objects, there is absorption, reflection and transmission. On average 30% of light striking the Earth is reflected back. This is known as albedo. Albedo is the ratio of the outgoing reflected flux to the incoming flux. Flux is the energy that passes through a physically defined

surface that may not be aligned in the direction of propagation. When that happens the incoming energy, or radiation is reflected or refracted. An object that has a high albedo (near 1) is very bright; an object that has a low albedo (near 0) is dark.

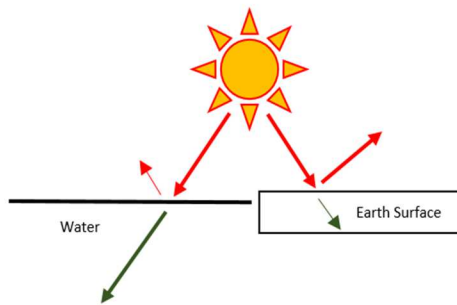


Figure 4. Albedo effect on earth surface

The albedo effect is eliminated from the temperature calculations to obtain the actual surface land temperature. Reflectivity data and the top of the atmosphere (TOA) given by the satellite do not account for the albedo effect from the atmosphere, so one has to estimate the albedo integrated across all wavelengths and directions. The reflectivity expected is expressed as the reflection coefficient

$$R = I_{\text{reflected}} / I_{\text{surface}}$$

Equation 3

Where I_{surface} is the solar radiation that has passed through the atmosphere and $I_{\text{reflected}}$ is the solar radiation reflected from the surface.

$$\text{Albedo} = \Sigma(R \cdot R_f)$$

Equation 4

Where R is the reflectivity obtained from Equation 4 and R_f is the energy fraction between incoming and reflected radiation. Emissivity and albedo are subtracted from the Landsat image values to estimate the land surface temperature. These two parameters are needed to calculate accurate Land Surface Temperatures.

4.1.5 Comparison of at-sensor radiance to at-satellite temperatures.

Once DNS are converted to spectral radiance and external factors are corrected for surface temperature can be calculated. The values retrieved are also called

effective at-satellite temperatures. The thermal band data (Band 6) can be converted from at sensor spectral radiance to effective at sensor temperature. Here we assume that earth's surface is a black body and consider emissivity as one. The conversion formula from the at sensor's spectral radiance to at sensor brightness temperature is

$$T_b = K_2 / [\ln (K_1/L_\lambda) + 1]^2 \quad \text{Equation 5}$$

Where T_b is the effective at sensor brightness temperature in Kelvin, K_2 is calibration constant 2, K_1 is calibration constant 1, and L_λ corresponds to the spectral radiance at the sensors aperture calculated with Equation 1. The constants K_1 and K_2 vary depending on the satellite used. The values for constant K_1 and K_2 were obtained from the NASA satellites Landsat 4 (TM), Landsat 5 (TM), and Landsat 7 (ETM+) and are showed in Table 2 [55].

Table 2

Constant Values for Equation 7

Constant	K1	K2
Units	W/(sq. m μ m)	Kelvin
L4 TM	671.62	1284.3
L5 TM	607.76	1260.56
L7 ETM	666.09	1282.71

4.1.6 Calculation of Land Surface Temperature (LST). Finally, the LST

can be calculated as shown in Equation 7 below

$$S_t = T_b / (1 + ((\lambda * T_b) / d) \times \ln e) \quad \text{Equation 6}$$

Where T_b is the reference black body temperature, λ is the wavelength of emitted radiance, d is the product of the Planck's constant ($6.26 \times 10^{-34} J \times s$) with the velocity of light ($3 \times 10^8 m/s$), divided by the Boltzmann constant ($1.38064852 \times 10^{-23} J/K$ and e is the land surface emissivity [57]. At this point the initial satellite data is completely converted into a color coded thermal map. The following results

demonstrate the applicability and advantages of the above-mentioned process as a tool for early landfill fire identification. Thermal infrared observations are made exclusively from satellites, which provide more than enough data to deduce where the landfill fire will occur.

4.2 Results

The USGS Earth Explorer (EE) tool provides the ability to query, search, and order satellite images, aerial photographs, and cartographic products from several sources. An example of the Landsat images for Atlantic Waste Landfill (AWL) can be found in Figure 5 and Figure 6. The landfill is the white area located in the center of the pictures. In particular, Figure 5 shows what the original raw images looked like, whereas Figure 6 shows the effect of calibration and atmospheric correction. In the output resulting from this initial processing the cloud cover and shadows have been removed and an overall improved picture is obtained. The outline of the landfill is visualized clearly in Figure 6, (g); however, it is still not possible to have a visual representation of the hotspots present on the landfill or any other temperature data.

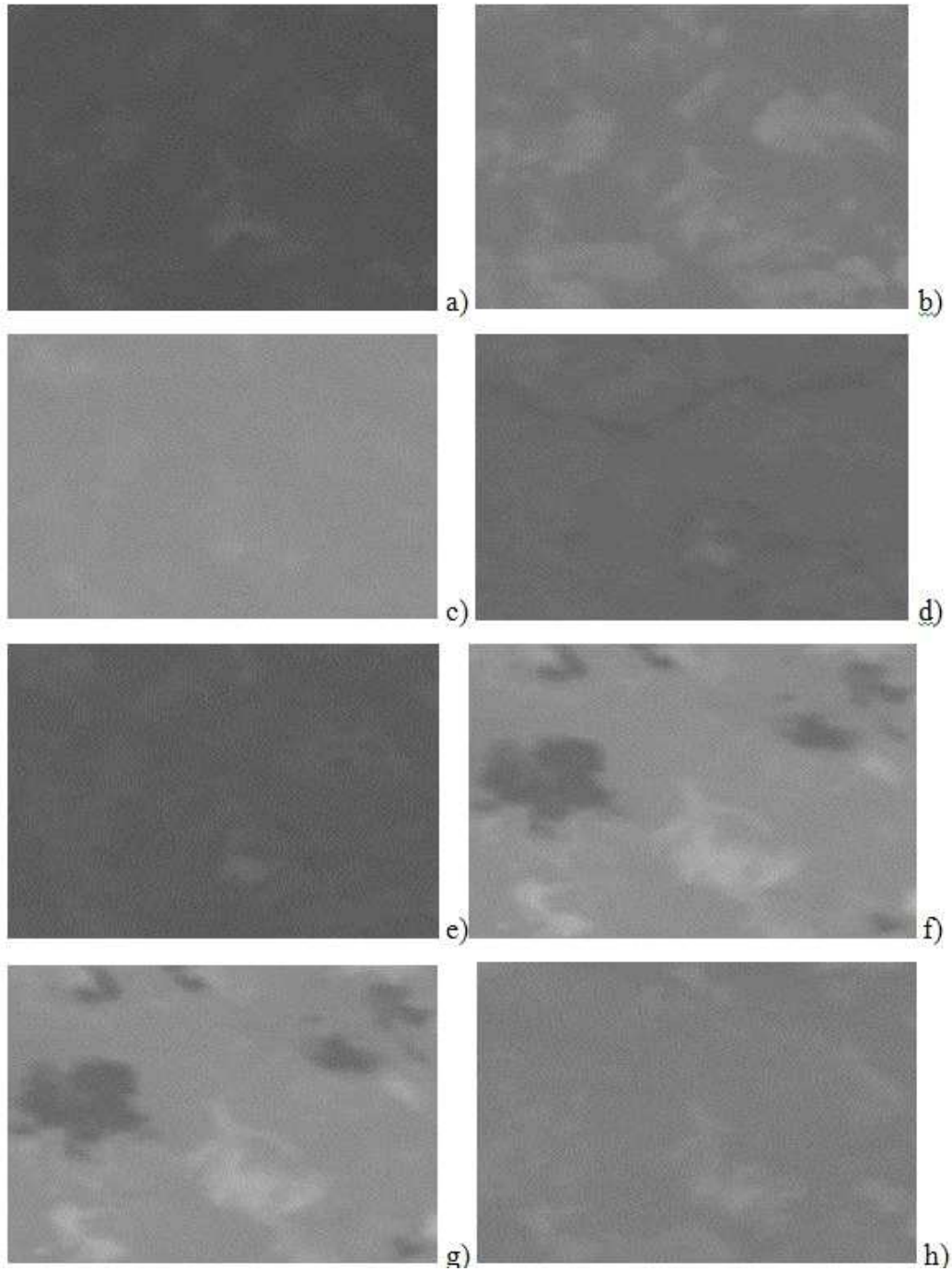


Figure 5. Non-calibrated images of Atlantic Waste Landfill January 23rd 2004 (a); April 28th 2004 (b); August 21st 2005 (c); January 26th 2006 (d); February 13th 2008 (e); May 25th 2008 (f); June 29th 2009 (g); October 9th 2011 (h).

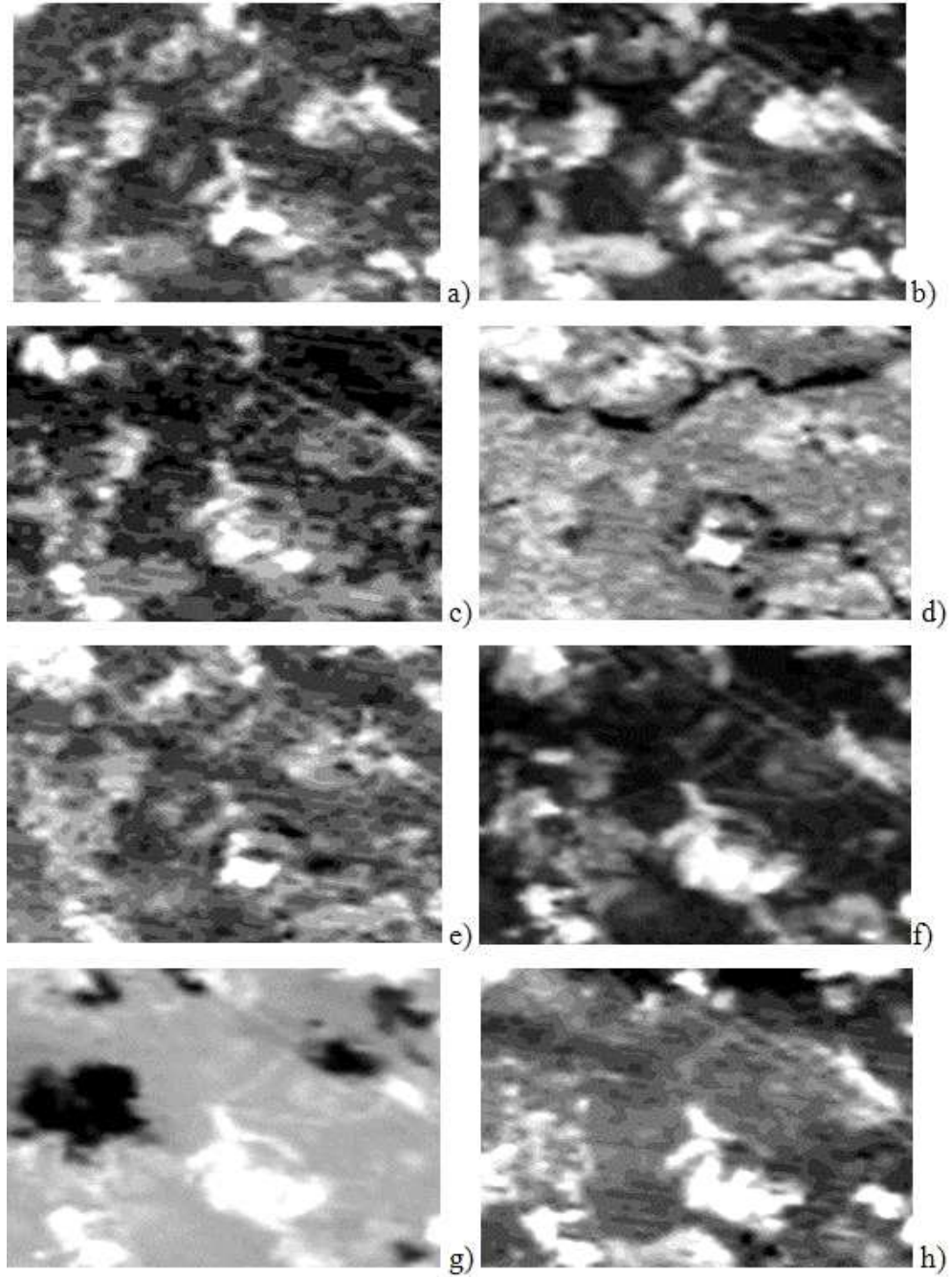


Figure 6. Landsat 8 images of Atlantic Waste Landfill after performing atmospheric correction. January 23rd 2004 (a); April 28th 2004 (b); August 21st 2005 (c); January 26th 2006 (d); February 13th 2008 (e); May 25th 2008 (f); June 29th 2009 (g); October 9th 2011 (h).

4.2.1 Comparison of LST and air temperature in two study areas. After the calibration and atmospheric correction is accomplished, data are in a suitable format for thermal mapping calculations. The rest of the image process, including hot spot identification was performed with the in-house developed “LST detection” Matlab program. The final results for the thermal mapping process of AWL in Virginia are shown in Figures 7, 9, 10, 11, and 14. As shown in Figures 7-15, it was possible to obtain a great variety of information regarding the status of both BL and AWL throughout a decade of data. Both values for maximum LST and average LST were obtained directly from the digital processing of the infrared band of the satellite data.

Figure 7 is a plot of the LST derived from the satellite images with the equivalent air temperature values for AWL. The comparison is made on a day-by-day basis with the LST values registered during the same date by the satellites within the same hour from the recording time. For each day that the data was acquired, two values are shown: the average LST of the landfill, and the temperature of the air above the landfill at that time. The average LST of the hotspots is indicated by yellow triangles while the air temperature collected at approximately the same time by the closest airport in Virginia is represented by green dots.

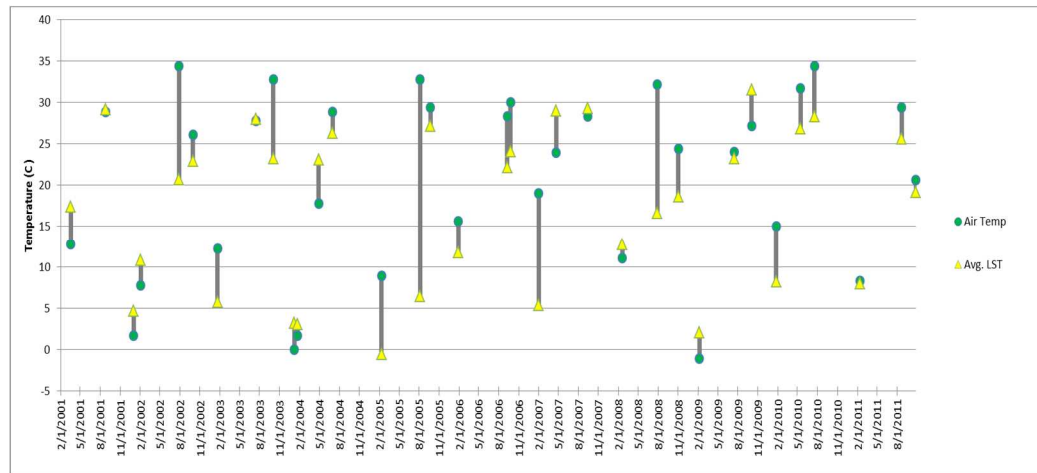


Figure 7. Day-by-day comparison of Avg. LST and Air Temperature for AWL, Virginia

The temperature difference between LST and air temperature varies from 1°C to 26°C. During winter months the temperature difference is at minimum. The cause of this phenomenon is related to the slowdown of the waste decomposition process during winter months due to the cold weather. Low temperature differences are mainly due to relatively low sky visibility and haze effects on the remote sensing images even after atmospheric correction is performed. Regardless, it is possible to notice a general trend for the LST values

for AWL, in fact, the air temperature is constantly higher than the LST throughout 8 years' worth of data. AWL is a site that has not been in the public eye until 2014, when residents of the Sussex County (Waverly, Virginia) started filing complaints about strong odors originating from AWL that were attributed to internal combustion reactions in the landfill [58]. Before that, it is likely that the landfill did not show LST values higher than air temperature but it still exhibited hotspots of higher temperature compared to the surroundings as it is shown in the figures in the next section. The interval of time considered in the analysis of images is the decade between 2000 and 2010. During this period of time it is likely that the subsurface reactions did not develop enough to cause the residents in Waverly to notice strong odors coming from AWL, but it still affected the LST of AWL periodically. This is the most probable cause of the variability observed in the graph where it is possible to notice few LST data points being higher than the air temperature even during winter months.

The opposite trend is noticeable in the result obtained from BL, in Missouri. Figure 8 shows a day-by-day comparison of the air temperature in Bridgeton, Missouri, with the LST values registered during the same date by the satellites within the same hour from the recording time. The crucial detail in this graph is the general trend of the LST constantly being higher than the air temperature. This

is only possible if the heat is moving to the surface from subsurface locations rather than via convection from the surrounding air.

Even though there is a minimal effect of the air temperature through convective heat transfer, its influence on the LST is minimal and does not interfere with the radiative, contact heat transfer from the heat developed by internal or surface activities of the landfills. Subsurface combustion can then be the only viable causes of the registered hotspots. The remaining days were characterized by air temperatures higher than LST. This can be due to seasonal temperature fluctuations and did not affect the LST since the convective heat transfer was not enough for it to impact the soil temperature. With the extrapolation of LST data from satellite images it was thus possible to derive exactly the temperature trends leading to the recent subsurface smoldering event.

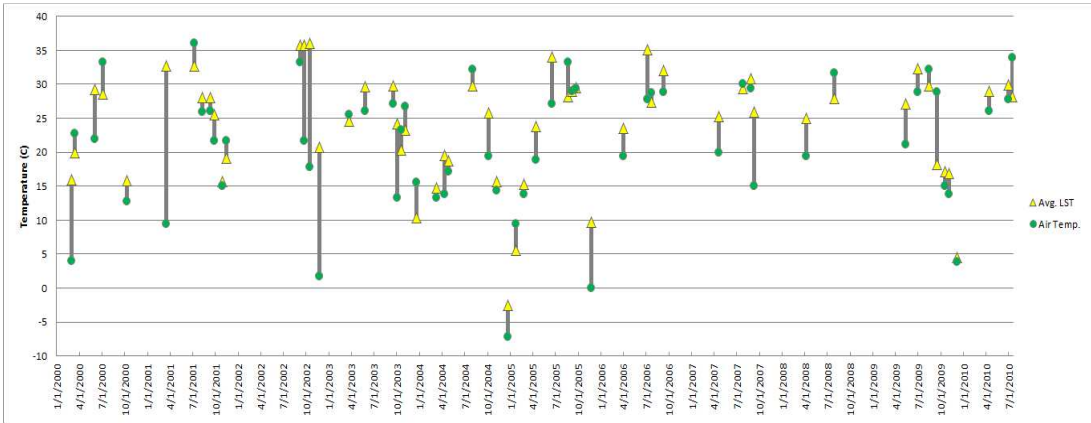


Figure 8. Day-by-day comparison of Avg. LST, Max. LST and Air Temperature for Bridgeton Landfill, Missouri.

4.2.2 “LST detection” Matlab program. A Matlab code was developed to evaluate the land surface temperature (LST) of the different landfills case studies. The code was given the name of “LST detection” program and can be applied to all the landfills in the United States for which usgs satellite data is available for download. “LST detection” Matlab program can accept hundreds of Landsat images as input and process the images in succession. The goal of this program is to process Level 1 geotiff satellite data from the USGS Earth Explorer portal and extract LST data from the thermal infrared band (band 6) and show the results in a clear display.

As the first step, the code prompts the user to decide how many areas of the landfill should be evaluated. At this point the user will be able to use the mouse cursor to select a polygon on the map that represents the landfill boundary. If more than one area is being evaluated, the user will be prompted to select multiple polygons of the landfill map. This command is extremely useful when a comparison of different locations is required. In this way, it is also possible to detect the exact location of a hotspot by comparing it to a different area of the landfill that is not experiencing smoldering events. After inserting the number of areas to be compared for temperature, the code will display the area of the landfill in a new window and the user will be invited to select the desired number of areas

in the image by moving the cursor on top of it. After the last area of interest is selected, the code will start processing all the input images of the provided database and will display a new window which showing a map of the landfill on the left and a chart where the average surface temperature and the maximum surface temperature are displayed as a function of time on the right of the Figure (Figures 9 and 12 in the next section). This LST detection program is a powerful tool because it allows users to remotely analyze LST data of virtually any landfill and can be used to draw conclusions about the state of hazardousness of waste sites.

4.2.3 Detection of consistent hot spots through time series analysis.

Figure 9 used to show maximum and average LST values for two different areas on the Atlantic Waste Landfill (AWL) over 12 years. In particular, the area delineated by the blue line contains a known hotspot while the area contoured with green dotted line does not. This feature of the “LST detection” Matlab program is very important because it allows the user to compare different parts of the landfill to better analyze the LST trends. Seasonal temperature changes and sun irradiation are the most probable cause of the similarity of trends for the two different areas. The three highest peaks in the data trend were zoomed in and shown in Figure 9; this is not obtained from the code output but it is illustrated for clarity purposes.

The maximum temperature peaks in the year of 2003 for the hotspot and the southern control area of AWL are separated by a difference of 6 °C. In the same fashion, two other maximum temperature peaks during 2007 differ by 4°C and 7 °C respectively. In 2009, an interval of 7 °C characterizes the difference between the maximum temperature of the hotspot and the control area in the south of the waste site. The choice of the control region is flexible, thus allowing the code user to compare different hotspots and different location within the same landfill study area. The output graph contains information about the temperature profiles of the chosen areas in terms of maximum temperature reached within the region and mean temperature of the same territories. From an image processing stand point this translates into analyzing all the pixels contained in the colored boundaries (blue, or green) and extrapolating the one that contains the highest temperature data associated with it (top graph of Figure 9). The three peaks selected from the top graph of Figure 7 were chosen because they exhibit the greatest temperature difference between the two regions. This proves that the area with the highest temperature is indeed a hotspot whose LST is much hotter than any other area in the landfill.

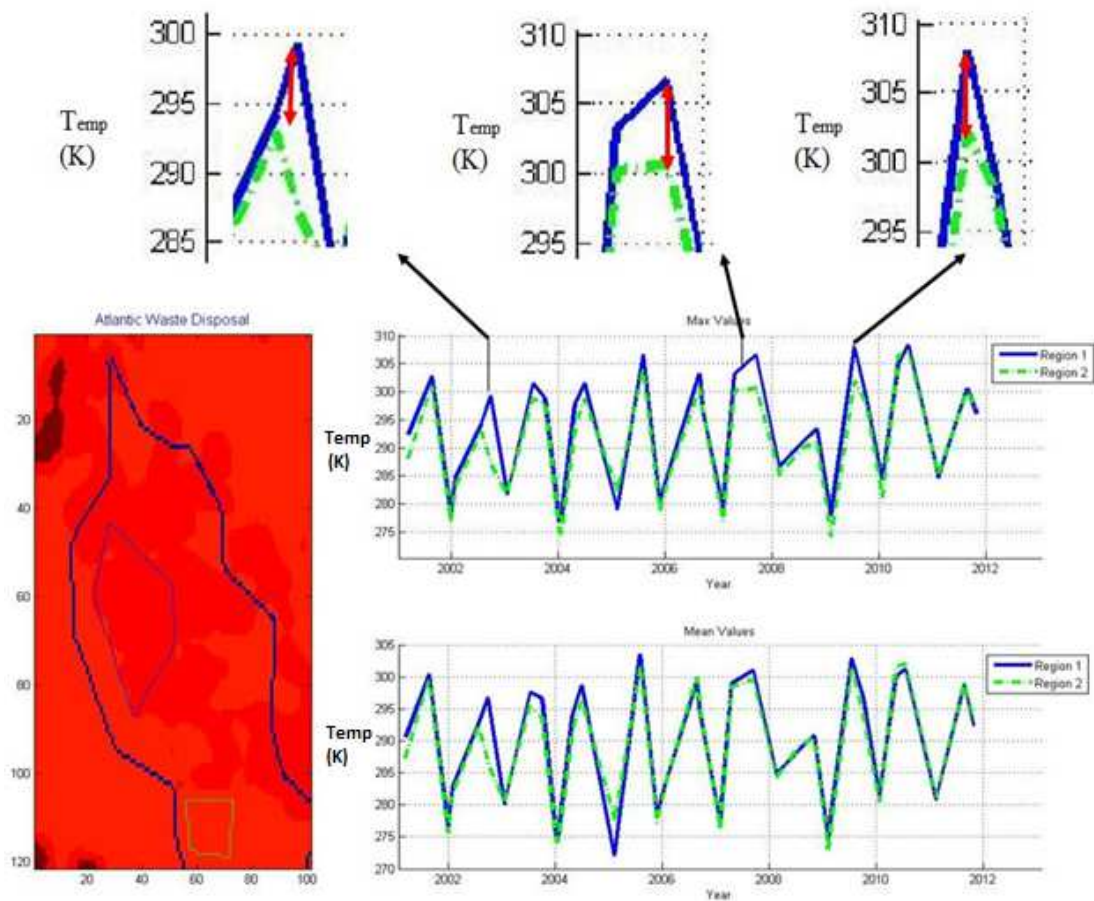


Figure 9. Relative temperature differences between a hotspot (blue) and a regular portion of the landfill (green) in a 12 year span for Atlantic Waste Landfill (AWL), Virginia

The bottom graph of Figure 9 is made by averaging all the temperature data in all the pixels of the contoured regions to find the mean temperature of that zone at that particular point in time.

The maps in Figure 10 show the temperature variation of the AWL area over a period of 12 years. The perimeter of the landfill territory is indicated by a dark blue contour for identification purposes and to emphasize how the location of the hotspots is internal to the landfill. The area representing the landfill could have been identified without showing its perimeter due to its darker shade than the surrounding area, an indicator of higher temperature. In particular, the red in the color range indicates the warmest region and the light blue color shows the cooler regions in comparison with the surrounding zones. The map indicates that the temperature is cooler near the borders of the landfill than certain areas located near the center, which are significantly higher in temperature. Figure 10 also shows average temperature difference between hot and cold regions on the surface of the landfill and how the location of the hotspots varies throughout the years.

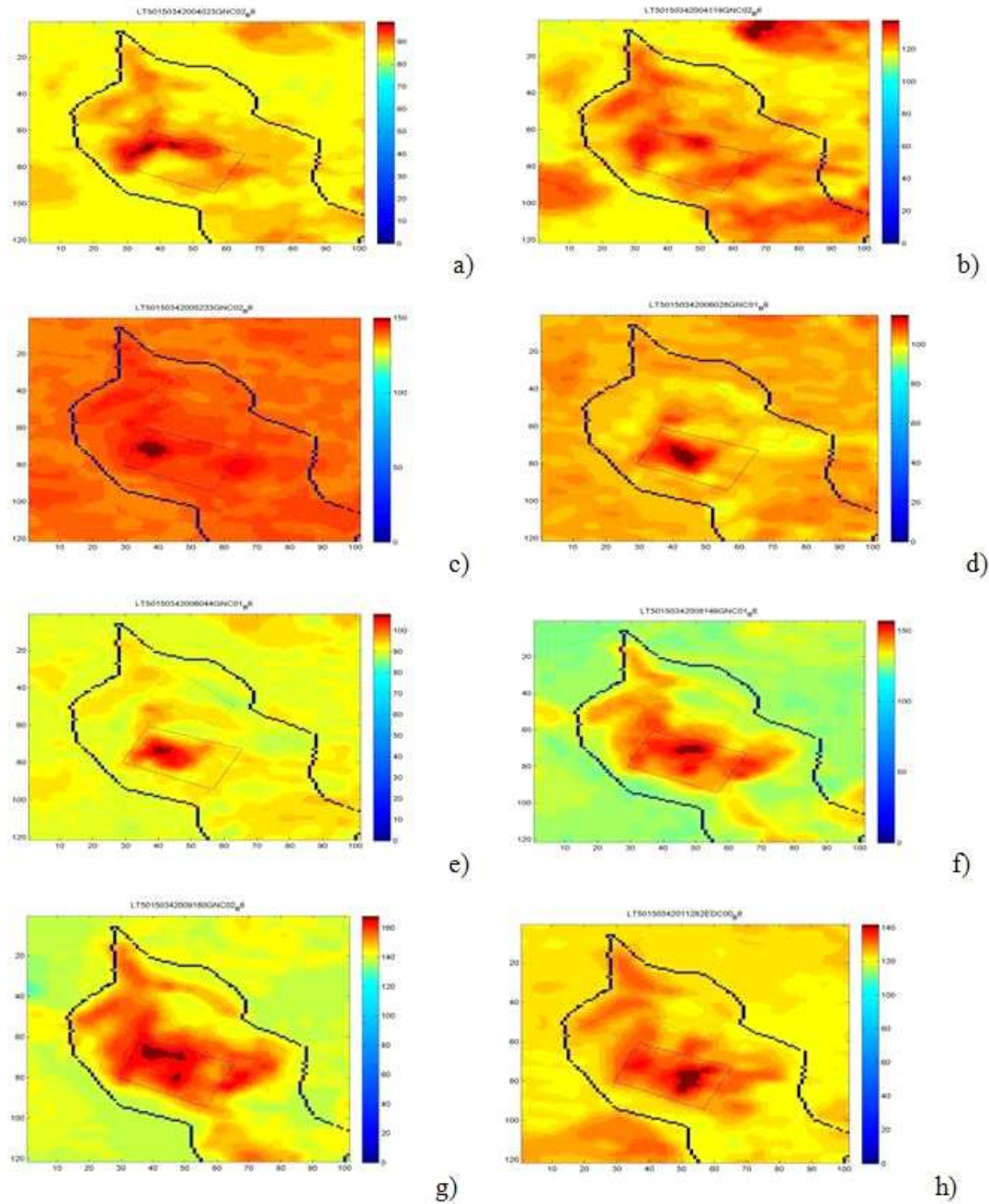


Figure 10. Thermal maps of Atlantic Waste Landfill (AWL) displaying the location of the hotspots relative to the perimeter of the landfill throughout the years. (a) January 23rd 2004; (b) April 28th 2004; (c) August 21st 2005; (d) January 26th 2006; (e) February 13th 2008; (f) May 25th 2008; (g) June 29th 2009; (h) October 9th 2011.

A careful comparison of the colored thermal images in series shows a suspicious temperature elevation during August 2005 (Figure 10, c). The hotspot in the central area of the landfill is dark red. Before August 2005 a slight difference in temperature is visible between the central and peripheral part of the landfill but it still does not appear to be concentrated in a single spot (Figure 10a, b). With the increase in temperature characteristic of the summer season, an interesting phenomenon is displayed (Figure 10, c). Now, both the entire landfill and surroundings are at roughly the same temperature, but a hotspot starts to form in the central part. The picture is indeed dominated by the color orange which corresponds to a higher temperature variation while the hotspot is dark red/brownish, indicating the highest temperature elevation in the field. The same hotspot increases in area in the following year of 2006 (Figure 10, d) while the surroundings are now at a lower temperature indicated by a bright yellow color. In the following years the hotspot is still there but it changes in area and location, moving slightly to the right (Figure 10 e, f, g, and h).

The trends of the maximum temperature difference and mean temperature difference throughout a time span of 12 years for two different areas on the BL surface are illustrated in Figure 11. The blue region shows higher mean and maximum temperature throughout the years compared to the green region.

However, both the green and blue regions have similar patterns, which is probably due to seasonal temperature changes and sun irradiation. Figure 12 is a multi-temporal map which focuses on the hotspots in the southern part of the landfill. It is easy to discern the hotspots on the landfill due to its LST which is much higher compared to the surroundings. The big hotspot areas are consistent throughout the years. The multi-temporal map shown in Figure 12 takes a closer look at the results obtained in Figure 11. Figure 12, a) through h), illustrates eight different snap shots of the LST hot spots existing in different areas of the landfill throughout 2000-2011. These hot spots are indeed moving throughout months and years signaling the presence of a possible biogas migration around the internal section of the landfill.

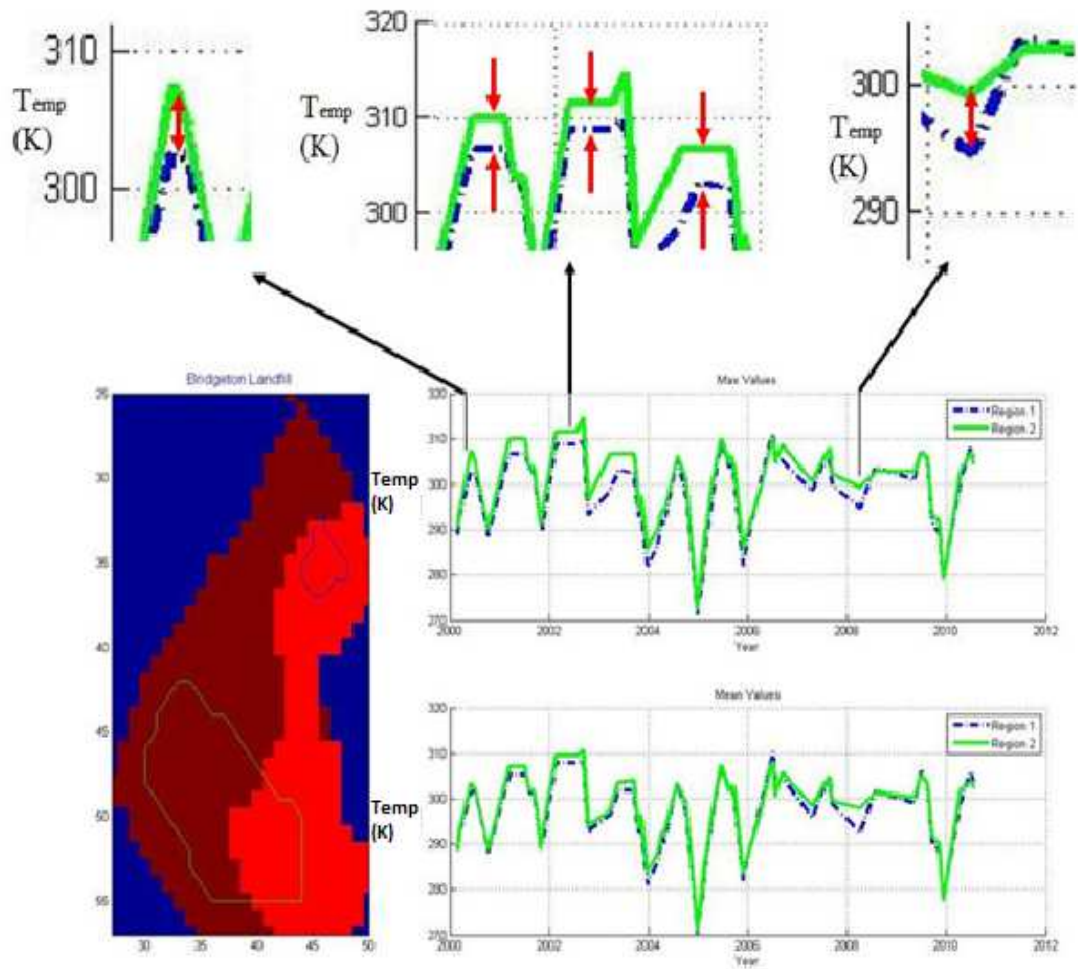


Figure 11. Relative temperature differences in a 12 year span for BL, Missouri

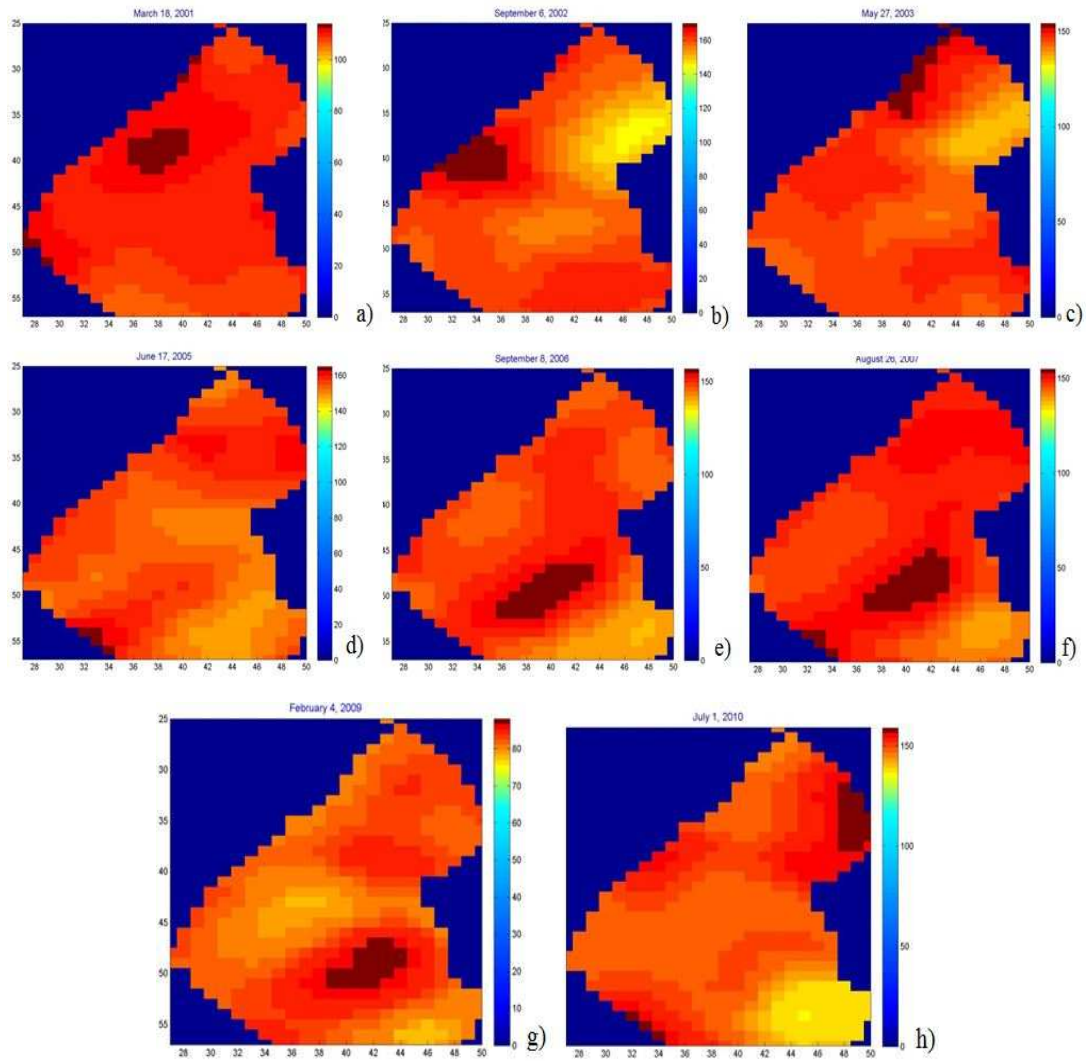


Figure 12. Thermal maps of Bridgeton Landfill displaying the location of the hotspots relative to the perimeter of the landfill throughout the years. January 20th 2000 (a); February 17th 2002 (b); July 4th 2002 (c); May 16th 2005 (d); December 22th 2006 (e); August 10th 2007 (f); August 25th 2009 (g); October 21st 2010 (h)

4.2.4 Composition of landfills maps superimposed by hotspots maps.

The frequency of maxima for Atlantic Waste Landfill (AWL), Virginia are depicted in Figure 13 *FIGURE 13*, in other words: the exact locations that reached the highest temperature values more frequently. The hotspots are clearly identified by the two red circles on the map. This information agrees with the results illustrated in Figure 9 and Figure 10 which show exactly the same location for the hotspot so it makes sense that the frequency of appearance in that area (Figure 13) would be higher. In contrast to the red dots corresponding to the hotspots, the lower the frequency of recurrence the darker the shade of color blue that was used in the graph to represent it.

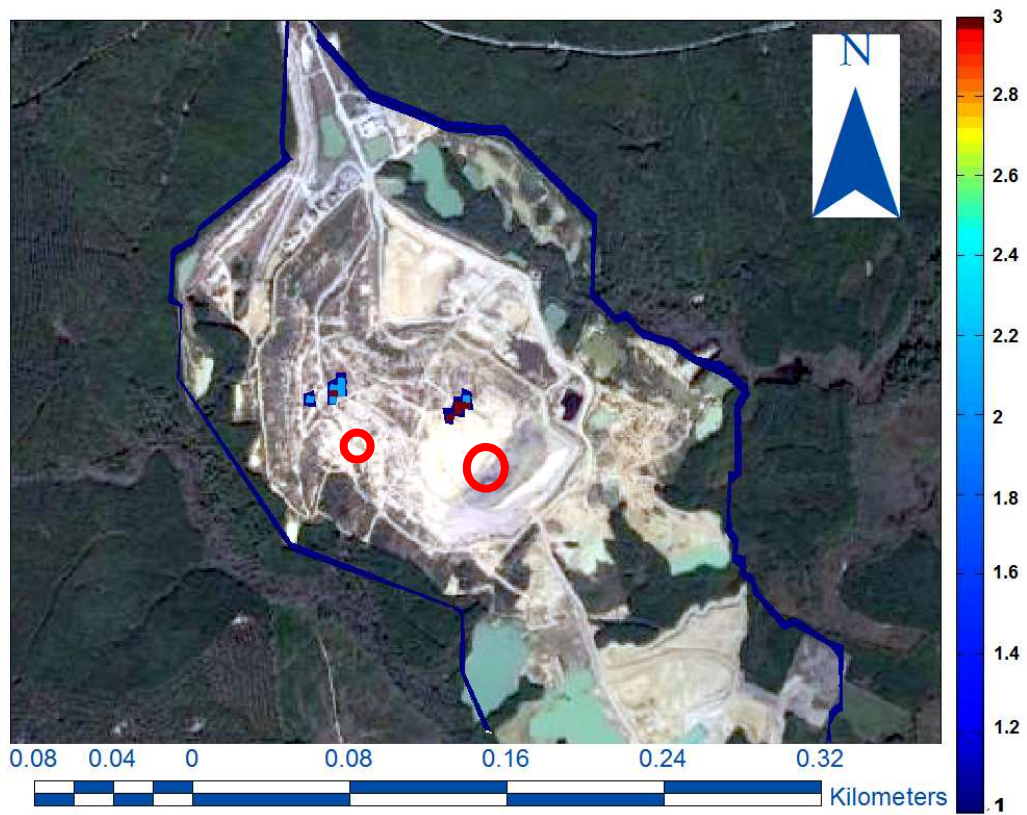


Figure 13. Location of frequency of maxima around the landfill site of Atlantic Waste Landfill (AWL), Virginia

In Figure 14, BL in Missouri is depicted and in particular, the exact locations that reached the highest temperature values more frequently are showed. From this information it is possible to predict exactly where an internal fire is about to occur or already occurring and the area of interest. The red parts on the landfill map correspond to hotspots in the northern radiological area (West Lake landfill). There are some other yellow heat signatures on the map belonging to the once active Sanitary Part of the landfill. This result confirms the subsurface smoldering event identified in 2013. The state health department should take action before the situation deteriorates further. A map of the location of the monitoring wells on BL territory is given in Appendix C. Moreover, Appendix C contains another BL map where the exact location of the smoldering event recorded in June 2013 is indicated.

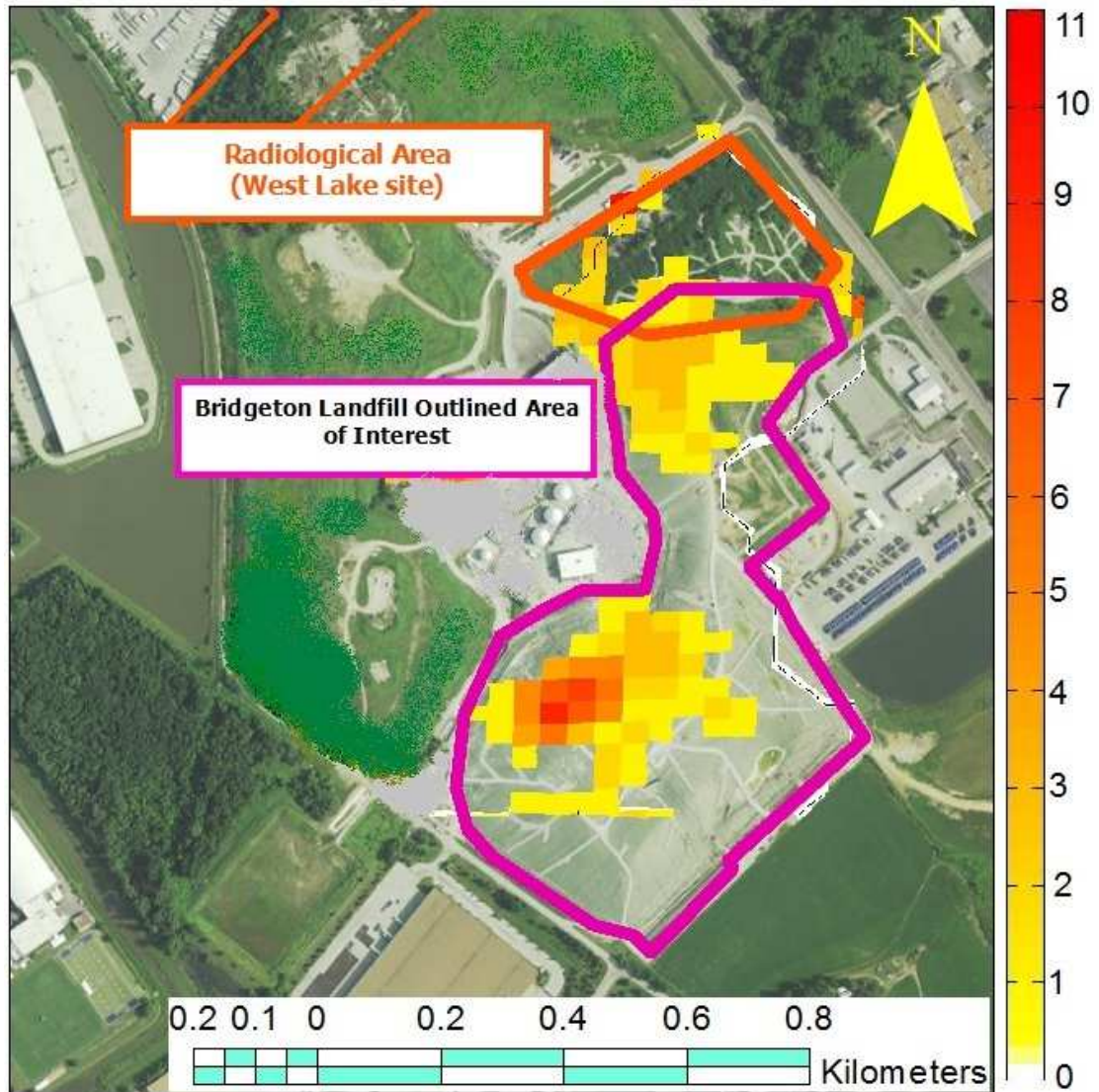


Figure 14. Location of frequency of maxima around the landfill site of Bridgeton Landfill, Missouri

Chapter 5

Development of Landfill Fire Index (LFI)

Another way to prevent smoldering events and fire outbreaks in a landfill is to identify what quantifiable factors can be measured and monitored in order to determine the specific circumstances leading to feasible conditions for combustion. For this purpose a Landfill Fire Index (LFI) was developed. A LFI is a statistical tool that can be used as a safety management resource that ensures the prevention of environmental disasters by increasing awareness of hazards. The use of a LFI for management and monitoring purposes is of foremost importance while deciding what control measures need to be enacted to reduce risk to an acceptable level. The LFI should be determined regularly, whether it be monthly, annually, or bi-annually. The 8 steps that should be used to successfully ensure a continuous prevention from landfill fire hazards are illustrated in Table 3, which constitutes also the action flow to be followed in case a hazardous scenario may occur.

The importance of a Landfill Fire Index (LFI) is to limit clean-up costs and minimize individual risk to the landfill personnel, by making them aware that a landfill fire is occurring. This study identified various factors that determine a landfill's increased probability to subsurface fire. In the following paragraphs different LFI factors will be analyzed and quantified for a clear understanding of

the numerous scenarios that can lead to hazardous conditions. Until now, these parameters have been treated as static risks, and independent from each other, meaning that only periodic assessment was deemed necessary in case an alert was triggered in the control system. The application of the LFI permits the dynamic treatment of LFI factors over time. In particular, the LFI takes into account the interdependency of each risk factor so when coupled with continuous monitoring, minimal effort will be required to stop the combustion processes within the landfill before a fire starts, preventing emergency situations.

Table 3

Eight-Step Risk Assessment Process

Step	Description
1. Identify the hazards	Hazards can be identified using observation, experience and talking to people who carry out the specific job. The following can be consulted: workforce, accident (ill health and near miss) data, instruction manuals, data sheets, hazard crib sheets, and workplace inspections.
2. Identify those at risk	Individuals who would be directly affected by the risk including: office staff, maintenance personnel, members of the public, machine operators
3. Identify existing control measures	Examine how the risks are already being controlled. These control measures can be analyzed to determine if they are adequate in controlling the risk and to help evaluate the risk.
4. Evaluate the risk	A risk is the likelihood that a hazard will cause harm. A risk can be calculated by multiplying the likelihood by the severity. A risk assessment chart can be used to determine the severity of the risk
5. Decide/implement control measures	If risk is not being properly controlled, new control measures are required to lower risks. The hierarchy of controls is as follows: <ul style="list-style-type: none"> • Elimination (get rid of the risk) • Substitution (exchange one risk for something less likely or severe) • Physical controls (separation/isolation, eliminate, contact with hazard) • Administrative controls (safe systems of work, rules in place to ensure safe use/contact with hazard) • Information, instruction, training and supervision (warn people of hazard and tell/show/help them how to deal with it) • Personal protective equipment (dress them appropriately to reduce severity of accident)
6. Record assessment	Keep copies of the risk assessments for future records and inspection
7. Monitor and review	To ensure that all control measures are working properly on reducing risks, the risk assessment must be constantly reviewed and scanned for changes.
8. Inform	The results of the risk assessment should be relayed to all individuals directly at risk

5.1 Methodology and Data

In the next two sections, a new risk detection method that involves the analysis of multiple quantitative factors to detect landfill fire occurrences is presented. A landfill fire database with 20 years of data was obtained from FEMA and was used to acquire information about the typology of recorded landfill fires during that period of time. An in-depth description of the eight risk factors used in the Landfill Fire Index (LFI) comes after that. The Risk Index is then applied to the two cases studies of Bridgeton (BL) and Burlington County Landfill (BCL). Finally, the decision model that was used to analyze the risk index and to prove its statistical significance is described.

5.1.1 Landfill Fire Index data analysis. Information about landfill fires was obtained from the National Fire Incident Reporting System (NFIRS), which is the standard national reporting system and it is made up of a collection of data on fire occurrences across the United States by the National Fire Administration (NFA) and the Federal Emergency Management Agency (FEMA). In order to get a preliminary understanding of the challenges encountered to preserve safety in a landfill, data from the NFIRS was collected about all reported landfill fire incidents happening between the years 1980-2001 (Figure 15). This analysis allowed to find trends in fire susceptibility between municipal waste landfills and construction

and demolition landfills, with particular attention on what was the first ignition sources for landfill fires in the United States.

The NFIRS database includes all types of fire events, therefore, it was necessary to isolate the landfill fire events from the rest of data. The trend in the number of landfill fires can be seen in Figure 15. A challenge encountered in the analysis of the data is that the NFIRS system combined landfill fires with illegal dumpsite fires for the years 1980 and 1989, whereas from 1990 onwards, only landfill fires were accounted for in the basic incident index. This explains why the amount of landfill fires was so high in the earlier years and why they lowered significantly after 1990. Data from the year 1992 could not be analyzed, as the files were corrupted.

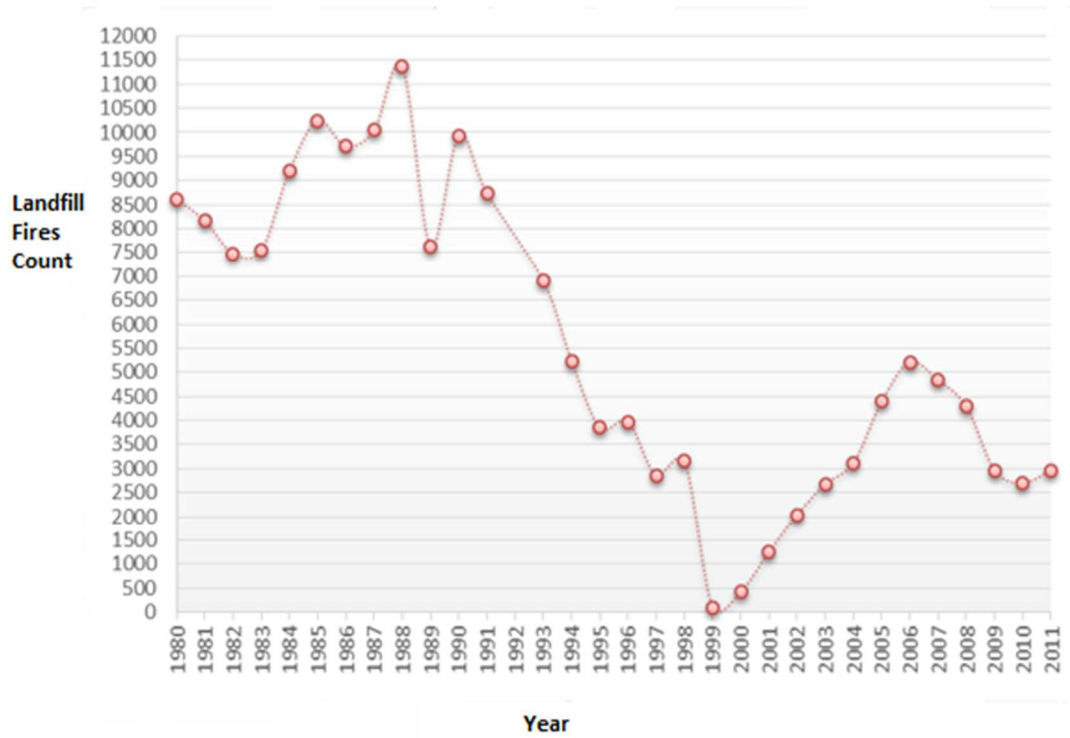


Figure 15. Number of Reported Landfill Fires in the United States between 1980 and 2011

5.1.2 Landfill classification data analysis. The landfill fire data set was analyzed further, to study trends in the data that related to increased fire susceptibility. The NFIRS data classifies landfills into two types: municipal solid waste, and construction and demolition landfills. It was found that during the 12 year period of 1999-2011, there were more construction and demolition landfills fires than municipal solid waste. This result directly corresponds with a FEMA report, "Landfill fires, their magnitude, characteristics and mitigation" which states construction and demolition landfills have a higher risk for fire due to the nature and composition of the material collected and based on "anecdotal remarks by landfill fire suppression professionals" [16]. Figure 16 shows the number of construction and municipal landfill fires from 1999-2011 in relation to the number of landfill total landfill reported fires each year. Between 49% and 67% of the reported landfill fires were construction landfill fires during this period of time. This confirms the fact that construction landfills are at a higher risk for fires than municipal landfill fires.

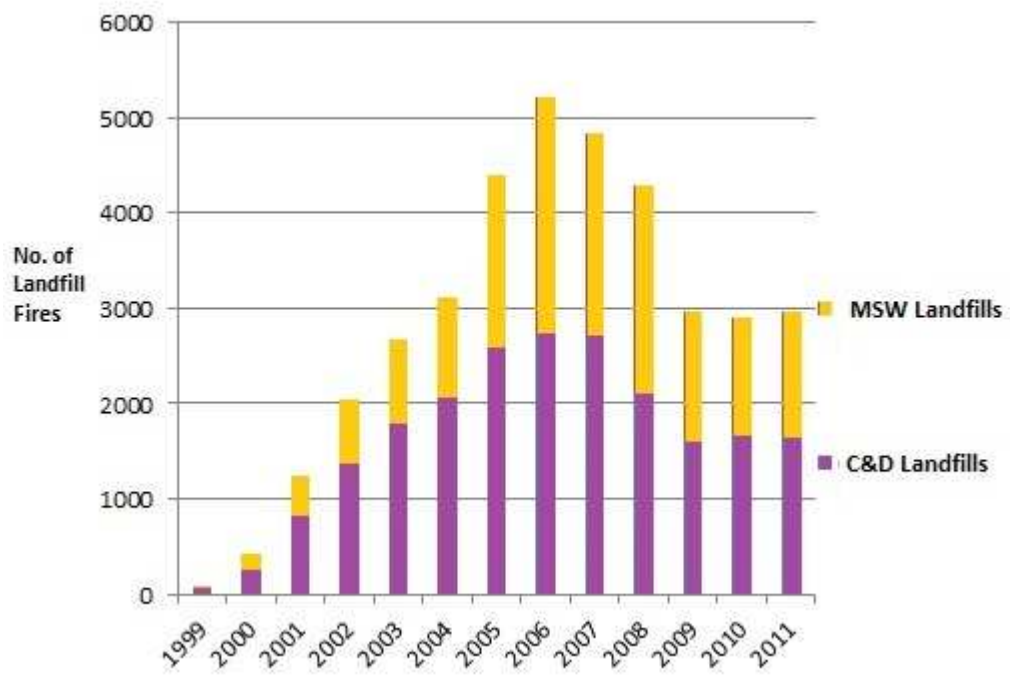


Figure 16. Number of landfill fire occurrences based on landfill classification (1999-2011)

5.1.3 First ignition source data analysis. Another important type of information obtainable from the database is the causes leading to a surface landfill fire, in other words, the different types of ignition sources. After the information stored in the FEMA database was filtered by means of ignition source, all the municipal solid waste (MSW) and construction and demolition landfill fire occurrences were categorized into 684 fire outbreaks. These 684 fires were then evaluated to establish the top ten ignition sources. Once all the ignition sources were ordered in terms of frequency, the top 10 ignition sources for landfill fires (Figure 17) : undetermined (45%); rubbish, trash or waste (21%); other (9%); light vegetation, not crop including grass (7%); organic materials (5%); heavy vegetation, not crop including trees (4%); multiple items first ignited (4%); magazine, newspaper, writing paper (2%); dust, fiber, lint, including sawdust and excelsior (1%); and electrical wire, cable insulation (1%). Due to the nature of subsurface events, it was found that there is no ignition source database for underground smoldering fires and that the detection of the fire happens only when the combustion reaction already started and when it is too late for the ignition source to be identifiable.

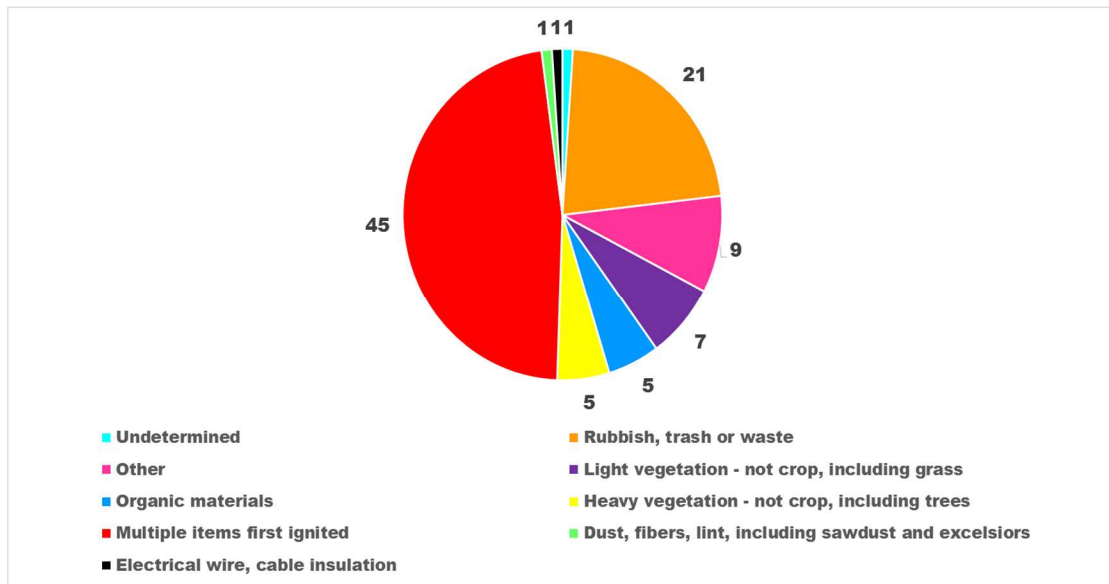


Figure 17. Top ten ignition sources for landfill fires

5.2 Landfill Fire Index Factors

Risk factors in landfills can be measured and prioritized in order to manage risk levels within defined tolerance thresholds or ranges without being over controlled. When considering risk factors it is important to take into account their area of influence. Landfill gas (LFG) emissions impact their surroundings in different ways and act on different scales [59], [60] as illustrated in Figure 18. Specifically, the hazardous consequences of a fire or subsurface event affect distant areas around the landfill. This means that not only nearby businesses but also highly populated towns in the vicinity of the disposal facility can be negatively affected by a fire outbreak. One of the negative factors that is usually neglected is

noise pollution. Noise pollution is a critical health concern that can lead to hearing loss, sleep disruption, cardiovascular disease, social handicaps, reduced productivity, impaired teaching and learning, absenteeism and accidents [61]. Chronic noise exposure can also diminish the serenity and calmness that people foresee to have during leisure times. Noise pollution adversely influences general health and well-being in the same way as chronic stress does. Mitigating measures should be proposed to keep the noise to minimum levels. In example, heavy equipment and machinery within the facility should be maintained in good condition at all times to avoid unnecessary noise and vibration. In order to keep civilians living in nearby cities away from noise pollution several practices should be implemented as engineered controls for noise reduction at sources or diversion in the trajectory of sound waves. As illustrated in Figure 18, noise pollution can affect nearby population up to a distance of 6 km [60]. Poisonous gas emissions instead are able to travel at least 8 km before getting mitigated by wind or other atmospheric events [59]. Even when landfill gases concentrations fall below dangerous levels, disruption of daily activities may be caused by unpleasant odor.

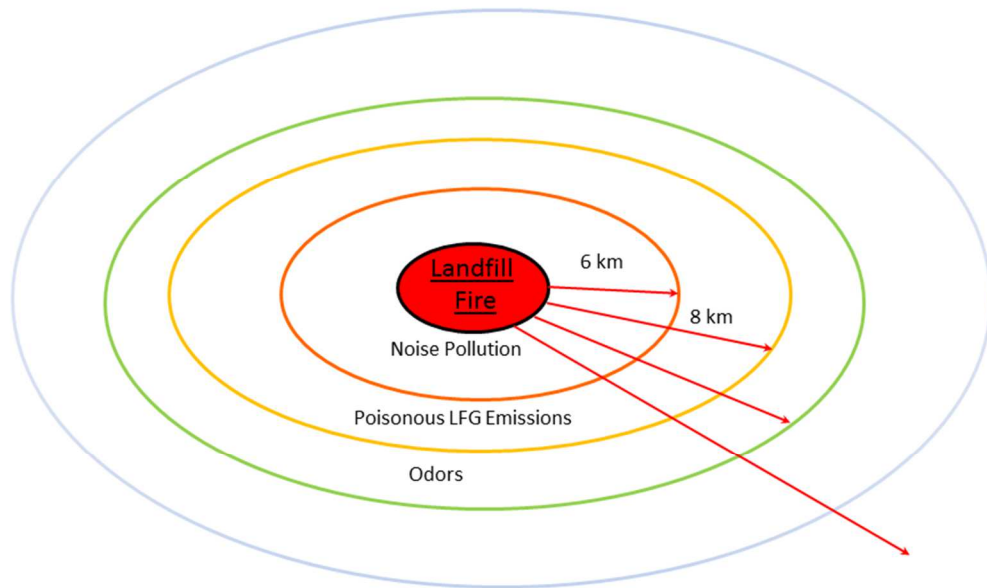


Figure 18. Risk factors area of influence around a general landfill

Poisonous gas emissions are able to travel at least 8 km before being mitigated by wind or other atmospheric events [59]. Even when landfill gases concentrations fall below dangerous levels, disruption of daily activities may be caused by unpleasant odors [59]. Subsurface events can have a great impact on water quality because the high temperatures and explosions can fracture the liner at the bottom of the landfill with leachate polluting the underlying aquifer. Since not all the landfills are positioned on top of an aquifer and different aquifers extend to different depths, it is difficult to predict the extension of the damage caused by

subsurface events on this matter. Besides having large spatial scale, landfill gases also act on different time scales. Underground chemical degradation, landfill gas emissions, and other processes occurring inside the landfill continue long after the waste has been disposed. The period of significant emissions can last up to hundreds of years [59]. Also, the life span of the compounds emitted varies greatly. For example, dust and odors are transient phenomena, whereas other more toxic trace compounds can accumulate in organisms and persist in natural ecosystems for extended periods of time [62].

5.2.1 Residual Nitrogen. Residual nitrogen is the occurrence of excess nitrogen gas present in a landfill due to aerobic decomposition. These aerobic conditions stem from fluctuations in the landfill gas collection system. The objectives of this gas collection system are: protecting the groundwater, control over subsurface gas migration, surface emission control, odor control, and for energy recovery use. Over-pulling air infiltration and under-pulling gas migration through the gas collection system results in the presence of excess nitrogen. When the vacuum in the gas collection system pulls in too much air the oxygen in the air kills off the methanogens and creates aerobic conditions. During this state of decomposition, oxygen is consumed and the nitrogen that is also present in the air is left inside the landfill. A report provided by the Solid Waste

Association of America states that the normal ratio of N_2 to O_2 is approximately 3.76 [63]. Both acceptable and non-acceptable ranges for residual nitrogen are illustrated in Table 4. Excess residual nitrogen can be an indicator of a subsurface fire occurring under aerobic conditions. Under aerobic conditions, the internal waste temperature can rise significantly, making spontaneous combustion more likely to occur. (Table 4)

Table 4

Residual Nitrogen Ranges for Landfills

Percentage	Meaning
0 – 12%	Normal operating range for interior extraction devices at most landfills
16 – 20%	May be necessary for perimeter migration control, side slope emission control, or where other compromise is required.
> 20%	Indicates aggressive landfill gas extraction, can lead to aerobic conditions

5.2.2 Oxygen exceedance. Oxygen exceedance recorded within a monitoring well can be a good indicator of significant air intrusion. Air intrusions through landfill cover can introduce oxygen into the landfill, which kill off methanogens and create aerobic decomposition. The aerobic bacteria consume the excess oxygen within the landfill, and leaves behind the nitrogen from the air. This process increases the nitrogen to oxygen ratio, as is referred to as residual nitrogen. The presence of oxygen increases aerobic bacterial activity within the landfill and elevates internal temperatures. Methane gas starts to be produced by the anaerobic bacteria only when the oxygen in the landfill is used up by the aerobic bacteria; therefore, any excess oxygen remaining in the landfill will slow methane production. Hotspots are created when the temperature rises due to anaerobic decomposition, they can migrate throughout the landfill, thus creating smoldering events. Even though smoldering waste exposed to an influx of oxygen can grow into dangerous fires, underground oxygen levels that are too low are actually more hazardous than moderate levels. Shadi y. Moqbel described heat generation occurring due to chemical oxidation even at volumetric concentrations of oxygen as low as 10% [64]. Results indicate a significant heat generation from exothermic pyrolysis in the absence of oxygen (0% - 10%). For concentrations between 10 - 20% by volume solid waste did not exhibit thermal runaway or flammable combustion. However, self-heating occurs due to slow pyrolysis and waste continues to

disintegrate, leaving only char, which is a product of smoldering. When oxygen levels are above 20% by volume, pyrolysis is attenuated due to higher oxygen levels [64]. Intuitively, an oxygen rich environment is considered more prone to fires, however, the oxygen-starved conditions of waste collected in a landfill make the compacted material prone to self-heating behavior due to pyrolysis.

5.2.3 Methane. Methane (CH_4) constitutes both a very short term and acute explosion hazard and has a much more far-reaching and long-term effect on global warming than other LFG as CO_2 in soils, methane undergoes oxidation and therefore impoverishes the soil of oxygen and increases the carbon dioxide levels [62]. Landfills are the third most influential anthropogenic source of methane emissions (approximately 20% of anthropogenic sources), where the human activities account world-wide for some 70% of the emissions. Methane is one of the main components of landfill gas with concentrations ranging between 30 and 60%. Methanogenesis and methane emissions can be retarded by accumulation of acids. Conversely, the increase of methane production helps avoiding acid accumulations and improve the water balance and distribution in the landfill soils [65]. The flammable range for methane is within concentrations of 50,000 ppm – 150,000 ppm [48]. Methane concentrations can be a good indicator of aerobic conditions. Methane producing bacteria (methanogens), which thrive in oxygen deficient environments, die off when exposed to oxygen and methane production

is significantly reduced. Therefore, reduced methane concentrations detected by a monitoring well can signify that aerobic decomposition is occurring. The average methane concentration should be between 460,000 ppm – 500,000 ppm. Concentrations less than this increase the likelihood of explosion and fire occurring since landfill gas will mix with air and become depleted in methane, through dilution and/or oxidation, and therefore fall within the flammability range [48].

5.2.4. Carbon monoxide. Carbon monoxide (CO) is a direct by-product of incomplete combustion and can make up 0 to 3 % vol of landfill gases while normal levels are usually at 0.001 % vol. According to the Occupational Safety and Health Administration (OSHA), carbon monoxide is a “poisonous, odorless and tasteless gas” [66], and workers should be limited to 50 ppm of co averaged over an 8 hour time period because causes respiratory failure and death above 5 000 ppm [20]. Subsurface landfill fires can produce co levels in excess of 50,000 ppm [16]. These high levels of exposure can severely impact the communities surrounding the landfill. Different types of combustion yield different amounts of co. If a subsurface fire has been burning underground, high CO gas concentrations can be detected in the monitoring wells, which are a sign of oxygen-starved burning of the refuse. Carbon monoxide is also released during combustion of

LFG, as a result of incomplete combustion. According to the Environmental Protection Agency, monitoring wells that read carbon monoxide levels between 100 and 1,000 ppm are viewed as suspicious, and need to be analyzed further with air and temperature monitoring. Any monitoring well with CO levels in excess of 1,000 indicates the presence of an active subsurface landfill fire [48]. The higher the carbon monoxide concentration, the poorer the combustion process. During an experimental landfill fire in Sweden 1600 ppm of CO were measured inside the burning waste mass [65]. There is no evidence to suggest that carbon monoxide is produced microbiologically from a landfill. Therefore, if carbon monoxide is present, it is an indicator of a fire. While carbon monoxide is a good indicator for subsurface fire detection, the gas itself is deadly in high concentrations. Carbon monoxide is harmful when breathed because it displaces oxygen in the blood, which deprives the heart, brain and other organs of oxygen.

5.2.5 Carbon dioxide. Carbon dioxide (CO_2) is a colorless and odorless gas and constitutes the predominant form of gaseous carbon. It is one of the products of biodegradation of waste and other organic compounds, under both aerobic and anaerobic conditions. Alongside methane, CO_2 is one of the two dominant gases generated in landfills, usually in concentrations reaching 20 to 50% of the gas [62]. Besides being toxic, carbon dioxide can result in asphyxia by

oxygen displacement or even toxicity to plant when high concentrations are attained in soils. Especially in landfill soils, high levels of CO_2 are toxic to plants roots even when enough oxygen is available. Indirect effects of CO_2 include pH lowering and, consequently, effect soil composition. Usually, CO_2 can be found in soils in concentrations fluctuating between 0.04 and 2 %. Vegetation can usually persists until 5 % is reached, even though tolerance varies between plant species. Carbon dioxide constitutes a serious safety threat in landfill environments since a few deaths due to carbon dioxide asphyxia happened on or near landfills, in drains, culverts and other underground and closed environments where LFG had accumulated. Building requirements for infrastructures situated on or near landfills do not demand CO_2 levels monitoring, but only methane levels. It would be more appropriate to include carbon dioxide monitoring into the basic requirements since methane can be rapidly oxidized to CO_2 in soils and could thus still indicate the presence of methane production. Absence of monitoring for CO_2 could indeed result in undetected, and therefore hazardous, migration of LFG [62], [18].

5.2.6 Moisture content. Unsaturated conditions in a landfill increase LFG production because it promotes bacterial decomposition. Moisture may also promote chemical reactions that produce gases. Wet surface soil conditions may

prevent landfill gas from migrating through the top of the landfill into the air above, thus increasing internal pressure and temperature. Moisture may also seep into the pore spaces in the landfill and displace air from these spaces thus promoting anaerobic conditions. Moisture content not only plays a strong role in waste degradation, it also has an effect on subsurface fire ignition. Certainly, very low moisture content can cause increasing temperature because reduced evaporation means less heat is carried off with the water particles. However, if the water content is too high, the excess moisture will result in bacterial growth and transport of nutrients and microorganism to all areas within a landfill. There will also be an increase in chemical self-heating due to increasing aerobic decomposition carried out by aerobic microbes. Compaction of waste delays flammable and explosive conditions since it increases the density of the landfill contents, thus diminishing the rate at which moisture can infiltrate the waste. Moisture content in a landfill should be limited to concentrations lower than 20 %. Moisture content between 20 and 45% greatly increases the risk of internal hot spots forming from increased bacterial activity [67].

5.2.7 Monitoring well temperature. Subsurface fires are directly related to an increase in internal temperature of a landfill. As the waste temperature rises, bacterial activity increases, resulting in increased gas production. Increased

temperature may also increase rates of volatilization and chemical reactions. Monitoring wells give an approximate temperature value of the gases in the surrounding landfill area. Therefore, if a subsurface fire is occurring in a specific cell, the nearest well may “pick up” the increased temperature. As determined by the New Source Performance Standards (NSPS), a wellhead temperature that exceeds or is equal to 131 °F (55 °C) should be investigated for subsurface fire occurrence. Wellhead temperatures over 140 °F (60 °C) indicate aerobic conditions that can alter the decomposition rate of waste, or viability of methane recovery [48]. Readings can be done by lowering a temperature probe into a monitoring well and recording measurements every 0.5 – 1 m. Abnormal elevated temperatures can be an indication of a fire present near that monitoring well. For in-situ measurements, a cone penetrometer (CPT) measures temperature, angle of decline and resistance to penetration. The electronics in this device can operate in temperatures up to 80 °C. Waste temperature readings can also be an indication of subsurface fire occurrence. Waste temperature can be obtained by performing borehole drilling or sampling to bring waste to the surface, and using hand-held scanning devices to determine a temperature reading. A waste temperature reading of 170°f or more is a direct indication that a landfill fire is occurring [19].

5.2.8. Buried waste density. Subsurface fires are ignited by several different factors; however the intensity and area of the fire can be related to waste density. Air intrusions, whether naturally occurring through small cracks in the cover, or by excessive gas extraction, allow oxygen to flow within the subsurface of the landfill. Buried waste with a lower density has excess air voids present that allows oxygen and other gases to propagate in the form of hot pockets and spread the subsurface fire. If waste is loosely buried or frequently disturbed, more oxygen is available, so that aerobic bacteria will live longer and produce carbon dioxide and water for longer periods of time. This will result in an increase in temperature of the waste due to aerobic decomposition and thus enhancing the probability of fire outbreaks. If hot spots (areas where waste temperatures have increased) are present, the presence of low waste density can allow these small smoldering heat events to grow into a full blaze. On the contrary, waste with a higher density is more compact and limits the propagation of these gases and smoldering fires. In highly compacted waste, methane production will begin promptly since aerobic bacteria will be replaced by methane-producing anaerobic bacteria. To ensure proper compaction and limit the propagation of fire and gases, a buried density between 5.20 and 10.70 kN/m^3 is most ideal [18].

The landfill box model given in Figure 19 is a great tool to clearly visualize the dynamics of the risk factors taking place inside the landfill. Figure 19 was indeed built from the LFI factors in Figure 20 and it helps to better visualize the connection between quantitative values of the risk factors and their risk values. Green arrows represent a negative dependency between the increase or decrease of a certain factor and their risk value. In particular, a green arrow pointing up implies that the higher the quantitative value of that particular risk factor, the lower the overall risk of fire. On the other hand, red arrows represent a positive dependency between the increase or decrease of a certain risk factor and their risk value. Subsurface events generate higher temperatures that reach both monitoring wells and surface alike. When the heat from subsurface events is transmitted to the surface, it creates hotspots that can be easily identified by thermocouples. Poisonous landfill gas emissions can be generated from the hotspots and start their journey to the nearby populated areas. When methane is pulled out from the landfill interior, dangerous aerobic conditions can take place, therefore, the red arrow next to the methane label symbolizes the higher risk of fire that arises from the diminished quantity of the chemical inside the landfill. On the contrary, high levels of carbon monoxide indicate incomplete combustion conditions, therefore, the red upward arrow symbolizes the greater risk of a fire outbreak given higher concentration of this chemical.

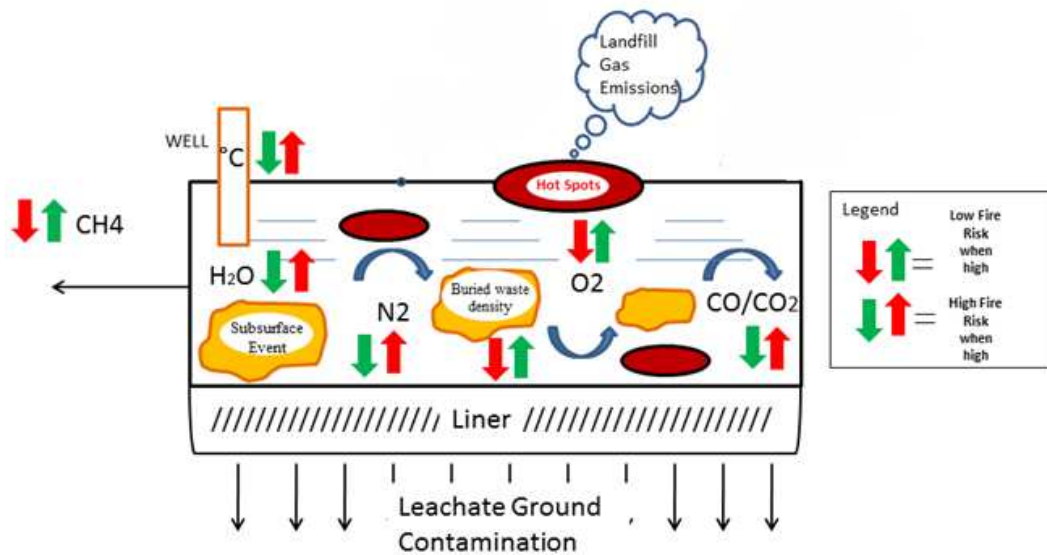


Figure 19. Landfill Box Model

5.3 Landfill Fire Index data for Bridgeton and Burlington Landfills

The data necessary to calculate the Landfill Fire Index for both Bridgeton Landfill and Burlington County Landfill were obtained in the form of tabular monitoring well recordings and is available in Appendix A and Appendix B. The active monitoring well networks provide basic statistics about the composition of the underground landfill gas. Five different dates and monitoring wells were selected as data points to prove the applicability of the Landfill Fire Index (LFI) for Bridgeton Landfill (BL). A map of the location of the monitoring wells on BL

territory is given in Appendix C. Moreover, Appendix C contains another BL map where the exact location of the smoldering event recorded in June 2013 is indicated. The choice of the 4 monitoring wells was then dictated by their location in respect to the recorded smoldering event, the data used was recorded on the same date for all the four wells. Data from GEW-028R instead, the fifth monitoring well analyzed, was recorded in 2015 and it is used to make a comparison between fire conditions in BL and Burlington County Landfill (BCL) controlled conditions.

Monitoring well data collected for May 2015 at Burlington County Landfill (BCL) was analyzed for fire risk. Burlington County Resource Recovery divided the facility into two separate landfills, 1 and 2. The monthly averages of the concentrations for each facility were used to compare Landfill Fire Index Factors. SCS Engineers conducted well-field monitoring in Burlington County's Landfill Nos. 1 and 2 to satisfy the EPA's New Source Performance Standards. The vertical extraction wells, horizontal collectors and leachate cleanouts were read at least once a month. The landfill Gas (LFG) collectors were monitored for gas quality, composition, static pressure, and gas temperature by using a landfill gas analyzer (Landtee GEM-2Nav or GEM 2000).

This section focuses on analyzing the vulnerable elements and parameters of a landfill and assigning a value for their level of hazardousness. The results are

an estimate of the conditions of a landfill with respect to smoldering events. The consequences of smoldering events are direct damages to the landfill and adjacent infrastructures, nearby roads and towns, direct losses such as cost of repairs and replacement, income loss for the little and big businesses nearby the landfill and the connected population, casualties, environmental hazards as air pollution and release of poisonous gases; and indirect losses, such as economic losses of companies which collaborate with landfills and leachate operations. It is not within the scope of this thesis to determine individual risk.

5.4 Analytical Hierarchy Process (AHP) calculation for Landfill Fire Index (LFI) determination

With the development of the Landfill Fire Index (LFI) it is also necessary to take into account the weight of each LFI factors. Especially for landfills, the determination of such weight values is very difficult due to the complexity of the system. The value of a specific LFI factor can indicate hazardous conditions but it can also be more or less influential compared to other factors on the overall state of hazardousness of a landfill. This situation is taken into account throughout the development of the LFI by applying statistical tools such as Analytical Hierarchy Process (AHP) techniques. In fact, AHP can help in many different scenarios of complex planning, energy, health, marketing, natural resources, and transportation problems.

The AHP method can be applied to scenarios where multiple criteria need to be considered to prioritize among criteria and alternatives. This method was first developed by Saaty in 1980 [68] and then revised by Saaty and Millet in 2000 [69]. When using AHP the system is decomposed into a hierarchy. Pair-wise comparisons are made and priorities are established among the elements of the hierarchy in the form of a pair-wise comparison matrix (PCM). The resulting matrix is normalized by averaging the values in each row to get the corresponding rating. The results are synthesized and the consistency ratio of the judgement is evaluated.

Equation 8 is a mathematical representation of the LFI. The probability to have a subsurface event inside a landfill can be calculated as a total risk, which is also called collective risk, and it is the sum of all the risks that arise from all the considered hazards scenarios and hazardous parameters (the Landfill Fire acting on all the factors at risk (LFI factors)). It can be expressed mathematically as

$$R = \sum R_{i,i} = \sum V_i \cdot F_i$$

Equation 7

$$R = V_N \cdot F_N + V_O \cdot F_O + V_M \cdot F_M + V_{CO} \cdot F_{CO} + V_{CO2} \cdot F_{CO2} + V_{MC} \cdot F_{MC} + V_{WT} \cdot F_{WT} + V_{WD} \cdot F_{WD} \quad \text{Equation 8}$$

Where V equals the weight of risk, F equals the LFI factor level, and the subscript are defined in Table 5. A graphical representation of the risk assessment index factors is showed in Figure 20. This is a diagram that illustrates the eight different parameters contributing to the risk of fire outbreak. As mentioned by the method described by Millet and Saaty [69] each level F_i is assigned a value between 0, 5, or 10 which can be later substituted into Equation 9. The choice between 0, 5, or 10 corresponds to low, medium, and high value of each LFI factor, respectively. LFI factor values can be easily obtained on the field from the data acquired from the monitoring wells. The measurement of each parameter falls within a specific range which corresponds to different severity levels. The descriptions of the eight LFI factors performed in the previous section: “5.2 Landfill Fire Index Factors” was used to obtain the final values of the Landfill Fire Index (LFI) factors in Figure 20.

Table 5

Explanation of symbols used in Equation 9

Symbol	Description
N	Probability or Risk factor relative to Residual nitrogen levels
O	Probability or Risk factor relative to Oxygen Exceedance levels
M	Probability or Risk factor relative to Methane levels
CO	Probability or Risk factor relative to Carbon Monoxide levels
CO ₂	Probability of Risk factor relative to Carbon Dioxide levels
MC	Probability or Risk factor relative to Moisture Content levels
WT	Probability or Risk factor relative to Well Temperature values
WD	Probability or Risk factor relative to Buried Waste Density values

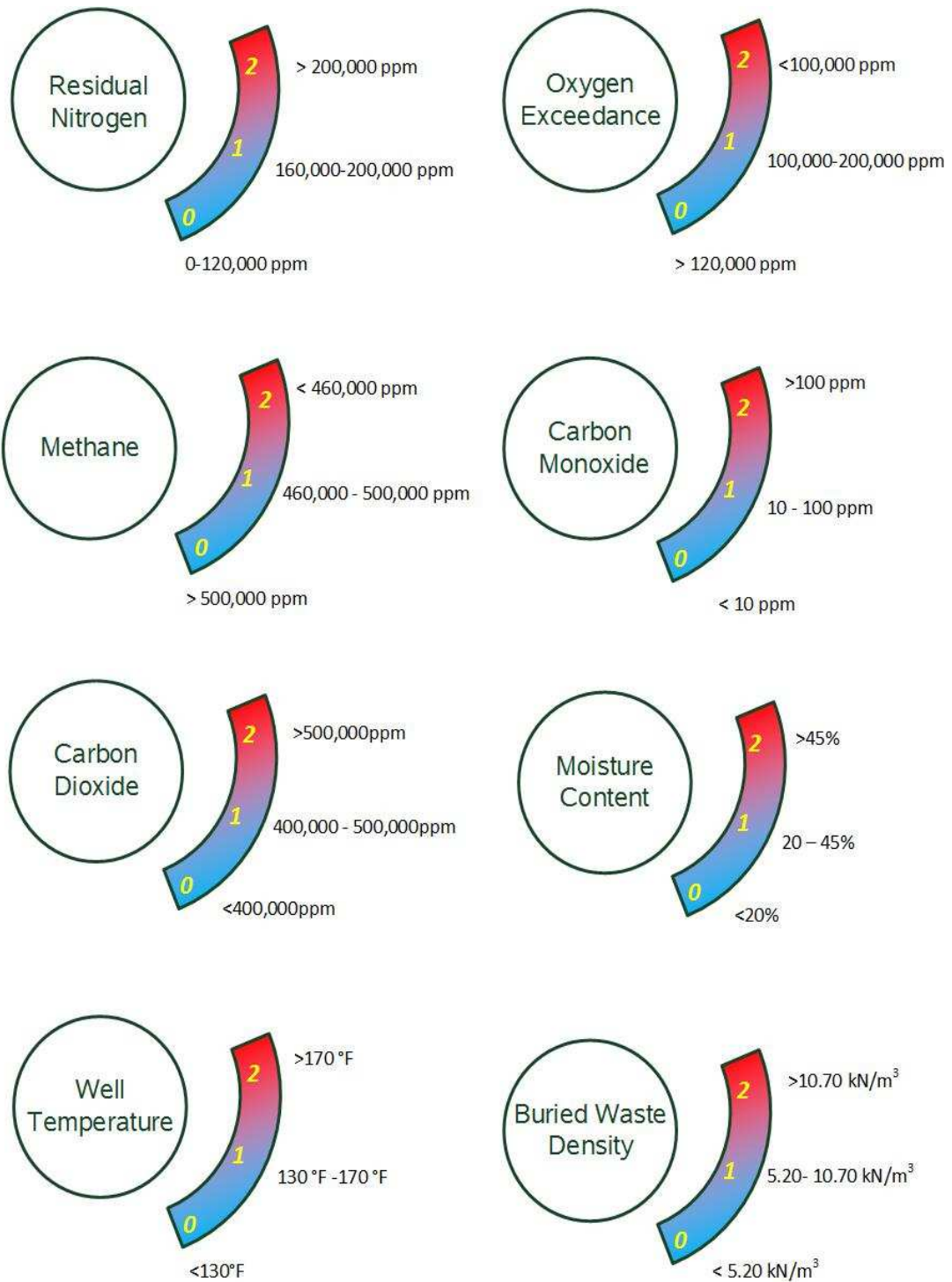


Figure 20. Landfill Fire Index factors: the eight parameters of the LFI

AHP was used to calculate the magnitude of weight coefficient, V_i for the 8 criteria, i . In this method, the criteria are compared in terms of importance in pairs. A comparison matrix (PCM) from the method illustrated by Saaty [68] is generated where the criteria in the row is being compared to the criteria in the column or, in mathematical form, the elements $V_{i,i}$ equal 1 and where the general element $V_{i,j}$ is equal to $1/V_{j,i}$. Notably, the relevance of the level F_i in respect to another level F_j is graded based on a standard index scale from 1/9 to 9 with the meaning of each number illustrated in Table 6. Two criteria (nitrogen and carbon monoxide for example) are evaluated at a time in terms of their relative importance. If criterion F_i is exactly as important as criterion F_j , this pair receives an index of 1. Obviously, the criterion F_i has the same importance relative to itself, therefore the diagonal of the matrix contains only values of 1. If F_i is extremely more important than F_j , the matrix element i, j equals 9. For a "less important" relationship, fractions from 1/2 to 1/9 are used. For instance, if F_i is extremely less important than F_j , the rating is 1/9, but all gradations are possible in between.

The numbers 1/8, 1/6, 1/4, 1/2, 2, 4, 6, and 8 are used to express intermediate gradations. For example, a value of 1/2 indicates that the factor F_i is not as "equally important" as the factor F_j but yet it cannot be considered "slightly less important" with respect to F_j . The same concept is true for the rest of the intermediate values.

The elements of the PCM are normalized by dividing each number in a column by its column sum. In this way, the normalized form of the PCM is obtained. The final weights (V_i) are the mean of the elements of each row of this second matrix. These weights are already normalized and together are called “priority vector” of the second matrix. The sum of the elements of the priority vector equals 1.

A statistically reliable estimate of the consistency of the resulting weights is made by calculating the consistency ratio (CR) coefficients. When the CR has a value lower than 0.1 the overall statistical consistency of the Pairwise Comparison

Table 6
Pair comparison rating parameters for AHP

Rating	Description
1/9	Extremely less important
1/7	Far less important
1/5	Much less important
1/3	Slightly less important
1	Equally important
3	Slightly more important
5	Much more important
7	Far more important
9	Extremely more important

Matrix is demonstrated. When this ratio is larger than 0.10 further analysis is required to obtain a more truthful representation of the 8 interdependent factors. When the results are perfectly consistent, the consistency ratio will be equal to zero. With real world systems subject to many variables, the consistency ratio will tend to zero even if it does not exactly match zero. The work of Saaty [68] demonstrated that the calculation of the CR requires to find the Consistency Index (CI) of the PCM to be divided by the Random Index (RI) in Equation 10 and 11. Both of them have no units. On the other hand, the calculation of the CI instead requires to find the maximum Eigen value of the PCM and plug it in Equation 10.

$$CI = \frac{(\lambda_{max} - N)}{(N - 1)} \quad \text{Equation 10}$$

Where N is the number of criteria considered, and λ_{max} is the maximum Eigen value of the PCM. The maximum Eigen value itself is the summation of the elements of the priority vector multiplied one-by-one by the sum of the elements of the PCM columns. In the work of Saaty, a reciprocal matrix was randomly generated using the scale found in Table 7 and then the random consistency index was obtained and proved to be less than 0.10. This Random Index (RI) is found in

literature [68] and depends on the number of criteria that comprise the PCM. The summary of RI from literature is presented in Table 7.

Table 7

Random Index table (Saaty, 1980)

<i>n</i>	1	2	3	4	5	6	7	8	9	10
<i>RI</i>	0	0	0.58	0.90	1.12	1.24	1.32	1.41	1.45	1.49

After that, the CR can be calculated with Equation 11.

$$CR = \frac{CI}{RI}$$

Equation 11

Where CI is the Consistency Index from Equation 10 and RI is the Random Index from Table 7.

5.5 Results Summary of AHP Model

The application of the Landfill Fire Index (LFI) factors and their respective statistical weights was the last step to rank the possibility of hazardous conditions to fire. The results from the application of the Analytical Hierarchy Process (AHP) to all the LFI factors considered is illustrated in Table 8.

Table 8

Pair-wise Comparison Matrix for V_i (Weights of the LFI factors)

Criteria	N	O	M	CO	CO2	MC	WD	WT	V_i
N	1	1	1	1/9	1	1	1	1	0.057
O	1	1	1/4	1/5	5	1/2	1/3	1	0.072
M	1	4	1	1/2	4	1/3	1/2	2	0.114
CO	9	5	2	1	8	2	2	3	0.262
CO2	1	1/5	1/4	1	1	1/7	1/9	1/3	0.025
MC	1	2	3	1/2	7	1	1/2	4	0.158
WD	1	3	2	1/2	9	2	1	3	0.244
WT	1	1	2	1/3	3	1/4	1/3	1	0.068

$$\lambda_{max} = 8.89 \text{ CR} = 0.0909 \ll 0.1$$

Each criteria in the row was compared to the criteria in the column and assigned a value from 1/9 to 9 depending on its importance respect to the criteria in the column. When a criteria in the row is compared onto itself, the element of the Pair-wise Comparison Matrix (PCM) is assigned a value of 1.

For example, Nitrogen is in the first row of the pair-wise comparison matrix (PCM) in Table 8, and when compared to oxygen it was assigned a value of 1. This is because, as explained in section “5.2 Landfill Fire Index Factors”, overpulling of landfill gases like methane is a huge problem that can easily escalate the hazardous conditions of the waste into fire, and when this happens it is the nitrogen level that is mostly affected and shows a level higher than safe conditions. In the same way, the oxygen level is as important because it is directly related to the most hazardous conditions of the waste site which are anaerobic conditions. The same reasoning was applied for the comparison between nitrogen level and all the other criteria, and all the pair-wise comparisons were assigned a value of 1 except for carbon monoxide. In this case, the value given to the comparison is 1/9, in other words nitrogen level is “extremely less important” than carbon monoxide. This is because carbon monoxide is one of the products of fire reactions while nitrogen is not. In particular, it is more likely to have a landfill fire when carbon monoxide levels are high and nitrogen is low than the opposite. With respect to methane, oxygen

exceedance is less important than methane (value of 1/4) because low methane levels indicate overpulling and are a direct cause of temperature increase which is obviously the primary cause of fire onset. Oxygen levels (and in particular, anaerobic conditions) are “much less important” than carbon monoxide because the presence of carbon monoxide is more directly related to combustion reactions than oxygen alone. On the other hand, oxygen is “much more important” than carbon dioxide (and the pair-wise value is equal to 5) because the biodegradation of waste (indicated by the amount of carbon dioxide) is not as dangerous as the temperature increase that can be produced by anaerobic conditions. Similarly, carbon monoxide can be considered in between “far” and “extremely more important” than carbon dioxide (pair-wise value is equal to 8) for the same reason mentioned above. The moisture content in the waste is more important than the oxygen levels (pair-wise value is equal to 2) because the saturated conditions created by high moisture content can increase the pressure and temperature of the system and thus create uncontrollable hazardous conditions faster than anaerobic conditions. When it is too low, the waste density value can induce immediate structural damage of the waste bulk other than enhancing the propagation of gases around the landfill and thus can be considered “slightly more important” (pair-wise value is equal to 3) than anaerobic conditions. By the same reasoning, waste density comparison with well temperature level is given a value of 3.

The values under the column named " V_i " are the statistical weights needed to complete both Equation 8 and Equation 9. The weight values were obtained from the interpretation of the hazardousness of the eight risk factors described in the previous section: "5.2 Landfill Fire Index Factors". The Eigen vector, λ_{max} equals 8.89 and the consistency ratio, CR equals 0.0909, which is lower than 0.10 thus indicating the consistency of the results. Equation 9 was evaluated for the worst case scenario: when all the risk factors possess the greatest value and therefore are assigned a value of 10. When this happens, the upper limit of the Landfill Fire Index (LFI) is obtained and it equals 10, as expected. In this case, the condition of the landfill is categorized as "Fire Present". This means that the waste site is currently under conditions where it is not possible to prevent a fire outbreak anymore and therefore preventive measures are futile, instead corrective actions are required to take place as soon as possible in order to prevent structural damage, life losses, and environmental disasters.

Equation 9 was applied 4 more times in order to set the rest of the LFI categories from 3 to 10. The names of the final categories are: "Very Low Hazardous Conditions for Fire" (LFI between 0 – 2), "Low Hazardous Conditions for fire" (LFI between 3 – 4), "Moderate Hazardous Conditions for fire" (LFI between 5 – 6), "High Hazardous Conditions for fire" (LFI between 7 – 8), and "Fire

present” (LFI between 9 – 10). The Landfill Fire Index (LFI) in Table 9 is based on the ranking of the LFI factors for a general landfill (Figure 20) and the weights of the different criteria in Table 8. This general instance can be applied to any landfill that provides monitoring wells data of the gas composition and characteristics of the landfill. Experience using LFI could result in being able to use Table 9 to indicate the level of response needed.

Table 9

Landfill Fire Index (LFI)

	Landfill Fire Index	Value
1	Very Low Hazardous Conditions for Fire	0 - 2
2	Low Hazardous Conditions for Fire	3- 4
3	Moderate Hazardous Conditions for Fire	5 - 6
4	High Hazardous Conditions for Fire	7 - 8
5	Fire Present	9 - 10

By reducing the determination of LFI important factors to a series of pairwise comparisons, and then synthesizing the results, the AHP helped to capture both subjective and objective aspects of the decision process. In addition, the AHP incorporates a useful technique for checking the consistency of the results, thus reducing the bias in the LFI factors determination.

5.6 Comparison of Calculated Landfill Fire Index Value for Two Landfills

The repeated application of the Analytical Hierarchy Process (AHP) method resulted in the complete evaluation of Bridgeton (BL) and Burlington County (BCL) Landfill Fire Index (LFI) even when some LFI factors were not recorded in the monitoring well reports. When information about one of the risk factors is missing, it is not appropriate to assume that the weight of that factor is equal to 0. Instead, the calculation of the weights needs to be revised and the pairwise comparison matrix, PCM needs to be normalized without taking into consideration the missing factors.

5.6.1 Bridgeton Landfill (BL). The data available for Bridgeton Landfill was missing the moisture content values and waste density data, therefore the Landfill Fire Index (LFI) was evaluated for 6 factors instead that 8. The results for the weight factors calculations are illustrated in table 10. For Bridgeton landfill, the Eigen vector, λ_{max} equals 8.89 and the consistency ration, CR equals 0.0764, which is greatly lower than 0.1 and proves once again the statistical significance of the results. Monitoring well data from BL are available to the public from official engineering reports [70]. The data relevant to the Analytical Hierarchy Process (AHP) and Landfill Fire Index (LFI) found in this chapter are available in Appendix A.

Table 10

PCM for Bridgeton Landfill weight factors

Criteria	N	O	M	CO	CO2	WT	Vi
N	1	1	1	1/9	1	1/6	0.065
O	1	1	1/4	1/5	5	1/3	0.076
M	1	4	1	1/2	4	1/2	0.17
CO	9	5	2	1	8	2	0.406
CO2	1	1/5	1/4	1	1	1/9	0.04
WT	6	3	2	1/2	9	1	0.244

$\lambda_{max} = 8.89$ CR = 0.0764 < 0.1

The monitoring wells chosen as a real life example for the application of LFI to real landfill fire conditions are GIW-05 and GEW-038. These two wells were selected among hundredths because they are located in the area affected by a known subsurface fire event, therefore they were most likely to exhibit a LFI reflecting “Fire Present” conditions. Particularly, GIW-05 is located exactly on top of the smoldering event whereas GEW-038 is very close to the smoldering event but not on top of it. If the LFI works, it can be predicted that GEW-038 will present a relatively high LFI, but a lower value respect to GIW-05. The location of these wells can be easily identified on the BL map in Appendix B. The relevant data used for the calculation of the LFI for GIW-05 and GEW-038 are found in Table 11.

An additional well presenting fire conditions (GEW-028R) was taken into account for BL but this time the data (Appendix A) was recorded in 2015 instead that 2013

as it is the case for GIW-05 and GEW-038. On the other hand, GEW-028R was chosen because it can be compared to the data collected during the same year of 2015 for wells of Burlington County Landfill (BCL) which are not located near known fires and do not present hazardous conditions. Landfill gas composition and properties were examined for well GEW-028R only for the period of time corresponding to July-October 2015. The only records available about the oxygen composition for GEW-028R are dated October 2015 but the rest of the risk factors values were recorded on July 9th 2015. Table 11 summarizes these findings. The LFI weight values, previously calculated, were combined with the results from the pair-wise comparison matrix, PCM, in Table 10 by substituting in the terms of Equation 9. Applying Equation 9 to the data from well GIW-05, one obtains a LFI of 10 (Figure 11). In a similar manner, Equation 9 was applied to the data of GEW-038 and resulted in a LFI equal to 7.37, whereas the application of Equation 9 to the data from GEW-28R resulted into a LFI of 9.81. The summary of the results of the LFI factors and the overall LFI determination for GIW-05 and GEW-038 is illustrated in Table 12 and Table 13 respectively.

Table 11

Summary of data from monitoring wells in Bridgeton Landfill

Risk Factor, F _j	GIW-10	GEW-038	GEW-028R	GEW-10
Residual Nitrogen (ppm)	281,000	20,000	290,000	39,000
Oxygen Exceedance (ppm)	3000	65,000	33,000	0
Methane (ppm)	12,000	56,000	40,000	530,000
Carbon Monoxide (ppm)	0	1,800	2,700	0
Carbon Dioxide (ppm)	704,000	630,000	400,000	360,000
Moisture Content (%)	N/A	N/A	N/A	N/A
Monitoring Well Temperature	172 °F	121 °F	194.2 °F	90 °F
Buried Waste Density (kN/m ³)	N/A	N/A	N/A	N/A

As expected, the LFI factors for the well located on top of the subsurface event (GIW-05) present a value of 10 (the highest value). LFI factors for GEW-028R instead are all equal to 10 except for the carbon dioxide content which is at a level quantitatively between the lowest and the highest level of hazardousness and therefore was assigned a middle value of 5. The results from the LFI calculations show a value of 9.81 out of 10 which is extremely high and falls into the category of “Fire Present” (Table 14). This means that the LFI value can indeed indicate the hazardous subsurface fire conditions present in Bridgeton Landfill (BL). The results were validated by reports of smoldering or landfill fires by contacting specific landfills within the study area [6], [70].

Table 12

Final Landfill Fire Index for GIW-05 (BL)

Risk Factor, Fj	GIW-10	Vi	Fj
Residual Nitrogen (ppm)	281,000	0.65	10
Oxygen Exceedance (ppm)	8,000	0.076	10
Methane (ppm)	11,000	0.17	10
Carbon Monoxide (ppm)	3,200	0.406	10
Carbon Dioxide (ppm)	700,000	0.04	10
Moisture Content (%)	N/A	N/A	N/A
Monitoring Well Temperature	172 °F	0.244	10
Buried Waste Density (kN/m3)	N/A	N/A	N/A
Risk			
LFI = 10		Assessment :	Fire Present

Table 13

Final Landfill Fire Index for GEW-038 (BL)

Risk Factor, Fj	GEW-038	Vi	Fj
Residual Nitrogen (ppm)	20,000	0.65	10
Oxygen Exceedance (ppm)	65,000	0.076	10
Methane (ppm)	56,000	0.17	10
Carbon Monoxide (ppm)	1,800	0.406	10
Carbon Dioxide (ppm)	630,000	0.04	10
Moisture Content (%)	N/A	N/A	N/A
Monitoring Well Temperature	121 °F	0.244	0
Buried Waste Density (kN/m3)	N/A	N/A	N/A
LFI = 7.37		Risk Assessment:	High Hazardous Conditions for Fire

Table 14

Final Landfill Fire Index for GEW-028R (BL)

Risk Factor, Fj	GIW-028R	Vi	Fj
Residual Nitrogen (ppm)	290,000	0.65	10
Oxygen Exceedance (ppm)	33,000	0.076	10
Methane (ppm)	40,000	0.17	10
Carbon Monoxide (ppm)	2,700	0.406	10
Carbon Dioxide (ppm)	400,000	0.04	5
Moisture Content (%)	N/A	N/A	N/A
Monitoring Well Temperature	194.2 °F	0.244	10
Buried Waste Density (kN/m3)	N/A	N/A	N/A
Risk Index =		Risk	
9.81		Assessment:	Fire Present

The last monitoring well belonging to BL that was analyzed was GEW-10. This well was chosen because it is located far away from the location of the smoldering event (Appendix C). Relevant data used for the calculation of the LFI for GEW-10 is illustrated in Table 15. The outcome from the pair-wise comparison matrix, PCM, is still in Table 10 and substituting the LFR factors value into Equation 9 results in an LFI of 0.760. The results of the LFI factors and overall LFI determination for GEW-10 are illustrated in Table 15. As expected, their distance from the smoldering event (Appendix C) affects the result of the LFI. The farther away from a subsurface fire, the lower the value of the LFI and therefore the lowest level of hazardousness of the landfill conditions with respect to fire. This well was taken into consideration because it is an example of non-hazardous conditions in BL and thus verifies that in absence of fire conditions the LFI results in the final category “Very Low Hazardous Conditions for Fire”.

Table 15

Final Landfill Fire Index for GEW-10 (BL)

Risk Factor, Fj	GEW-10	Vi	Fj
Residual Nitrogen (ppm)	39,000	0.65	0
Oxygen Exceedance (ppm)	0	0.076	10
Methane (ppm)	530,000	0.17	0
Carbon Monoxide (ppm)	0	0.406	0
Carbon Dioxide (ppm)	360,000	0.04	0
Moisture Content (%)	N/A	N/A	N/A
Monitoring Well Temperature	90 °F	0.244	0
Buried Waste Density (kN/m3)	N/A	N/A	N/A
Risk Index =			
.760		Risk Assessment:	Very Low Hazardous Conditions for fire

Some discussion has to be made about the choice of the monitoring wells which affects the overall success of the LFI. First of all, this LFI is only able to make an estimate of the hazardousness of the landfills conditions and does not represent a measure of risk. Transforming the Landfill Fire Index into a Risk Index was outside of the scope of this thesis and is left as future work. In order to make the results of the Analytical Hierarchy Process (AHP) statistically significant, more than 200 data points are required to be regressed into an equation. Another important part of the statistical process is the determination of outliers from the mathematical representation of risk. Ideally, one would have to record hundreds of data from three representative wells located in the fire zone, far away from the fire zone, and in between fire and non-fire zone respectively. Also, the mathematical analysis should be repeated several times for the same wells but at different times: before, during, and after the smoldering event took place.

Even though the statistical study described in this thesis covers only 4 data points, the wells analyzed are the best available and are definitely significant to the scope of this thesis because they are located in the smoldering zone (GIW-05), far away from the smoldering zone (GEW-10), and in between smoldering and non-smoldering zone(GEW-038).

Underground combustion can happen anywhere in the interior of the landfill and the decomposition process takes place continuously for the entire life of the landfill. There is not accurate information available in the literature review to establish exactly how long it takes for the mixture of materials that waste is composed of to reach the ignition point. This is due to the fact different landfills collect very different constituents and it is very difficult to monitor the exact conditions of the waste at any given point in time or space. For this reason, this analysis focused only on the few points in space at one point in time that turned out to be relevant for the purpose of this thesis. If the landfill is operated properly it will never catch fire; therefore, the application of the LFI described in this thesis can be used as an assessment tool to understand the conditions of the landfill and so that preventive measures can be established before an environmental disaster can occur.

5.6.2 Burlington County Landfill (BCL). Monitoring well data collected for May 2015 by SCS Engineers [71] in Burlington County Landfill (BCL) was analyzed for hazardous conditions leading to fire. BCL divided the facility into two separate landfills, 1 and 2. SCS engineers conducted well-field monitoring in both BCL 1 and 2 to satisfy the EPA's New Source Performance Standards (NSPS) [71]. The data available for BCL are missing information about the moisture content values, carbon monoxide and waste density, and therefore the Landfill

Fire Index (LFI) was evaluated for 5 factors instead that 8. The results for the weight factors calculations are illustrated in Table 16. For Bridgeton landfill, the Eigen vector, λ_{max} equals 5.315 and the consistency ration, CR equals 0.0787, which is lower than 0.1 and showed the consistency of the results.

Table 16

PCM for Burlington County Landfill weight factors

Criteria	N	O	M	CO2	WT	Vi
N	1	1	1	1/9	1/6	0.069
O	1	1	1/4	1/5	1/3	0.074
M	1	4	1	1/2	½	0.178
CO	9	5	2	1	2	0.429
WT	6	3	2	1	1	0.251
$\lambda_{max}= 5.315$ CR = 0.0787 << 0.1						

The vertical extraction wells, horizontal collectors and leachate cleanouts were read at least once a month. The landfill gas (LFG) collectors were monitored for gas quality, static pressure, and gas temperature by using a landfill gas analyzer (Landtee GEM-2Nav or GEM 2000). The following gases were monitored for gas quality: methane, carbon dioxide, oxygen and the balanced gas, nitrogen. The wells were adjusted when they did not meet operational guidelines or exceeded concentration limits set by NSPS. Under NSPS, monitoring wells must not exceed a concentration of over 5% oxygen. Site flows are averaged over a

month period, and divided by the total number of minutes in that month to determine the average methane concentration. Monitoring of the landfill under EPA's NSPS standards includes: flare temperatures, flare run times and LFG combusted, system downtime, and startup, shutdown and malfunction reporting. Monitoring of the landfill under EPA's NSPS standards includes: flare temperatures, flare run times and LFG combusted, system downtime, and startup, shutdown and malfunction reporting. The monthly averages for concentrations were used to compare risk factors. Table 17 lists the risk factor values for BCL 1, 2 (West), 2 (East) and the data provided by SCS Engineering.

Table 17

LFI Factors Assessment for Burlington County Landfill (BCL)

Risk Factor, F_j	Landfill 1	Landfill 2 (East)	Landfill 2 (West)
Residual Nitrogen (ppm)	148,000	100,000	145,000
Oxygen Exceedance (ppm)	6,000	15,000	53,000
Methane (ppm)	460,000	470,000	328,000
Carbon Monoxide (ppm)	N/A	N/A	N/A
Carbon Dioxide (ppm)	360,000	360,000	360,000
Moisture Content (%)	N/A	N/A	N/A
Monitoring Well Temperature	91.3 °F	105 °F	105 °F
Buried Waste Density (kN/m ³)	N/A	N/A	N/A

The LFI factor values, previously calculated, were combined with the results from the pair-wise comparison matrix, PCM, in Table 16 by substituting in the terms of Equation 9. The results of the LFI for the areas named Landfill 1, Landfill 2 (east), and Landfill 2 (West) are 0/10, 0/10, and 1.26 respectively. Table 18, Figure 19, and Figure 20 illustrates the summary for the evaluation of the BCL Landfill Fire Index (LFI) for all the parts in which BCL is divided (1, 2 West, 2 East respectively). As showed, all the LFI factors for BCL 1 present the lowest LFI factor values with a final LFI of 0/10. This means that all those conditions are absolutely stable and non-hazardous and falls into the category of "Very Low Hazardous Conditions for Fire". The same can be said for BCL 2 (West) which has the lowest LFI factors with a final LFI of 0/10. On the other hand, the oxygen exceedance and the methane are present at a level which is in between the lowest and highest level of hazardousness and therefore was assigned a middle value of 5. The results from the LFI calculations show a value of 1.26 out of 10 which is still low and falls into the category of "Very Low Hazardous Conditions for Fire". These results agree with the engineering reports available from SCS Engineering which never reported any subsurface event or fire in BCL.

Table 18

LFI for BCL - Landfill 1

Risk Factor, Fj	Landfill 1	Vi	Fj
Residual Nitrogen (ppm)	148,000	0.069	0
Oxygen Exceedance (ppm)	6,000	0.074	0
Methane (ppm)	460,000	0.178	0
Carbon Monoxide (ppm)	N/A	N/A	N/A
Carbon Dioxide (ppm)	361,000	0.429	0
Moisture Content (%)	N/A	N/A	N/A
Monitoring Well Temperature	91.3 °F	0.251	0
Buried Waste Density (kN/m3)	N/A	N/A	N/A
LFI = 0		Risk Assessment:	Very Low Hazardous Conditions for Fire

Table 19

LFI for BCL - Landfill 2 (East)

Risk Factor, Fj	Landfill 2 (East)	Vi	Fj
Residual Nitrogen (ppm)	100,000	0.069	0
Oxygen Exceedance (ppm)	15,000	0.074	0
Methane (ppm)	470,000	0.178	0
Carbon Monoxide (ppm)	N/A	N/A	N/A
Carbon Dioxide (ppm)	275,000	0.429	0
Moisture Content (%)	N/A	N/A	N/A
Monitoring Well Temperature	105 °F	0.251	0
Buried Waste Density (kN/m3)	N/A	N/A	N/A
LFI = 0		Risk Assessment:	Very Low Hazardous Conditions for Fire

Table 20

LFI for BCL - Landfill 2 (West)

Risk Factor, Fj	Landfill 2 (West)	Vi	Fj
Residual Nitrogen (ppm)	145,000	0.069	0
Oxygen Exceedance (ppm)	53,000	0.074	5
Methane (ppm)	328,000	0.178	5
Carbon Monoxide (ppm)	N/A	N/A	N/A
Carbon Dioxide (ppm)	360,000	0.429	0
Moisture Content (%)	N/A	N/A	N/A
Monitoring Well Temperature	105 °F	0.251	0
Buried Waste Density (kN/m3)	N/A	N/A	N/A
		Risk	Very Low Hazardous
LFI = 1.26		Assessment:	Conditions for Fire

5.7 Comparison of AHP for 4 and 7 factors

The statistical work illustrated in the previous sections showed how the Analytical Hierarchy Process (AHP) can be reproduced for different number of factors. In particular, the process was used to calculate the ideal scenario when all 8 criteria are available for data collection. In this way the Landfill Fire Index (LFI) chart was obtained. Successively, the data available for Bridgeton Landfill (BL) and Burlington County Landfill (BCL) provided the required information for executing the AHP process for 6 and 5 criteria. In the following paragraphs, the application of the AHP analysis will be analyzed also for 4 and 7 factors instead that 8.

Table 21 contains the Pair-wise Comparison Matrix (PCM) for 7 criteria. Carbon Dioxide was purposely omitted because out of all the factors it is the criteria which affects hazardous conditions less directly. The elements of the PCM were left unaltered from the original comparison matrix in Table 7. The resulting Eigen vector, λ_{max} equals 7.75 and the consistency ration, CR equals 0.094, which is lower than 0.1 thus indicating the consistency of the results. The values for the weights, V_i are found the last column of Table 21

Table 21

PCM for 7 criteria

Criteria	N	O	M	CO	MC	WT	WD	Vi
N	1	1	1	1/9	1	1	1	0.057
O	1	1	1/4	1/5	1/2	1/3	1	0.072
M	1	4	1	1/2	1/3	1/2	2	0.114
CO	9	5	2	1	2	2	3	0.262
MC	1	2	3	1/2	1	1/2	4	0.025
WT	1	3	2	1/2	2	1	3	0.158
WD	1	1	1/2	1/3	1/4	1/3	1	0.244

$$\lambda_{max} = 7.75 \text{ CR} = 0.0942 < 0.1$$

The AHP process was repeated once again to find the PCM for 4 criteria (Table 22). In this case the resulting Eigen vector, λ_{max} equals 4.11 and the consistency ratio, CR equals 0.043, which is lower than 0.1 thus indicating the consistency of the results. After removing carbon dioxide from the list of the initial 8 criteria, the successive factors omitted were nitrogen, moisture content, and waste density. For the sake of the statistical analysis, what was left is oxygen, methane, carbon monoxide, and well temperature. By comparing the AHP results from both Table 21 and Table 22 it is noticeable that the value for carbon monoxide is the only one that significantly changed. In fact, its Vi value almost doubled from 0.262 to 0.452 from 7 criteria down to 4. In other words, as the number criteria decreased, the importance of carbon monoxide increased. This can be explained by the fact that carbon monoxide is indeed the most important factors in landfill

fire prevention and fire hazardous conditions identifications. Due to their nature, smoldering events that take place in the depths on the waste mass are not always associated to an extreme high temperature value, instead they are easily identified with high carbon monoxide levels.

Table 22
PCM for 4 criteria

Criteria	O	M	CO	WT	Vi
O	1	1/4	1/5	1/3	0.08
M	4	1	1/2	1/2	0.2
CO	5	2	1	2	0.452
WT	3	2	1/2	1	0.267

$\lambda_{max} = 7.75$ CR = 0.0942 < 0.1

This newly developed Landfill Fire Index (LFI) was successfully employed to assess the conditions of Bridgeton Landfill and Burlington County Landfill, thus proving its effectiveness in pinpointing ongoing and future subsurface events. The LFI can be used by landfill management teams to assess the potential of a landfill fire; thus, helping both the regular and emergency decision process.

Chapter 6

Conclusions and Future Work

Surprisingly, there are not many published papers about monitoring landfill fires. This is the first study to evaluate an interdisciplinary method to monitor and predict landfill fire events in United States. Since many landfills and other disposal facilities have closed throughout the past 40 years [16], the number of neglected waste sites increased together with the chance of subsurface events happening. Thus, there are many closed and abandoned waste sites around the United States that need to be monitored for subsurface activities and potential hazardousness. Remote sensing can be used to address this problem by monitoring the thermal signature of these waste sites and locate hotspots. Hotspots can be an indication of fire and hazardous materials contamination that threatens human health and the environment. This thesis presented a non-invasive method of temperature monitoring that allows the collection of enough information such that subsurface events can be detected and be acted upon in a timely manner to ensure the effectiveness of preventive measures. As shown in Chapter 4, it was possible to successfully detect and monitor the exact location of the hotspots that developed in both Atlantic Waste Landfill (AWL), and Bridgeton Landfill (BL). Multi-temporal LST thermal maps were successfully plotted for the two case studies: it was proved that the presence of hotspots is entirely due to

subsurface events inside the landfills and that they can be remotely sensed through the application of the LST detection Matlab code. Given the availability of public data from USGS Explorer satellite images database, the same method can be applied to any other landfill present on US territory to predict onsets of fire.

Safety is an important component to the health and well-being of individuals in all types of settings. In order to safeguard safety, assessments of hazardous conditions are implemented wherever possible, especially in environments such as landfills where different threatening scenarios may occur. Due to their importance, landfills require an assessments of hazardous conditions that is practical, sustainable, and easy to understand. The Landfill Fire Index (LFI) here proposed is generic enough to allow its application to landfills of different sizes, complexity or geographic reach. At the same time, the LFI in this paper can be considered extremely useful and sustainable for decision-making because it takes into account the diversity of all the particular factors that are landfill specific. The results shown in the previous chapter illustrate how AHP was successfully applied to different landfills to create the LFI and thus assess the hazardousness of landfills conditions. Data from several monitoring wells from both Bridgeton Landfill (BL) and Burlington County Landfill (BCL) were used to calculate their LFI. In particular, BL is experiencing a subsurface event in its Southern region

while BCL is not experiencing hazardous conditions. The LFI in both landfills was able to describe the conditions in both BL and BCL. The use of the LFI could be able to evaluate how substantial the possibility of hazardous fire conditions are in any landfill in the United States, thus localizing possible fire outbreaks and to lay the groundwork for risk response for fire prevention.

Landfill fires are an ongoing problem that can be detrimental to the surrounding environment, by infiltrating the surrounding water tables, soil, and releasing volatile particles into the atmosphere. In fact, current methods for fire preventions are inadequate since they are useful to fire detection only after a fire has already occurred. As the impact of landfill fires is studied more, various methods have been researched into how to predict and prevent them. However, a preliminary detection method in the form of LFI eliminates expensive clean-up costs and environmental catastrophe. During the completion of the LFI, the primary characteristics that increase a landfill's susceptibility to fire were identified and analyzed to find the ranges that increased fire potential. The eight LFI factors identified were: residual nitrogen, oxygen exceedance, methane level, carbon monoxide level, carbon dioxide level, moisture content, monitoring well temperature, and buried waste density. The completed LFI can be used by landfill personnel during their weekly monitoring well checks, and can become additional monthly landfill protocol. This method ensures the safety and health of landfill

personnel, the surrounding communities and environment and reduces the risk of fire fighter fatalities. Landfill operators can use the LFI to aid them in avoiding possible fire catastrophes and allow them to take preliminary measures that reduce economic and environmental costs.

Several recommendations can be made regarding the future work that can be implemented to this work. Temporal assessment of the Landfill Fire Index (LFI) can be accomplished so that different wells located on the territory that experienced a fire can be analyzed before and after a subsurface event. Also, more landfills should be analyzed and hundreds of data points should be collected to calculate their LFI. The remote sensing analysis should be completed for other waste sites around US along with the application of the LST detection for hotspots recognition. The final goal is the development of a system for comparison of the LFI to the satellite data from the LST detection code and incorporate this method to a satellite-based landfill monitoring system, which will use thermal infrared observations from Landsat satellites to assess the thermal state of the landfill surface and identify anomalous thermal patterns and anomalous changes in the thermal state of any landfill in the United States. This information will further be used to issue warnings of potential landfill fires. The results generated from this

study are a perfect data input for the monitoring system, involving an efficient satellite image classification algorithm and a physically-based land surface temperature retrieval algorithm.

Thermal remote sensing is indeed an effective tool to monitor landfill internal activities and a great method to predict fire outbreaks and thus prevent possible environmental disasters. It is hoped that thanks to this method, collaboration with public health departments will be possible and will result in public health messaging being issued once a fire outbreak will be detected or considered imminent.

References

- [1] USGS - United States Geological Survey, "Earth Explorer," NASA,[Online]. Available: <http://earthexplorer.usgs.gov/>. [Accessed 6 June 2016].
- [2] D. Landgrebe, "Computer-Based Remote Sensing Technology: A look to the future.," *Remote Sensing of the Environment*, vol. 5, pp. 229-246, 1976.
- [3] J. B. Campbell, *Introduction to Remote Sensing*, New York - London: The Guildford Press, 2007.
- [4] F. Cecchi, P. Pavan, A. Musacco, J. Mata-Alvarez and G. Vallini, "Digesting the organic fraction of municipal solid waste: Moving from mesophilic (37°C) to thermophilic (55°C) conditions," *Waste Management Resources*, vol. 11, p. 403–414, 1993.
- [5] Johnson County Department of Public Health, "After Action Review – Air Quality Monitoring Activities during Iowa City Landfill Fire," Johnson County Department of Public Health, Johnson County, Iowa, 2012.
- [6] Thalhamer, Todd, "Data Evaluation of the Subsurface Smoldering Event at the Bridgeton Landfill," Hammer Consulting Service, Cameron Park, CA, 2013.
- [7] T. Thalhamer, "Fires at Solid Waste Facilities, Landfill Fire Guidance Document," CalRecycle, 2010.
- [8] J. DeHann, *Kirk's Fire Investigation*, 6th ed., Upper Saddle River, New Jersey: Pearson Prentice Hall, 2007.

- [9] J. Martin, T. Stark, T. Thalhamer, G. Gerbasi and R. Gortner, "Detection of Aluminum Waste Reactions and Waste Fires," *Journal of Hazards, Toxic, and Radioactive Waste*, vol. 17, no. 3, pp. 164-174, 2013.
- [10] T. G., H. Theisen and S. Vigil, *Integrated Solid Waste Management: Engineering Principles and Management Issues*, McGraw Hill, 1993.
- [11] F. B. DeWalle, E. S. K. Chian and E. Hammerberg, "Gas production from solid waste in landfills," *Journal of Environmental Engineering (ASCE)*, vol. EE3, no. 104, p. 415-432, 1978.
- [12] K. E. Hartz, R. E. Klink and R. K. Ham, "Temperature effects: methane generation from landfill samples," *Journal of Environmental Engineering (ASCE)*, vol. 108, no. 4, p. 629-638, 1982.
- [13] J. F. Rees, "The fate of carbon compounds in the landfill disposal of organic matter," *Journal of Chemical Technology and Biotechnology*, vol. 30, no. 4, pp. 161-175, 1980.
- [14] D. Houi, E. Paul and C. Couturier, "Heat and mass transfer in landfills and biogas recovery," in *Proc., 6th Int. Waste Management and Landfill Symp*, Pisa, Italy, 1997.
- [15] G. J. Farquhar and F. A. Rovers, "Gas production during refuse decomposition," *Water, Air, & Soil Pollution*, vol. 4, no. 2, p. 483-495, 1973.
- [16] FEMA/USFA, "Landfill Fires: Their Magnitude, Characteristics and Mitigation," Federal Emergency Management Agency, Arlington, Virginia, 2002.

- [17] P. Foss-Smith, "Understanding landfill fires," Waste Management World, 1 August 2010. [Online]. Available: <https://waste-management-world.com/a/understanding-landfill-fires>. [Accessed 8 July 2016].
- [18] J. Hanson, N. Yesiller, S. Von Stockhausen and W. Wong, "Compaction Characteristics of Municipal Solid Waste," Journal of Geotechnical and Geoenvironmental Engineering, vol. 136, no. 8, pp. 1095-1102, 2010.
- [19] EPA, "Subsurface Heating Events at Solid Waste and Construction and Demolition Debris Landfills: Best Management Practices," Ohio Environmental Protection Agency, EPA, Ohio, 2011. S, 2011.
- [20] N. O. a. A. A. -. NOAA, "NOAA's Geostationary and Polar-Orbiting Weather Satellites," 5 March 2014. [Online]. Available: <http://noaasis.noaa.gov/NOAASIS/ml/genlsatl.html>. [Accessed 6 July 2016].
- [21] NASA, "Benefits to you," Landsat Science, 2 July 2016. [Online]. Available: http://landsat.gsfc.nasa.gov/?page_id=3510. [Accessed 6 July 2016].
- [22] US Dept of Commerce, National Oceanic and Atmospheric Administration, National Weather Service, "Weather Satellites," JetStream, [Online]. Available: <http://www.srh.noaa.gov/srh/jetstream/remote/satellite.html>. [Accessed 6 July 2016].
- [23] S. K. a. T. H. v. d. Haar, Satellite meteorology - An introduction, Academic Press, 1995.
- [24] U.S. Geological Survey, "Landsat Project Description," U.S.G.S., 1 December 2015. [Online]. Available: http://landsat.usgs.gov/about_project_descriptions.php. [Accessed 27 May 2016].

- [25] S. J., J. C. J.-. M. A. and L. Paolini, "Land Surface temperature retrieval from Landsat TM 5," *Remote Sensing of Environment*, vol. 90, no. 4, pp. 434-440, 2004.
- [26] P. Tyagi and U. Bhosle, "Atmospheric correction of remotely sensed Images in Spatial and Transform Domain," *International Journal of Image Processing*, vol. 5, no. 5, pp. 564-579, 2011.
- [27] K. A. Y. and A.-E. A., "Assessment of Kuwait's Al-Qurain Landfill Using Remotely Sensed Data," *Journal of Environmental Science and Health, Part A: Toxic/Hazardous Substances and Environmental Engineering*, vol. 39, no. 2,, pp. 351-364, 2004.
- [28] P. R. T. Yang K., M. Y., K. T., W. M. M., C. S. J., Z. Y. and S. P., "Evaluation of satellite estimates of downward shortwave radiation over the Tibetan Plateau," *Journal of Geophysical Research*, vol. 113, no. D17204, 2008.
- [29] NSIDC, "Remote Sensing: Visible," National Snow & Ice Data Center, 2016. [Online]. Available: https://nsidc.org/cryosphere/seaice/study/visible_remote_sensing.html. [Accessed 8 July 2016].
- [30] N. M. Shor, "Vegetation Applications: Agriculture, Forestry, and Ecology," EOS-Goddard Program Office. NASA, 1 November 2005. [Online]. Available: https://fas.org/irp/imint/docs/rst/Sect3/Sect3_1.html. [Accessed 4 August 2016].
- [31] Copernicus Global Land Service, "Land Surface Temperature," Copernicus. Europe's Eyes on Earth, 2016. [Online]. Available: <http://land.copernicus.eu/global/products/lst>. [Accessed 03 June 2016].

- [32] S. C. Freitas, I. F. Trigo, J. Macedoa, C. Barroso, R. Silva and R. Perdigão, "Land surface temperature from multiple geostationary satellites," *International Journal of Remote Sensing*, vol. 34, no. 9–10, p. 3051–3068, 2013.
- [33] M. Jin, "Analysis of Land Skin Temperature Using AVHRR Observations," *Bulletin of the American Meteorological Society*, vol. 85, p. 587–600, 2004.
- [34] M. Jin, R. E. Dickinson and D.-L. Zang, "The footprint of urban areas on global climate as characterized by MODIS," *Journal of Climate*, vol. 18, pp. 1551-1565, 2005.
- [35] Y. Yu, C. S. Nat. Oceanic & Atmos. Adm., J. L. Privette and A. C. Pinheiro, "Evaluation of Split-Window Land Surface Temperature Algorithms for Generating Climate Data Records," *IEEE Transactions on Geoscience and Remote Sensing*, vol. 46, no. 1, pp. 179-192, January 2008.
- [36] J. J. Settle, N. A. Bharmal, G. J. Robinson and A. Slingo, "Sampling Uncertainties in Surface Radiation Budget Calculations in RADAGAST," *Journal of Geophysical Research*, vol. 113, no. D13, 16 July 2008.
- [37] Peg Shippert, "Digital Number, Radiance, and Reflectance," Harris geospatial solutions, 23 August 2013. [Online]. Available: <http://www.harrisgeospatial.com/Home/NewsUpdates/TabId/170/ArtMID/735/ArticleID/13592/Digital-Number-Radiance-and-Reflectance.aspx>. [Accessed 06 June 2016].
- [38] G. B. Franca and A. P. Cracknell, "Retrieval of land and sea surface temperature using NOAA-11 AVHRR data in north-eastern Brazil," *International Journal of Remote Sensing*, vol. 15, pp. 1695-1712, 1994.

- [39] Patrick, Minnis; Mandana, M., Khaiyer,, "Anisotropy of Land Surface Skin Temperature Derived from Satellite Data," NASA, Hampton, Virginia, 1999.
- [40] M. Akul, "Introduction to the Electromagnetic Spectrum and Spectroscopy," Pharma Change, 24 August 2011. [Online]. Available: <http://pharmaxchange.info/press/2011/08/introduction-to-the-electromagnetic-spectrum-and-spectroscopy/>. [Accessed 28 June 2016].
- [41] Irons, R. James;, "The Thematic Mapper," NASA, 27 June 2016. [Online]. Available: <http://landsat.gsfc.nasa.gov/?p=3229>. [Accessed 28 June 2016].
- [42] Iron, James R.; Taylor, Michael P.; Rocchio, Laura;, "The Multispectral Scanner System," NASA, 27 June 2016. [Online]. Available: <http://landsat.gsfc.nasa.gov/?p=3229>. [Accessed 28 June 2016].
- [43] C. Chunmei, W. Yuchun, X. Jianjun and Y. Zhaojie, "Remote sensing estimation of Chlorophyll a and suspended sediment concentration in turbid water based on spectral separation," *Optik - International Journal for Light and Electron Optics*, vol. 124, no. 24, p. 6815–6819, 2013.
- [44] M. A. Network, "Electro-Optical Imaging Systems," Federation of American Scientists , [Online]. Available: https://fas.org/man/dod-101/navy/docs/es310/EO_image/EO_Image.htm. [Accessed 28 June 2016].
- [45] Google Earth, 38° 45' 29.56" N and 90° 28' 42.99" , "Bridgeton Landfill," 2 February 2016. [Online]. [Accessed 1 July 2016].
- [46] Google Earth, 37° 03' 25.60" N and 77° 10' 19.67" W, "Atlantic Waste Landfill," 25 October 2014. [Online]. [Accessed 1 July 2016].

- [47] Google Earth, 40° 04' 32" N and 74° 45' 53.86" W, "Burlington County Landfill," 16 April 2016. [Online]. [Accessed 1 July 2016].
- [48] EPA - Environmental Protection Agency, "West Lake Landfill Superfund Site," US Environmental Protection Agency October 2011. [Online]. Available: <https://www.epa.gov/mo/west-lake-landfill>. [Accessed 1 April 2016].
- [49] Tony Sperling, "Review of Subsurface Self Sustaining Exothermic Reaction Incident at Bridgeton Landfill," Landfill Fire Control Inc., North vancouver, 2015.
- [50] Tony Sperling, "Data Evaluation of the Subsurface Smoldering Event at the Bridgeton Landfill," Hammer Consulting Service, Cameron Park, CA, 2013.
- [51] Associated Press, "State issues notices of violation to Sussex County Landfill," The Washington Times, 4 January 2016.
- [52] B. County, "Solid Waste," [Online]. Available: <http://www.co.burlington.nj.us/344/Solid-Waste>. [Accessed 29 June 2016].
- [53] S. Thomas, "SOLID WASTE FACILITY PERMIT - Burlington Landfill," Division of Solid and Hazardous Waste, Trenton, 1999.
- [54] Center of Earth Observation - Yale, "Converting Digital Numbers to Top of Atmosphere (ToA) Reflectance," 2013. [Online]. Available: http://www.yale.edu/ceo/Documentation/Landsat_DN_ti_Reflectance.pdf. [Accessed 10 January 2016].

- [55] C. Gyanesh, L. M. Brian and L. H. Dennis, "Summary of Current radiometric calibrations coefficients for Landsat MSS, TM, ETM+ & E 0-1 ALI Sensors," *Remote Sensing of the Environment*, vol. 113, pp. 893-903, 2009.
- [56] J. Zhang, Y. Wang and Y. Li, "A C++ program for retrieving land surface temperature from the data of Landsat TM/ETM+ Band6," *Computers and Geosciences*, vol. 32, no. 10, pp. 1796-1805, 2006.
- [57] Q. Weng, D. Lu and J. Schubring, "Estimation of Land Surface Temperature-vegetation abundance relationship for urban heat island studies," *Remote Sensing of the Environment*, vol. 89, no. 4, pp. 467-483, 2004.
- [58] M. Buettner, "Landfill creating road woes in region," *The Progress-Index*, 3 April 2016.
- [59] P. Moy, "A health risk comparison of landfill disposal and waste-to-energy (WTE) treatment of municipal solid wastes in New York City (NYC).(Master Thesis)," Earth Engineering Center, Columbia University , New York City, New York, 2005.
- [60] A. S. Farah, O. Dasimah and K. Subramaniam, "Environmental Health Impact Assessment of a Sanitary Landfill in an Urban Setting," *Procedia - Social and Behavioral Sciences*, vol. 85, pp. 82-91, 2013.
- [61] D. Prasher, T. C. P. Morata, L. Fechter, A. C. Johnson, S. P. Lund, K. Pawlas, J. Starck, M. Sliwinska-Kowalska and W. Sulkowski, "A European Commission research project on the effects of exposure to noise and industrial chemicals on hearing and balance," *Noise Health*, vol. 4, no. 14, pp. 41-48, 2002.

- [62] F. Catherine, M. Christian and L. Anders, "Gas Emission from Landfills. An overview of issues and research needs," Swedish Environmental Protection Agency, Stockholm, 1999.
- [63] E. E. Matthew, "Using residual nitrogen to troubleshoot wellfield performance," in Swana Northern New England and Southern New, 2013.
- [64] Y. M. Shadi, "Characterizing Spontaneous Fires in Landfills," Department of Civil, Environmental and Construction Engineering. University of Central Florida, Orlando, Florida, 2009.
- [65] A. Lagerkvist, "Landfill Technology," Luleå University of Technology, Department of Environmental Engineering, Division of Landfill Science & Technology, Luleå, 1999.
- [66] US Consumer Product Safety Commission, "Carbon Monoxide Questions and Answers," [Online]. Available: <http://www.cpsc.gov/en/Safety-Education/Safety-Education-Centers/Carbon-Monoxide-Information-Center/Carbon-Monoxide-Questions-and-Answers-/>. [Accessed 15 July 2016].
- [67] M. Y. Shadi, "Characterizing Spontaneous Fires In Landfills," Department of Civil, Environmental and Construction Engineering, University of Central Florida, Orlando, Florida, 2009.
- [68] T. L. Saaty, *The Analytic Hierarchy Process: Planning, Priority Setting, Resource Allocation*, McGraw-Hill International Book Co, 1980.
- [69] I. a. S. T. Millet, "On the relativity of relative measures-accommodating both rank preservation and rank reversals in the AHP," . *European Journal of Operational Research*, vol. 121, no. 1, pp. 202-212, 2000.

- [70] Missouri Department of Natural Resources, "Reports - Bridgeton Sanitary Landfill," 1 August 2016. [Online]. Available: <http://dnr.mo.gov/bridgeton/BridgetonSanitaryLandfillReports.htm>. [Accessed 8 August 2016].
- [71] SCS Engineers, "Burlington County Resource Recovery Complex: Monthly Operations and Maintenance Report.," SCS Engineers, Madison, Wisconsin, May 2015.
- [72] T. G., H. Theisen and S. Vigil, *Integrated Solid Waste Management: Engineering Principles and Management Issues*, McGraw Hill, 1993.
- [73] Irons, James R.; Taylor, Michael P.; Rocchio, Laura,, "The Thematic Mapper," NASA, 27 June 2016. [Online]. Available: <http://landsat.gsfc.nasa.gov/?p=3229>. [Accessed 6 James R. Irons June 2016].

Appendix A

Bridgeton Landfill Monitoring Wells Raw Data

GW ID#	Reading Date	CH4 (% Vol.)	CO2 (% Vol.)	Oxygen (% Vol.)	Balance (% Vol.)	Wellhead Temp. (F)	Pressure (In W.C.)	Pump Operational (Y/N)	Comments
GIW-05	04/08/13	0.2	72.4	0	27.4	160	-0.1	N	
GIW-05	04/09/13	0.6	66.7	2.5	30.2	170	-0.3	Y	
GIW-05	04/10/13	0.3	72.5	0.3	26.9	170	-0.2	Y	
GIW-05	04/11/13	0.3	73.2	0.2	26.3	165	-0.5	Y	
GIW-05	04/12/13	0.3	72.5	0.2	27	160	-0.7	Y	
GIW-05	04/13/13	0.3	72.2	0.2	27.3	160	-0.9	Y	
GIW-05	04/14/13	0.2	75.1	0.2	24.5	160	1	Y	
GIW-05	04/15/13	0.7	72.3	0.3	26.7	170	-0.5	Y	
GIW-05	04/16/13	0.9	71.6	0.2	27.3	170	-1.8	Y	
GIW-05	04/17/13	1.8	71.3	0.3	26.6	160	-2.2	Y	
GIW-05	04/18/13	0.3	74.2	0.2	25.3	165	-1	Y	
GIW-05	04/19/13	1.8	69.4	1.2	27.6	165	-2.9	Y	
GIW-05	04/20/13	0.3	71.3	0.2	28.2	165	-2.6	Y	
GIW-05	04/21/13	1.1	70	0.8	28.1	172	-3	Y	
GIW-05	04/22/13	0.2	79.6	0.3	19.9	170	-2	Y	
GIW-05	04/23/13	0.4	71	0.5	28.1	170	-4.2	Y	

April 2013 Wellfield Monitoring Data - Bridgeton Landfill

Well Name	Date Sampled	Methane	CO ₂	O ₂	Balance Gas	Init Temp °F	Adj Temp	Init Flow scfm	Adj Flow	Init Static Press	Adj Static Press	H ₂ O		System Pressure	Baro
												Init Diff Press	Adj Diff Press		
GEW-09	4/2/2013 10:41	54.4	42.9	0	2.7	82	83	5	9	-0.7	-0.7	0.006	0.02	-27.36	29.7
	4/9/2013 10:10	52	43.6	0.3	4.1	87	87	18	19	-0.5	-0.5	0.082	0.089	-23.9	29.26
	4/16/2013 10:26	55.6	44.3	0	0.1	66	68	28	29	-0.1	-0.1	0.19	0.201	-19.17	29.62
	4/23/2013 10:29	50.8	42.2	0.6	6.4	84	84	16	15	-0.5	-0.5	0.068	0.058	-25.31	29.49
	4/29/2013 10:06	52.8	42.5	0.4	4.3	100	100	6	6	-0.6	-0.6	0.012	0.012	-20.69	29.42
GEW-10	4/2/2013 11:18	36.9	57.6	0.2	15.3	102	102	8	8	-15.3	-15.3	0.021	0.024	-25.18	29.67
	4/10/2013 8:46	30.4	62.9	0.1	6.6	106	106	18	16	-12.8	-12.8	0.106	0.09	-17.86	29.19
	4/17/2013 11:23	31.6	55.6	0.5	12.3	108	108			-15.2	-15.2	-0.005	-0.035	-22.27	29.48
	4/22/2013 15:55	30.5	44.1	0.1	25.3	102	102	14	14	-15.2	-15.3	0.049	0.065	-22.15	29.43
	4/22/2013 16:00	31.2	43	0.1	25.7	102	102	15	14	-15.6	-15.6	0.066	0.062	-21.78	29.43
GEW-11	4/29/2013 11:01	31.1	42.7	0.6	25.6	108	108	13	16	-14.3	-14.3	0.051	0.076	-20.09	29.41
	4/10/2013 14:03	11.3	65	0.3	23.4	162	162	34	32	-13.3	-13.1	0.437	0.39	-13.11	29.08
	4/10/2013 9:42	9.8	70.8	0.1	19.3	168	168	24	26	-6.2	-6.3	0.231	0.27	-6.3	29.22
	4/17/2013 14:08	25.1	67.5	0.3	7.1	170	170	26	27	-7.7	-7.7	0.244	0.259	-7.6	29.41
	4/22/2013 16:13	10.1	68.9	0	21	168	168	13	16	-7.1	-7.4	0.073	0.103	-7	29.43
GEW-12A	4/22/2013 16:18	10.7	69.2	0.1	20	168	168	27	27	-8.4	-8.9	0.274	0.287	-9.07	29.43
	4/29/2013 11:48	9.3	66.8	0.6	23.3	170	170	16	20	-9.1	-9.6	0.104	0.161	-10.12	29.42
	4/2/2013 14:12	0.3	69.2	0.8	29.7	110	110			-9.7	-10	-10.876	-8.681	-12.95	29.67
	4/10/2013 9:53	0.3	74.4	0	25.3	170	170	44	42	6.7	3.9	6.492	5.939	1.99	29.2
	4/17/2013 14:16	7.1	65.7	2.2	25	162	162	49	17	4.8	3.8	7.662	9.905	0.67	29.4
GEW-13	4/22/2013 16:26	1.2	67.8	1.1	29.9	148	148	29	29	-1.4	-1.6	2.667	-2.254	-2	29.42
	4/22/2013 16:33	1.4	65.6	1.7	31.3	150	150	26	26	3.4	1.3	2.198	-5.705	3.33	29.42
	4/29/2013 13:39	0.3	65.2	1.8	32.7	156	156	47	1	2.5	1.7	7.019	-2.669	2.5	29.36
	4/10/2013 10:01	0.2	86.4	0	13.4	150	150	2	1	-6.3	-6.4	0.013	0.006	-6.58	29.21
	4/17/2013 16:24	14.1	85.8	0	0.1	140	140	1		-7.3	-7.1	0.002	-0.14	-8.82	29.39
GEW-14A	4/22/2013 16:29	0.2	85.5	0	14.3	146	146			-7.3	-7.1	-0.367	-0.284	-7.16	29.51
	4/29/2013 13:46	0.3	84	0.7	15	154	146	8	1	-8.1	-7.6	-0.383	-0.649	-8.19	29.51
	4/2/2013 14:23	13.3	75	0	11.7	120	120	35	18	-4.9	-4.5	0.438	0.123	-5.43	29.67
	4/10/2013 10:07	12.4	79.5	0	8.1	122	122	16	8	-2.7	-2.8	0.093	0.026	-3.19	29.21
	4/17/2013 14:28	19.5	76.5	0	4	104	104	9	32	-0.3	-0.2	0.031	0.349	-0.41	29.39
GEW-15	4/22/2013 16:14	17	68.3	2.1	12.6	70	70	29	17	-2.7	-2.8	-0.239	-0.149	-2.88	29.51
	4/22/2013 16:20	19.3	74.7	0	6	70	70	29	17	0.7	0.8	0.256	0.095	-2.76	29.51
	4/29/2013 13:49	8.7	60.8	2.8	27.7	80	80	13	8	-0.3	-0.3	0.058	0.022	-0.38	29.36
	4/2/2013 15:07	2.7	72.8	0	24.5	136	136	71	68	0	0	1.78	1.627	-1.87	29.61
	4/10/2013 10:44	3.2	73.5	0	23.3	136	136	46	47	1.4	1.5	0.751	0.782	0.41	29.19
GEW-16R	4/17/2013 15:04	3.1	73.5	0	23.4	140	140	48	47	3.1	2.9	0.826	0.789	0.61	29.31
	4/22/2013 16:03	2.9	71.1	0.2	25.8	140	140	77	72	1.3	1.5	2.082	1.823	0.35	29.48
	4/22/2013 16:10	2.9	70.7	0.1	26.3	140	140	74	71	1.2	1.3	1.877	1.745	0.23	29.48
	4/10/2013 10:40	3.4	77.6	0	19	148	148			7	7	-15.899	-15.825	0.36	29.23
	4/4/2013 8:35	0.5	77.8	0.2	21.5	140	140	63	12	-2.8	-2.6	1.448	0.064	-1.96	29.62
GEW-17R	4/10/2013 14:28	0.3	77.9	0	21.8	140	140	8	15	0.8	0.8	0.026	0.086	0.8	29.11
	4/19/2013 9:21	0.5	77.2	0.4	21.9	150	150	60	43	-3.3	-3.4	1.361	0.69	-2.43	29.2
	4/25/2013 11:12	0.4	77.8	0	21.8	160	160	33	33	-0.8	-0.8	0.435	-0.49	-0.23	29.8
	4/25/2013 11:16	0.4	77.6	0	22	160	160	51	45	-0.5	-0.5	1.005	0.769	-0.54	29.8
	4/30/2013 8:59	0.5	77.3	0	22.2	170	170	48	40	1.1	0.8	0.89	0.619	1.06	29.33

April 2013 Wellfield Monitoring Data - Bridgeton Landfill

Well Name	Date Sampled	Methane	CO ₂	O ₂	Balance Gas	Init Temp °F	Adj Temp	Init Flow scfm	Adj Flow	Init Static Press	Adj Static Press	H ₂ O		System Pressure	Baro
												Init Diff Press	Adj Diff Press		
GEW-25A	4/4/2013 8:59	15.8	71.5	0	12.7	136	136	21	26	-0.8	-0.8	0.165	0.239	-2.47	29.64
	4/10/2013 14:55	11.5	75.7	0	12.8	134	134			1.8	1.7	-1.202	-1.076	0.33	29.12
	4/19/2013 10:19	16.8	74.5	0	8.7	132	132	12		-0.8	-0.8	0.056	-0.039	-3.58	29.18
	4/25/2013 12:15	14	72.6	0	13.4	132	132			0.7	0.6	-1.612	-1.702	-0.86	29.69
	4/25/2013 12:20	14.1	72.9	0	13	132	132			0.7	0.8	-1.322	-1.305	-0.44	29.69
	4/30/2013 9:24	13.5	73.8	0	12.7	140	140			0.7	0.7	-1.812	-1.823	-0.24	29.36
GEW-26R	4/4/2013 9:02	0.8	76.1	0	23.1	180	180			2	2.1	-7.457	-7.725	-1.25	29.63
	4/19/2013 10:22	0.8	79.9	0	19.3	175	175			1.7	1.8	-9.363	-8.587	-1.86	29.18
	4/25/2013 12:23	0.6	78.6	0	20.8	175	175			3.3	3.3	-6.809	-6.747	3.4	29.69
	4/25/2013 12:31	0.5	79.3	0	20.2	175	175			3.4	3.7	-5.958	-6.418	3.88	29.69
GEW-27A	4/30/2013 9:27	0.6	79	0	20.4	180	180			4.1	4.1	-4.208	-4.278	1	29.36
	4/4/2013 9:04	21.8	74.6	0	3.6	140	140	50	47	-1.8	-1.7	0.843	0.756	-1.99	29.63
	4/10/2013 14:58	18.1	73.5	0	8.4	142	142	48	51	0.8	0.8	0.784	0.884	0.75	29.11
	4/19/2013 10:25	20.2	74.8	0	5	140	140	47	45	-2.5	-2.4	0.775	0.695	-1.5	29.18
	4/25/2013 12:11	20.9	70.4	0	8.7	140	140	40	43	-0.1	0	0.628	0.542	-0.69	29.81
	4/25/2013 12:16	21.3	69.8	0	8.9	140	140	39	42	0	-0.2	0.527	0.587	-0.3	29.81
GEW-28R	4/30/2013 9:29	19.6	73.1	0	7.3	140	140	36	34	0.7	0.6	0.448	0.396	0.49	29.35
	4/4/2013 9:07	21.6	70.2	0	8.2	124	124	24	30	-1.3	-1.3	0.205	0.294	-3.84	29.63
	4/10/2013 15:00	19.8	70.8	0	9.4	124	124	36	33	0.9	0.9	0.431	0.365	-0.69	29.1
	4/19/2013 10:27	23.1	71.1	0	5.8	120	120	24	22	-3.6	-3.6	0.199	0.172	-3.74	29.19
	4/25/2013 12:18	21.8	69.2	0	9	124	124	21	28	-0.6	-0.8	0.153	0.27	-1.58	29.82
	4/25/2013 12:23	22.1	69	0	8.9	124	124	28	24	-0.6	-0.7	0.256	0.2	-1.72	29.82
GEW-29	4/30/2013 9:31	19.9	70.4	0	9.7	124	124	21	25	0	0	0.15	0.218	-0.41	29.35
	4/4/2013 9:14	9.8	73.8	0	16.4	122	122	66	64	0	0	1.483	1.376	-1.52	29.59
	4/10/2013 16:16	8.4	74.6	0	17	126	126	63	64	2.5	2.5	1.341	1.397	0.62	29.04
	4/22/2013 10:13	8	73.7	0	18.3	125	125	69	62	0.8	0.8	1.607	1.309	-0.62	29.52
	4/22/2013 10:18	8.1	73.9	0	18	125	125	61	60	0.9	1	1.26	1.24	-0.55	29.52
	4/30/2013 10:12	7.7	74.3	0	18	128	128	64	57	1.9	2.1	1.396	1.121	0.61	29.32
GEW-30R	4/4/2013 9:17	15.1	71.3	0	13.6	164	164	19	21	-3.5	-3.3	1.034	1.225	-4.04	29.62
	4/10/2013 16:19	11.7	74	0	14.3	160	160	19	20	-0.4	-0.3	0.961	1.108	-1.1	29.05
	4/22/2013 10:23	25.7	66	0	8.3	150	150	11	11	-3.6	-3.5	0.331	0.345	-3.86	29.53
	4/22/2013 10:32	26	65.2	0	8.8	150	150	12	15	-3.5	-3.7	0.367	0.602	-3.75	29.53
	4/30/2013 10:15	20.4	69.5	0	10.1	156	156	13	12	-2.2	-2.2	0.479	0.379	-2.54	29.35
	4/4/2013 10:16	0.3	76.3	0	23.4	54	54			-1.1	-0.9	-0.995	-0.845	-0.9	29.65
GEW-31R	4/10/2013 17:27	0.3	78	0	21.7	64	64			-1.5	-1.6	-1.816	-1.855	-1.66	29.03
	4/4/2013 9:22	1	70.3	0	28.7	190	190			-4.2	-4.9	-1.104	-8.901	-4.53	29.64
	4/10/2013 16:30	0.9	71.9	0	27.2	184	184			-3.7	-4.8	-4.507	-3.458	-4.36	29.07
	4/4/2013 9:25	0.4	67.6	0	32	194	194			-9.7	-10.1	-10.352	-10.164	-9.91	29.65
GEW-33R	4/22/2013 10:59	0.3	66.9	0	31.8	190	190			-7.4	-7	-7.852	-7.658	-7.84	29.56
	4/22/2013 11:04	0.3	67.1	0	32.6	190	190			-8.1	-7.8	-8.538	-8.241	-8.32	29.56
	4/30/2013 10:37	0.5	67.5	0	32	190	190			-13.7	-13.3	-13.407	-13.985	-13.86	29.38
GEW-34	4/4/2013 9:28	2.9	36.6	11	49.5	60	60	14	14	-10.7	-11.7	0.062	0.06	-13.88	29.05
	4/10/2013 16:54	1	12.1	17.4	69.5	64	64	13	11	-11	-11.1	0.046	0.034	-12.05	29.02
	4/22/2013 11:11	3.8	32.3	11.2	52.7	70	70	18	18	-12.3	-14	0.102	-0.014	-11.86	29.54
	4/22/2013 11:19	1.6	14.5	16.1	67.8	70	70	18	9	-12.9	-12.4	0.088	0.027	-11.86	29.54
	4/30/2013 10:40	0.5	8.3	17.6	73.6	80	80	18	9	-13.8	-15	-0.03	-0.019	-16.37	29.36

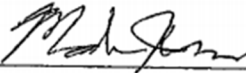
April 2013 Wellfield Monitoring Data - Bridgeton Landfill

Well Name	Date Sampled	Methane	CO ₂	O ₂	Balance Gas	°F		scfm		Init Static Press	Adj Static Press	*H ₂ O		System Pressure	Baro
						Init Temp	Adj Temp	Init Flow	Adj Flow			Init Diff Press	Adj Diff Press		
GEW-35	4/4/2013 9:33	0.4	78.3	0.1	21.2	188	188	41	41	-10	-10.7	0.707	0.685	-22.78	29.64
	4/10/2013 16:59	0.5	75	0	24.5	160	160	11	10	-15	-15.4	0.055	0.046	-17.62	29.03
	4/22/2013 14:07	10.1	54.3	5	30.6	130	130	38	37	-20	-20.2	0.497	0.476	-20.85	29.59
	4/22/2013 14:13	15.3	34.3	6.4	44	130	130	29	28	-20	-19.8	0.259	0.252	-20.76	29.59
	4/30/2013 10:46	0.5	37.6	8.6	53.3	140	140	3	3	-18.1	-18.1	-0.026	-0.002	-18.9	29.37
GEW-36	4/4/2013 9:37	0.3	70.7	0	29	168	168	10	10	-14.7	-15.1	0.034	-0.208	-16.13	29.63
	4/10/2013 17:02	0.3	70.9	0	28.8	154	154	10	10	-13.5	-14.7	-0.084	-0.281	-13.93	29.04
	4/22/2013 14:17	23.7	43.8	7.2	25.3	82	82	4	4	-20.8	-19.8	0.206	-0.048	-20.95	29.57
	4/22/2013 14:22	30	42.9	7.3	19.8	82	82	5	5	-19.6	-19.6	-0.276	0.041	-20.69	29.57
	4/30/2013 10:49	0.3	32.5	10.8	56.4	92	92	16	14	-17.7	-17.5	0.062	-0.408	-19.23	29.38
GEW-37	4/4/2013 9:40	0.2	75.2	0	24.6	180	180	16	14	-6.6	-6.6	0.116	0.089	-19.84	29.63
	4/10/2013 17:09	0.2	50.1	6	43.7	142	142	12	10	-12.3	-11.8	0.053	0.041	-14.37	29.04
	4/22/2013 14:28	36.3	61.1	2.4	32	154	154	18	16	-18.9	-19.8	0.119	0.094	-19.78	29.57
	4/22/2013 14:35	0.3	66.3	0.7	32.7	152	152	10	8	-18	-18.1	0.047	0.026	-18.82	29.57
	4/30/2013 10:52	0.5	46	6.9	46.6	146	146	12	12	-17.1	-17.5	0.057	-0.047	-18.48	29.37
GEW-38	4/4/2013 9:43	11	73.4	0	15.6	126	126	23	23	-10.8	-10.8	-0.3	0.189	-29.1	29.64
	4/10/2013 17:13	10.7	75.4	0	13.9	120	120	39	42	-7.6	-7.7	0.543	0.607	-22.86	29.03
	4/22/2013 14:30	6.2	71.1	0	22.7	120	120	10	12	-7.6	-7.5	0.036	0.052	-24.02	29.47
	4/22/2013 14:35	6.2	70.9	0	22.9	120	120	7	12	-7.5	-7.5	0.023	0.055	-25.78	29.47
	4/30/2013 10:54	6.7	70	0	23.3	126	126	21	22	-4.7	-4.5	0.169	0.182	-23.82	29.38
GEW-39	4/4/2013 9:45	40.7	56.7	0	2.6	110	110	102	101	-6.8	-6.7	2.852	2.798	-21.01	29.63
	4/10/2013 17:16	39.7	60.2	0	0.1	118	118	89	96	-5.3	-5.4	2.232	2.612	-17.18	29.03
	4/22/2013 14:40	39.8	56.2	0	4	110	110	94	89	-6.2	-6.4	2.417	2.18	-19.6	29.46
	4/22/2013 14:45	40.6	54.3	0	5.1	110	110	96	93	-6.3	-6.3	2.49	2.335	-18.57	29.46
	4/30/2013 10:57	42.5	56.8	0	0.7	112	112	84	82	-7	-6.8	1.934	1.84	-17.48	29.38
GEW-40	4/2/2013 9:08	52.5	47.1	0	0.4	94	94	18	19	-1.9	-2	0.086	0.093	-32.56	29.68
	4/9/2013 8:49	50.8	46.5	0	2.7	95	95	14	16	-1.7	-1.7	0.055	0.07	-24.49	29.22
	4/16/2013 8:54	50.7	47.7	0	1.6	89	89	20	19	-0.8	-0.8	0.105	0.094	-18.73	29.6
	4/23/2013 9:18	51	46	0.1	2.9	93	93	19	20	-1.8	-1.8	0.091	0.11	-23.75	29.5
	4/29/2013 8:42	52.5	45.4	0.2	1.9	94	94	17	18	-1.3	-1.3	0.081	0.089	-20.18	29.41
GEW-41R	4/9/2013 8:51	46	37.1	0.2	16.7	109	110	58	67	-1.8	-1.8	0.829	1.116	-22.49	29.23
	4/16/2013 8:57	51.2	39.8	0.3	8.7	103	103	48	52	-1.2	-1.3	0.559	0.667	-19.18	29.59
	4/23/2013 9:20	44.9	37.3	0.3	17.5	106	107	66	55	-1.9	-2	1.055	0.762	-22.03	29.5
	4/29/2013 8:45	46.5	38	0.3	15.2	107	107	21	18	-0.8	-0.8	0.115	0.091	-19.01	29.43
	4/29/2013 8:53	33.9	31.2	0	34.9	89	89	5	6	-0.6	-0.6	0.009	0.009	-22.67	29.22
GEW-42R	4/16/2013 8:59	34.6	31.4	0	34	70	70	17	16	-0.5	-0.5	0.071	0.067	-15.79	29.58
	4/23/2013 9:22	29.3	31	0	39.7	81	81	14	14	-0.9	-0.9	0.051	0.051	-22.39	29.5
	4/29/2013 8:47	34	34.7	0.2	31.1	81	82	24	24	-0.6	-0.6	0.149	0.148	-18.07	29.42
	4/7/2013 9:18	52.8	41.8	0.4	5	85	86	17	21	-0.6	-0.6	0.073	0.114	-27.62	29.68
	4/9/2013 8:57	53.8	42.8	0.1	3.3	107	107	12	10	-0.4	-0.4	0.038	0.03	-22.61	29.21
GEW-43R	4/16/2013 9:02	56.3	43.6	0	0.1	77	77	2	1	-0.2	-0.2	0.001	0	-15.52	29.49
	4/23/2013 9:25	56.3	43	0	0.7	88	88	15	11	-0.7	-0.7	0.055	0.033	-20.93	29.49
	4/29/2013 8:50	55.7	44.2	0	0.1	80	81	14	13	-0.2	-0.2	0.052	0.045	-16.87	29.41
	4/29/2013 8:53	55.6	44.3	0	0.1	86	87	28	29	-0.3	-0.3	0.198	0.21	-17.2	29.41

Client: Republic Services
Attn: Mike Lambrich
Project Name: Bridgeton Landfill
Project No.: North Quarry Samples
Date Received: 06/10/13
Matrix: Air
Reporting Units: % v/v

ASTM D1946								
Lab No.:	E061001-29		E061001-30		E061001-31		E061001-32	
Client Sample I.D.:	GIW 4		GIW 5		GIW 6		GIW 7	
Date Sampled:	06/06/13		06/06/13		06/06/13		06/06/13	
Date Analyzed:	06/10/13		06/10/13		06/10/13		06/10/13	
QC Batch No.:	130610GC8A1		130610GC8A1		130610GC8A1		130610GC8A1	
Analyst Initials:	MJ		MJ		MJ		MJ	
Dilution Factor:	3.2		3.4		3.4		3.6	
ANALYTE	Result	RL	Result	RL	Result	RL	Result	RL
	% v/v	% v/v	% v/v	% v/v	% v/v	% v/v	% v/v	% v/v
Carbon Monoxide	0.50	0.0032	0.52	0.0034	0.60	0.0034	0.37	0.0036

ND = Not Detected (below RL)
 RL = Reporting Limit

Reviewed/Approved By: 
 Mark Johnson
 Operations Manager

Date 6-12-13

The cover letter is an integral part of this analytical report

Laboratory Analysis - Bridgeton Landfill

Well Name	Date Sampled	Methane	CO ₂	O ₂ /Argon	Nitrogen	Hydrogen	Carbon Monoxide
							(ppm)
GEW-10	1/23/2013	36	52	1	8.6	2	340
	2/13/2013	38	38	4	20	ND	42
	3/5/2013	30	55	2	10	0	390
	4/22/2013	30	41	ND	28	ND	60

GEW-28R	1/23/2013	13	64	ND	ND	13	1,300
	2/12/2013	16	55	4	16	8.6	980
	3/6/2013	13	46	7	25	8.3	960
	4/25/2013	20	65	ND	ND	13	1,200
	1/23/2013	15	65	1	3.4	15	1,800

Laboratory Analysis - Bridgeton Landfill

Well Name	Date Sampled	Methane	CO ₂	O ₂ /Argon	Nitrogen	Hydrogen	Carbon Monoxide
							(ppm)
GEW-36	1/23/2013	1	61	1	3.2	33	3,900
	2/12/2013	0.32	52	4	15	28	2,900
	3/5/2013	0.7	61	0	0	34	3,300
	4/22/2013	0.14	38	8	30	22	1,900
GEW-37	1/23/2013	15	52	2	19	12	2,000
	2/12/2013	15	64	1	6	13	1,900
	3/5/2013	0.2	66	0	4	28	4,700
	4/22/2013	0.15	45	6	21	26	2,600
GEW-38	1/23/2013	4.3	64	1	3.9	26	3,200
	2/12/2013	5	66	1	2.6	25	2,100
	3/5/2013	6.7	63	2	6.5	22	1,600
	4/22/2013	5.6	63	ND	ND	27	1,800
GEW-39	1/23/2013	35	62	1	2.7	ND	98
	2/12/2013	35	60	1	2.6	1	170
	3/5/2013	43	53	0	0	ND	100
	4/22/2013	40	52	ND	5.5	ND	140

Appendix C

Map of The Smoldering Event in 2013

Data Evaluation Report, June 2013

